Manipulation of host cell death and innate immune signaling pathways by Coxsackievirus B3

by

Katharine Grace Harris

B.S. in Microbiology, Purdue University, 2010

Submitted to the Graduate Faculty of

the School of Medicine in partial fulfillment

of the requirements for the degree of

Doctor of Philosophy in Molecular Virology and Microbiology

University of Pittsburgh

2015

UNIVERSITY OF PITTSBURGH

SCHOOL OF MEDICINE

This dissertation was presented

by

Katharine Grace Harris

It was defended on

May 4, 2015

and approved by

Carolyn B. Coyne, PhD, Associate Professor of Microbiology and Molecular Genetics

Jennifer Bomberger, PhD, Assistant Professor of Microbiology and Molecular Genetic

Sarah Gaffen, PhD, Professor of Medicine

Saumendra Sarkar, PhD, Assistant Professor of Microbiology and Molecular Genetics

Jian Yu, PhD, Associate Professor of Pathology

Dissertation Advisor: Carolyn B. Coyne, PhD, Associate Professor of Microbiology and Molecular Genetics

Manipulation of host cell death and innate immune signaling pathways by Coxsackievirus B3

Katharine G Harris

University of Pittsburgh, 2015

Coxsackievirus B3 (CVB), an enterovirus, is a small, ssRNA virus with a genome of approximately 7 kB. There are 2 million symptomatic CVB infections annually in the United States, ranging from mild febrile illnesses to myocarditis, meningoencephalitis, or pancreatitis. CVB is a fecal-oral pathogen and must overcome diverse cellular barriers to cause disease, including the polarized epithelium lining the gastrointestinal tract. Viral infection of a host cell results in a variety of cellular responses that serve to control the viral infection. Once such response is the activation of intracellular innate immune signaling; this results in the production of type I interferon, which signals in an auto- and paracrine fashion to alter the transcriptional profile of a cell to inhibit viral replication. A second response to viral infection is the induction of cell death pathways; as viruses utilize host cell machinery for replication, early cell death of a host cell can result in an abortive infection. Here, I examine the ways in which CVB interfaces with these host cell pathways that affect viral replication. A primary mechanism utilized by CVB for altering host cell pathways is the production of the virally-encoded cysteine protease $3C^{pro}$. $3C^{pro}$ is required to process the viral polypeptide but is also known to target cellular protein targets for proteolysis. Here, I identify two cellular proteins targeted for proteolysis by $3C^{pro}$, Unc93b and RIP3, that are involved in the intracellular innate immune signaling and cell death pathways, respectively. I then characterize the roles of these proteins and their cleavage during CVB infection. In summary, I explore the ways in which CVB manipulates its host cell through

proteolysis of host cell proteins by the virally-encoded protease $3C^{pro}$ and find that the balance between virus and host is finely tuned through the activity of this protease.

TABLE OF CONTENTS

LIST OF TABLES

LIST OF FIGURES

PREFACE

This work would not have been possible without the support of many people and organizations. I'd like to thank Carolyn for acting as my mentor in every sense of the word – for being an incredible example of a scientist driven by curiosity, for copious amounts of advice and encouragement, and for always reminding me to 'enjoy my youth'. I'm also very grateful to the rest of the members of the Coyne lab, past and present. You people are fun to be around, you're fun to talk science with, and you're always there to help me out when I need an extra hand, to bounce an idea off someone, or help finding something I've lost deep in the recesses of the -80.

I'd also like to thank the other members of my thesis committee – Jen, Saumen, Sarah, and Jian, for their support. My committee meetings were always positive experiences and after each one I came away with new perspective on my project and new ideas for surmounting experimental and theoretical obstacles. Thanks for shepherding me through this process.

Additionally, I'd like to thank the funding sources that have made this work possible – the NIAID and the Burroughs Wellcome fund. I'd also like to thank the ARCS Foundation, Pittsburgh chapter, particularly the three couples who funded my scholarship through that foundation – to Charlotte and Henry Beukema, Beth and Russ Wainwright, and Cynthia Carrow and Jim Kyper, thank you for your encouragement, your interest, and all the lovely food and conversation.

In addition, I'd like to thank those within the University of Pittsburgh and those outside of it who have provided support in the completion of this work. Drs. Saumen Sarkar, Donna Stolz, Joanne Flynn, and Neal DeLuca (University of Pittsburgh), Dr. Xiaodong Wang (UTSW and NIBS), Drs. Cheryl Nickerson and Shameema Sarkar (Arizona State University), Drs. Harmit Malik and Maulik Patel (Fred Hutchinson Cancer Research Center), Drs. Sara Cherry and Jeff Bergelson (University of Pennsylvania), Dr. William Humphries (B&B microscopes), JoAnn Polk, John Viaropulos, Mary Lou Meyer, and Kristin DiGiacomo (University of Pittsburgh).

Finally, I'd like to thank my family and friends. To my parents, Mark and Lisa, you two are the best support system I've ever encountered. Thanks for your cards, visits, and unflagging confidence and thanks for always being a safe spot to land. To my brother, Sam, you are possibly the wisest brother anyone has ever had; you make me better and I'm grateful. To my partner, Allen, thanks for being genuinely interested in my work, even the boring parts, and being everlastingly patient when I claim an experiment will only take me 5 more minutes. I'm also endlessly grateful to my community of people at home in Indiana and here in Pittsburgh. There are too many kind people and kind actions to list here, but I'm overwhelmed when I think about all the love that has come my way while I've been working on this project.

1.0 INTRODUCTION

1.1 COXSACKIEVIRUS B3

1.1.1 Pathogenesis of CVB

Coxsackievirus B3 (CVB) is a non-enveloped virus in the enterovirus genus with a positive-sense RNA genome 7 kB in length. Enteroviruses are the most common human viral pathogens [1, 2] and cause a diverse range of diseases. Here, the pathogenesis of CVB is discussed.

1.1.1.1 History of CVB Pathogenesis. Originally isolated in Coxsackie, New York in 1947 [3], investigation into coxsackieviruses began in the context of the public health fight against epidemics of poliomyelitis. Non-paralytic poliomyelitis is characterized by an aseptic meningitis, in which the meninges become inflamed without evidence of a bacterial infection. A subset of cases progress to paralytic poliomyelitis, which is marked by destruction of motor neurons in the anterior horn of the spinal cord and subsequent flaccid paralysis.

In the 1800s, physicians began assembling detailed case studies of flaccid paralysis cases[4-6]; observations of the destruction of the gray matter of the spinal cord in these cases led to adoption of the name poliomyelitis (from the Greek for gray, *polios*). Though it had been

concluded based on epidemiological information that paralytic poliomyelitis was caused by an infectious agent [7, 8], in the early 1900s it was shown that spinal cord suspensions from patients who succumbed to paralytic poliomyelitis caused a paralytic disease in monkeys, that this disease was transmissible from monkey to monkey, and that the infectious agent was found in spinal cord suspensions from which bacteria and parasites had been removed [9, 10]. These observations led to the conclusion that the etiologic agent for poliomyelitis was a virus, subsequently dubbed poliovirus. By the 1940s, it was understood that poliovirus was transmitted primarily by a fecal-oral route, and techniques had been developed to isolate virus shed in the feces of patients [11].

In 1947, two children in Coxsackie, New York, presented with poliomyelitis-like symptoms, but the virus isolated from their fecal samples was not poliovirus, as expected. This virus was not neutralized by serum targeting poliovirus and induced pathologies in animal models divergent from that seen with poliovirus [3]. Subsequent clinical isolations of several serologically distinct viruses with similar pathologies in animal models led to the establishment of a group of viruses known as coxsackieviruses [12]. By 1950, the coxsackieviruses had been divided into 2 groups, A and B, based on the pathology caused in a suckling mouse model of infection [13]. Individual strains within these groups were distinguished by their antigenic diversity [14], this nomenclature persists to the present. In 1957, the genus enterovirus was established to contain poliovirus, the coxsackieviruses, and another newly discovered group of viruses known as the enteric cytopathic human orphan (ECHO) viruses [15].

Researchers now turned their attention to establishing the role of coxsackieviruses in human disease. It was unclear at this point whether coxsackieviruses were the etiologic agents of

poliomyelitis-like symptoms in the patients from which they had been isolated, or whether the presence of coxsackievirus was incidental in these patients [16]. It was recognized that seroprevalance for antibodies directed against coxsackieviruses was high in the general population, without accompanying reports of major illness, indicating that many infections caused subclinical infection [17, 18]. However, through extensive clinical surveillance, it was determined that coxsackieviruses from group B, particularly Coxsackievirus B3 (here, CVB) were responsible for cases of aseptic meningitis, resembling non-paralytic poliomyelitis, as well as myocarditis in infants and adults [19, 20]. Though it was observed soon after discovery of coxsackieviruses that group B coxsackieviruses exhibited tropism for the pancreas in mouse models [21, 22], it was not until almost 20 years later that a correlation between antibodies to group B coxsackievirus and onset of type I diabetes was observed [23], leading to an active field of research describing the role of coxsackievirus infection in the destruction of pancreatic β cells and subsequent development of diabetes [24].

The story of the discovery of coxsackieviruses is a lesson in the importance of careful observation in science. In seeking to isolate poliovirus, an entire group of viruses with a significant impact on human health were found, in an era before genetic techniques or even mammalian tissue culture were available for virus discovery work. The meticulous work that was undertaken to determine the role for coxsackieviruses in human disease inaugurated the modern field of coxsackievirus research.

1.1.1.2 Route of CVB Infection. Much of the knowledge about how CVB enters the body and causes disease is derived from studies done with poliovirus. As detailed above, poliovirus is

spread through the fecal-oral route, and the initial isolation of CVB was made from fecal samples. If the intestinal epithelial barrier is breached, a primary viremia may result. This viremia appears before any major symptoms of disease, commonly occurs among infected individuals, and also can occur in abortive illnesses, those in which no serious symptoms ever result [25, 26]. A secondary or 'major' viremia occurs in a subset of people due to continued viral replication in secondary sites of infection [27]. It is upon this secondary viremia that the virus gains access to distal organs including the central nervous system (CNS), heart, and pancreas and causes disease in these organs (Figure 1), the pathogenesis of these diseases are detailed in the following sections.

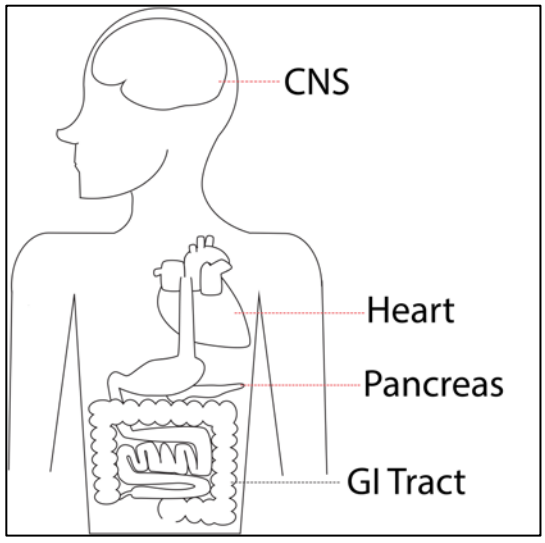

Figure 1. CVB intestinal infection and dissemination.

CVB infects a new host through the fecal-oral route. After replicating in and breaching the GI tract (black line), a primary viremia may result. After this, a secondary major viremia may result due to continued viral replication in secondary sites of infection. This viremia can lead to infection of distal sites including the CNS, heart, or pancreas (red lines), where serious pathologies may occur.

1.1.1.3 CVB infection of the heart. One of the most serious potential outcomes of a CVB infection is the dissemination of the virus to the heart and the subsequent development of

myocarditis, which can then further progress to dilated cardiomyopathy. These conditions are major causes of heart failure, particularly among children and adolescents [28]. Evidence of an enterovirus infection is found in up to 50% of cardiomyopathy cases [29-31]. CVB infections contribute to development of cardiomyopathy in two distinct ways—(1) the virus can directly infect and induce the cell death of cardiomyocytes or (2) they can trigger an autoimmune response in which the host's own immune system destroys cardiomyocytes and leads to the characteristic inflammation seen in cardiomyopathy. CVB infection does indeed directly cause apoptosis of cardiomyocytes *in vitro*. Primary cardiomyocytes isolated from mice or rats are killed upon CVB infection [32, 33], and a murine cardiac muscle cell line, HL-1 [34], undergoes apoptosis upon CVB infection [35]. Human patients presenting with enterovirus-induced myocarditis who had cardiac biopsies taken showed a strong positive correlation between cardiomyocytes staining positive for enterovirus capsid protein and those undergoing apoptosis [36]. Perhaps the most convincing evidence for direct CVB-mediated cell death comes from mice with severe combined immunodeficiency (SCID mice). SCID mice lack all mature T- and B- cell responses, and therefore are incapable of developing autoimmunity. Even in a SCID mouse model of CVB-induced myocarditis, death of cardiomyocytes correlates with the development of cardiomyopathy [37]. Despite these convincing results, it remains probable that autoimmune responses contribute to CVB-induced myocarditis, acting in combination with cell death caused directly by CVB replication. In mouse models of CVB-induced myocarditis, CVB infection leads to the generation of heart specific autoantibodies [38], and human patients with viral-induced myocarditis also have autoantibodies in their sera [39]. Therefore, it is likely that

both CVB-induced cell death and CVB-induced autoimmunity contribute to the destruction of cardiomyocytes in CVB-associated cardiomyopathy.

1.1.1.4 CVB infection of the central nervous system. As detailed in Section 1.1.1.1, CVB was initially isolated from patients with poliomyelitis-like symptoms. For this reason, neurological complications arising from CVB infections are well-studied. Both aseptic meningitis and meningoencephalitis, in which the brain itself is inflamed in addition to the meninges, can result from coxsackievirus infections [40], with neonates at particular risk [1]. An observational study of children admitted to a single hospital with confirmed CVB infections over an 8-year period noted that the most common diagnosis for these children was aseptic meningitis [41]. In a neonatal mouse model of CVB infection, viral protein was found exclusively in neurons and neuronal stem cells and the authors observed death of infected cells [42]. Additionally, neonatal mice infected with sublethal doses of CVB showed reduction in brain weight due to CVB-induced apoptosis of neuronal stem cells and consequent decreased neuronal proliferation [43]. This animal model evidence, coupled with observations of viral antigen from group B coxsackieviruses in neurons and glial cells of a patient with encephalitis [44] suggests that viral replication in and lysis of host cells in the central nervous system (CNS) contributes to CNS pathology upon CVB infection, in addition to the established role for immune infiltrate in aseptic meningitis [45].

1.1.1.5 CVB infection of the pancreas. The contribution of environmental factors to the onset of type I diabetes in children, in which the insulin producing β-cells of the pancreatic islet are

destroyed, has long been suspected, and there is strong evidence suggesting that viral infections, and enterovirus infections in particular, can precipitate its development [24]. A meta-analysis of the available literature showed that patients with type I diabetes were significantly more likely to have evidence of an acute enterovirus infection than the general population [46], and patients with recent-onset type I diabetes were significantly more likely to have evidence of enteroviral protein in their pancreatic islets than non-diabetic controls [47]. In perhaps the most convincing evidence for enterovirus-induced diabetes, CVB4 was isolated from the pancreas of a young patient who died from diabetic ketoacidosis and this strain of CVB4 was able to cause death of β-cells and subsequent hyperglycemia in mice [48]. Additionally, an analysis of the pancreases of organ donors with type I diabetes found that 3 of the 6 pancreases had capsid protein from CVB4 in the β-cells of their pancreatic islets compared to 0 of 26 control pancreases [49]. There is also evidence that β-cell destruction upon CVB-infection may be due to molecular mimicry, in which a CVB protein bears molecular similarity to an autoantigen [50, 51], or by the release of a normally sequestered autoantigen by CVB-infection of pancreatic islets [52], both of which lead to an autoimmune response directed against the pancreatic islets. Clearly, group B coxsackievirus infections can both directly and indirectly contribute to the β-cell destruction that results in development of type I diabetes, though CVB4 seems to be more important in this pathology than CVB3.

1.1.2 Viral Life Cycle

As research on the role of CVB in the pathogenesis of human disease was progressing, scientists understood that it was also important to understand the life cycle of CVB at a cellular level. To that end, much effort has been applied to understanding the mechanisms of entry, replication, and egress of CVB in cell culture models.

1.1.2.1 Viral Entry. In order to enter a host cell, CVB must attach to its receptor, known as the coxsackievirus-adenovirus receptor (CAR) [53]. This attachment is mediated by the insertion of CAR into the 'canyon' of CVB, a depression surrounding each five-fold axis of symmetry of the viral capsid [54, 55]. However, as CAR is localized to the tight junction in the intestinal epithelium and is therefore inaccessible to CVB approaching from the intestinal lumen, it has been shown that CVB first binds and clusters decay-accelerating factor (DAF), a membrane-anchored protein found at the apical surface [56]. This induces cytoskeletal rearrangements that allow access to CAR [56]. Once bound to CAR, CVB undergoes a conformational change involving rearrangement of the viral capsid proteins to become what is known as an 'A-particle', a necessary step for subsequent uncoating of the genome after internalization [57]. This altered particle is then endocystosed using a variety of endocytic pathways, depending on the cell type [56, 58-61]. The process of uncoating is not completely understood for CVB, but based on data from other enteroviruses, it is likely that the conformational change experienced upon A-particle transition results in the exposure of the terminus of the viral capsid protein VP1, expulsion of VP4 from the capsid, and expansion of a pore at the two-fold axis of symmetry of the viral capsid. The helical amphipathic tail of VP1 then inserts into the endocytic membrane, VP4 forms a pore in the endocytic membrane, and the expansion of the capsid at the two-fold axis of

symmetry allows the viral genome to exit through the VP4 pore into the cytoplasm, leaving behind an empty capsid in the endosome [62-66].

1.1.2.2 Viral Replication. Once uncoating has occurred, the now cytoplasmic RNA genome must be both replicated and translated. The mechanisms of these processes were first thoroughly investigated for poliovirus, and much of the knowledge of CVB replication is extrapolated from these studies. As CVB does not package a polymerase within its viral capsid, translation of the genome must first occur in order to produce the virally-encoded polymerase. The genome of CVB does not contain a 5'-cap, which is used for eukaryotic translation initiation, but is instead covalently linked to the VPg protein at its 5'-end [67, 68]. Therefore, translation initiation occurs via the genomic internal ribosomal entry site (IRES) and host-cell ribosomes [69, 70]. This produces a polyprotein that is autoprocessed by the viral cysteine proteases $2A^{pro}$ and $3C^{pro}$ (Figure 2) [71]. These proteases also target numerous cellular proteins for cleavage and are well conserved amongst enteroviruses [72-74]. The processing of $3D^{pol}$, the viral polymerase, enables it to begin negative-strand synthesis from the positive-strand genome. From this negative-strand template, many new copies of the viral genome are synthesized [75], which are then packaged into capsids [76]. The process of viral replication is localized to viral replication complexes (VRCs) that are induced by viral proteins and require the remodeling of host subcellular membranes to use as platforms [77]. This process is more thoroughly introduced in section 1.7.

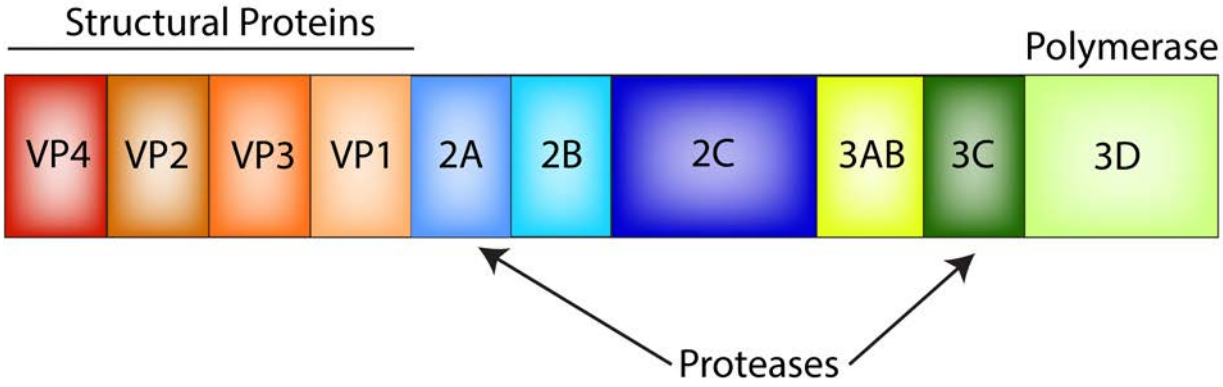

Figure 2. Polyprotein of CVB.

The CVB genome is translated as one polyprotein that is then processed or autoprocessed into individual proteins by the viral protease.

1.1.2.3 Viral Egress. Newly packaged CVB capsids must exit the cell to start a new round of replication in a new host cell or to exit the host. As interaction with CAR is required for the formation of the A-particle, and RNA cannot exit the capsid without this transition, there is no possibility for a newly formed virus to restart an infection in its cell of origin. It has been long observed that CVB infections cause cell death *in vivo* and in tissue culture (see section 1.2). For the preponderance of its spread, CVB relies on this cell death to escape the cell. Indeed, blocking apoptotic cell death in HeLa cells upon CVB infection led to large reductions in release of extracellular virus [78]. Conversely, increasing apoptotic cell death in CVB infected HeLa cells through ectopic expression of the pro-apoptotic protein Cyr61 led to an increase in extracellular virus release, while siRNA-mediated knockdown of Cyr61 decreased extracellular virus release [79]. Additionally, blocking CVB-induced necrosis in intestinal epithelial cell lines through a variety of mechanisms all led to a decrease in extracellular virus titers [80]. The fact that diverse

mechanisms of cell death inhibition in different cell lines upon CVB infection all resulted in a reduction or delay of viral release strongly implicates cell death in the process of viral egress and minimizes the possibility that inhibitors of cell death were having an off target effect on a separate aspect of the viral life cycle.

Despite the strong evidence cited above for the link between viral egress and cell death, there is also data that suggests that there may be secondary routes of viral egress that occur temporally before and independently of cell death. One such route may involve autophagy, which is thoroughly introduced in section 1.7. Neural progenitor cells infected with CVB shed extracellular microvesicles derived from autophagic pathways containing infectious CVB virions before any signs of cell death [81], and HeLa cells shed CVB in phosphatidylserine lipid-enriched vesicles before lysis [82]. Additionally, pharmacologically blocking the autophagy pathway in CVB-infected HeLa cells resulted in a reduction of extracellular virus, though this data is difficult to interpret in the context of autophagy as an egress pathway as treatment also reduced intracellular virus replication [83].

1.2 CVB INFECTION AND CELL DEATH

It is quite clear from the discussion of CVB pathogenesis in section 1.1.1 that cell death caused by CVB infection has serious consequences for human health. Cell death upon viral infection causes pathologies in the heart, CNS, and pancreas. Much research has been done concerning the mechanisms by which cell death occurs upon CVB infection.

Cells possess diverse routes of cell death initiation, from cell surface receptors such as the tumor necrosis factor receptor 1 (TNFR1) [84], to intracellular receptors known as pattern recognition receptors (PRRs) that sense pathogen or damage associated molecular patterns (PAMPs or DAMPs, respectively) [85], to the detection of DNA damage. Additionally, distinct forms of cell death can occur downstream of these triggers. Apoptosis, in either its caspase-dependent or caspase-independent form, is a tightly regulated form of cell death that results in chromatin condensation, DNA fragmentation, and the eventual disruption of the cell into apoptotic blebs [86]. Caspases are proteases that require proteolytic processing for activation, and, once activated, cleave downstream substrates to induce apoptotic cell death [87, 88]. Apoptosis is further categorized as intrinsic or extrinsic. Intrinsic apoptosis is mediated by the mitochondria and is dependent on the release of cytochrome C from the mitochondria, a process that is regulated by the Bcl-2 family of proteins. Pro-apoptotic Bcl-2 family members act to release cytochrome C from the mitochondria whereas anti-apoptotic family members act to prevent cytochrome C release. Extrinsic apoptosis, on the other hand, proceeds from cell surface receptors and is independent of the mitochondria [89]. Necrosis was long thought to be an unregulated form of cell death, characterized by loss of membrane integrity and a release of intracellular contents into the extracellular space that provoked a highly inflammatory reaction. Recently, programmed forms of necrosis have been discovered, with tightly regulated signaling cascades that result in membrane permeabilization by the mixed lineage kinase like protein (MLKL) and/or generation of reactive oxygen species (ROS) and lead to the necrotic death phenotype [90] (discussed thoroughly in section 1.5). [91]. *In vitro* studies of CVB infections in

cell culture models reveal that multiple redundant pathways are likely triggered to initiate cell death upon infection and the cell death pathways induced are cell type specific.

1.2.1 CVB-Induced Apoptosis

There is much evidence to suggest that apoptosis is a relevant *in vivo* form of cell death induced by CVB. Infected cardiomyocytes from patients with enterovirus-induced myocarditis were apoptotic [36], and primary rat pancreatic cell cultures died by apoptosis upon CVB5 infection [92]. Further *in vitro* work shows that infection with various CVB serotypes in HeLa cells leads to cytochrome C release from the mitochondria [78], a hallmark of intrinsic apoptosis. This release is followed by caspase-activation [93], specifically caspase 9 [78, 94], an initiator caspase that cleaves other caspases. Indeed, CVB infection results in activation of caspases-2, -3, -6, -7, -8, and -9 in HeLa cells [78, 93].

Although these studies clearly show that CVB induces apoptotic cell death in specific cell types both *in vivo* and *in vitro*, it remains to be explained how this apoptosis is mechanistically induced during viral infection. One such apoptosis-inducing mechanism is the activation of the unfolded protein response (UPR). The UPR, under normal cellular circumstances, is a cell-wide response to the accumulation of unfolded proteins in the endoplasmic reticulum (ER) [95], and can trigger apoptotic cell death [96]. CVB infection in HeLa cells induced the UPR through each of the three distinct UPR initiation pathways (the PERK, IRE1, and ATF6 dependent pathways) [97], and resulted in activation of caspase-12, a UPR specific caspase [98], and upregulated expression of CHOP, a pro-apoptotic transcription factor classically implicated in UPR-initiated

cell death [97, 99]. Alternatively, CVB infection can trigger apoptosis through the activation of stress activated protein kinases (SAPKs). SAPKs, including JNK and p38MAPK, are responsible for sensing cell stressors and transducing the signal to induce cellular responses to those stressors, including induction of cell death pathways [100, 101]. p38MAPK was phosphorylated and activated upon CVB infection of HeLa cells or a murine cardiomyocyte cell line [102, 103], and pharmacological inhibition of p38MAPK reduced CVB-induced cell death [102].

There is also much data available on the subject of the mechanisms by which CVB infection initiates the above cell death pathways. Transient overexpression of the CVB-encoded cysteine proteases $2A^{pro}$ or $3C^{pro}$ in HeLa cells is sufficient to reduce cell viability, activate caspases, and induce cytochrome C release from the mitochondria [104]. The mechanism of death induction by these proteases is dependent on proteolytic activity, as a catalytically inactive mutant of $3C^{pro}$ cloned from a closely related enterovirus, EV71, was incapable of inducing the apoptotic cell death induced by the wild-type protease in a glioblastoma cell line [105]. Cleavage of host cell proteins by these proteases likely feeds into the apoptotic pathways discussed above in multiple ways. A second mechanism by which apoptosis is triggered during CVB infections may be through production of double-stranded (ds)RNA during the course of genome replication. dsRNA is a highly immunogenic PAMP that can also lead to the induction of cell death [85, 106]. Multiple intracellular sensors of dsRNA exist and serve to activate innate immune signaling and can cross-talk with cell death pathways. Melanoma differentiation associated 5 (MDA5), a cytosolic dsRNA sensor, and toll-like receptor 3 (TLR3), an endosomal dsRNA sensor are both key sensors of CVB infection [107] (see section 1.3), and CVB infection induces expression of another cytosolic dsRNA sensor, protein kinase R (PKR) [108]. Finally,

viral capsid proteins themselves may serve to initiate apoptosis. CVB-encoded VP2, one of four viral proteins that compose CVB capsids [72], physically interacts with the pro-apoptotic host protein Siva [109, 110]. Siva functions by binding to Bcl-XL, an anti-apoptotic member of the Bcl-2 family and sequestering it, thus preventing it from carrying out its anti-apoptotic function [111]. Infection of a mouse model with CVB containing a mutation in VP2 preventing SIVA binding showed lower levels of cell death in the pancreas than wild-type CVB, despite similar viral titers [109]. The mechanism(s) by which VP2 binding to SIVA enhances its apoptotic function is not fully understood.

1.2.2 CVB-Induced Necrosis

In contrast to the large amount of data available on apoptotic cell death during CVB infection, much less is known about the contribution of necrotic cell death. One reason for this dearth of data is the only recent development of the programmed necrosis ('necroptosis') field. Another is that in many of the cell types studied *in vitro*, the main cell death pathway induced upon CVB infection is apoptosis and necrosis seems to be uninvolved, or not involved to any significant degree (as discussed in section 1.2.1). However, our group has recently shown that a polarized intestinal epithelial cell (IEC) line undergoes calpain-mediated necrotic cell death upon CVB infection, dependent upon Ca^{2+} release from the ER [80]. Another study showed that a pancreatic islet cell line that undergoes apoptosis when infected with CVB5 at a low multiplicity of infection (MOI), may instead undergo necrosis at higher MOIs. However, the method used here to characterize and quantify necrosis was not robust [112]. It is likely that both necrosis and

apoptosis are relevant forms of cell death *in vivo*, as EV infections must cross the polarized IEC barrier to cause initial viremia, and intestinal epithelial cells die necrotically *in vitro* (above, [80]) whereas apoptotic cell death seems most relevant at the distal sites of infection resulting in pathology (myocardium, pancreatic islets, and the CNS).

1.3 CVB INFECTION AND INNATE IMMUNE SIGNALING

In addition to being the cause of a number of pathologies associated with CVB infection and necessary for CVB egress, cell death can also be an important part of the innate immune response to an intracellular pathogen. It has long been appreciated that the intracellular innate immune response, comprised of a variety of signaling pathways designed to alert a host cell and its neighboring cells to a pathogenic invader, is necessary for the induction of the subsequent adaptive immune response [113, 114]. Innate immunity to pathogens is largely mediated by PRRs, which recognize a variety of PAMPs that are highly conserved amongst classes of pathogens [115]. During a viral infection, PRRs induce an intracellular signaling cascade in response to recognition of their cognate PAMP that results in the alteration of the transcription profile of the host cell or may lead to cell death. Two major classes of transcription factors are activated in response to this signaling: Interferon Regulatory Factors (IRFs) and nuclear factor kappa-light-chain-enhancer of B cells (NF-κB) family members. These transcription factors act in concert to induce the expression of type I interferon (IFN) [116]. These auto- and paracrine signaling molecules serve to upregulate a cadre of genes, known as interferon stimulated genes

(ISGs). The effects of type I IFNs and ISGs are legion; they are pro-inflammatory [117], enhance adaptive immunity [118], and are directly antiviral [119]. Additionally, NF-κB activation induces a host of pro-inflammatory and pro-survival genes independently of type I IFN induction [120-123] and may be required for full induction of type I IFNs [121, 124]. The two classes of PRRs known to be most critical in sensing CVB infection (detailed below) are the TLRs and the RIG-I like receptors (RLRs).

TLRs 1-13 are transmembrane PRRs that recognize a diverse range of PAMPs. TLRs can be divided into two broad categories—those that are localized to the cell surface and those that are localized to the endosomal lumen. TLRs that are present on the cell surface are important in recognition of bacterial pathogens. In contrast, TLRs that are localized to the lumen of endosomes, TLRs 3, 7, 8, and 9, serve to recognize nucleic acids and are thus traditionally thought to be the most important in the promotion of an antiviral response. TLR3 recognizes dsRNA and the synthetic dsRNA structural homolog poly(I:C) [106]. TLR7 and TLR8 recognize ssRNA and imidazoquinoline compounds [125-128]. TLR9 recognizes unmethylated deoxycytidylate-phosphate-deoxyguanylate (CpG) DNA, found almost exclusively in bacteria [129, 130].

RLRs are a group of cytoplasmic PRRs comprised of three members: retinoic acid-inducible gene (RIG)-I, MDA5, and laboratory of genetics and physiology (LGP)2. RIG-I recognizes cytoplasmic short dsRNA and 5'ppp-ssRNA [131-134]. MDA5 binds the internal duplex structure of cytoplasmic long dsRNA and cooperatively assembles into a filamentous oligomer composed of MDA5 dimers [132, 135-140]. The role of LGP2 has not been thoroughly elucidated. Early studies suggested that it acted as a negative regulator of RIG-I and

MDA5 [141-143]. However, further studies revealed that LGP2 was essential for type I IFN response to picornavirus infections in mice and that LGP2 with active helicase activity is required for IFNβ production in response to various RNA viruses in dendritic cells (DCs) and mouse embryonic fibroblasts (MEFs) [144]. Further studies of LGP2 have yielded equally disparate results, as both overexpression of chicken LGP2 and knockdown of endogenous LGP2 in chicken cells resulted in reduced IFNβ production in response to avian influenza infection [145].

1.3.1 TLR-mediated CVB sensing

TLR3 has been shown to play an essential and non-redundant role in the response to CVB, and may be the most critical TLR in the control of CVB infection. TLR3-deficient mice exhibit significantly increased mortality in response to a dose of CVB4 that is sublethal in control mice [146]. TLR3 also plays a protective role in restricting CVB infection in the heart as $TLR3^{-/-}$ mice infected with CVB display increased mortality and myocarditis [147]. $TRIF^{-/-}$ mice infected with CVB display increased viral replication in myocytes, decreased left ventricular functioning, and increased cardiac fibrosis [148]. Further supporting a role for TLR3 in CVB-triggered innate immune signaling, human patients diagnosed with enterovirus-induced myocarditis have increased frequencies of two single-nucleotide polymorphisms (SNPs) in TLR3 which result in variants that exhibit a reduced capacity to promote type I IFN and NF-κB signaling *in vitro* in response to poly(I:C) or CVB infection [149]. This suggests that sensing CVB-infection by TLR3 is key to activation of an effective immune response that can eliminate infection.

In addition to TLR3, several other TLRs have been shown to be important in the sensing of CVB infections. TLR4, which is localized to the cell surface, has also been shown to be important in the detection of CVB, although it is mainly studied in the context of bacterial pathogens. It has been shown that TLR4 mediates the production of tumor necrosis factor (TNF)α and interleukin (IL)-6 in pancreatic cells infected with CVB4, suggesting a role for TLR4 in recognizing not only bacterial lipopolysaccharides (LPS), but viral proteins as well [150], and implicating TLR4 in the production of pro-inflammatory cytokines that may contribute to pancreatic damage in CVB-precipitated type I diabetes. Additionally, the level of TLR4 expression and the level of enteroviral RNA present in endomyocardial tissue of patients with myocarditis are positively correlated [151]. However, in contrast to the studies described above related to TLR3 signaling, much less is known regarding the consequences of TLR4 signaling on CVB infection *in vivo*.

The ssRNA sensors TLR7 and TLR8 have also been shown to play some role in the induction of antiviral signaling in response to CVB infection, although their precise function remains largely unclear [152-154]. TLR7 has been shown to be required in plasmacytoid dendritic cells (pDCs), also known as interferon-producing cells because of their role in producing copious amounts of type I IFNs [155], for the production of IFNα and IL-12p40 in response to CVB, although this role was dependent on CVB specific antibody-mediated opsonization of the virus [154]. It has been shown that knockdown of endogenous TLR8 in primary human cardiac cells critically abrogates the capacity of those cells to produce IL-6 in response to CVB infection [153]. This suggests that the damaging cardiac inflammation seen in

CVB-induced myocarditis may be mediated through sensing of viral RNA by TLR8. However, little is known regarding the role of these TLRs in the control of CVB infections *in vivo*.

1.3.2 RLR-mediated CVB sensing

As the CVB genome is covalently linked to the VPg protein, it does not have a 5'-ppp motif that would be expected to be sensed by RIG-I. Indeed, MDA5, but not RIG-I serves as a cytoplasmic sensor for CVB. *In vitro*, MDA5$^{-/-}$ MEFs but not RIG$^{-/-}$ MEFS were unable to produce type I IFN in response to transfection of CVB genomic RNA [156]. MDA5 mediated responses to CVB RNA have been shown to be largely dependent on direct interaction of MDA5 with the dsRNA replicative intermediate form [139, 156]. The role of MDA5 also seems relevant *in vivo*, as in one study both MAVS and MDA5 deficient mice showed increased mortality and decreased systemic and tissue specific type I IFN upon CVB infection [157]. While a second study confirmed that MDA5 deficient mice were indeed more susceptible to CVB infection, as demonstrated by increased mortality, this study found that MDA5 seemed to be dispensable for production of systemic IFNα and tissue specific IFNβ in CVB3-infected mice [158]. These disparate results may be due to differences in the MDA5$^{-/-}$ mice used in the studies; the two studies used MDA5$^{-/-}$ mice generated on disparate genetic backgrounds [157] [158].

A link between the development of fulminant type I diabetes, a subset of type 1 diabetes characterized by rapid onset [159], and the sensing of CVB infection via RLRs has also been suggested. Both α- and β-cells in the pancreas of fulminant type I diabetics with enterovirus infection showed hyperexpression of RIG-I and MDA5 whereas non-fulminant diabetics without

enterovirus infections did not show this association [160]. However, the molecular basis for these results requires further study.

1.4 VIRUS-HOST CELL INTERACTIONS DURING CVB INFECTION

Section 1.1.2.2 introduced the extensive remodeling of the host cell effected by viral proteins in order to set up viral replication complexes. Here, the ways in which viral proteins, particularly viral proteases, alter host cell translation, cell death signaling, and innate immune signaling are thoroughly examined. These interactions are summarized in **Table 1**.

CVB Protein	Role in Interacting with Host Cell
$3C^{pro}$	Cleaves TRIF
$3C^{pro}$	Cleaves MAVS
$3C^{pro}$	Cleaves FAK
$2A^{pro}$	Cleaves PABP
$2A^{pro}$	Cleaves eIF4-G
2B	Inserts into ER membrane

Table 1. Virus-Host Cell Interactions

1.4.1 CVB and host cell translation

There is a significant body of work detailing the ability of the CVB proteases $2A^{pro}$ or $3C^{pro}$ to cleave a number of factors involved in host-cell transcription and translation. As CVB utilizes its own encoded polymerase to copy its genome and an IRES to initiate translation (section 1.1.2),

this allows the virus to disable host cell protein production while continuing to produce its own proteins [161]. Several host cell proteins required for the initiation of mRNA translation are cleaved directly by $2A^{pro}$, including eukaryotic initiation factor 4G (eIF4-G) [162, 163] and poly(A)-binding protein (PABP) [164]. In the case of poliovirus infection, proteins involved in the transcription of host cell genes are also targeted by viral proteases for cleavage, such as transcription factor IIIC (TFIIIC) [165], and the TATA-binding protein (TBP) [166]; it has not been interrogated whether TFIIIC and TBP are also targeted for cleavage during CVB infection, though the high degree of conservation among enteroviruses of the sequence identity and function of the virally-encoded proteases suggests that this is likely.

1.4.2 CVB and cell death signaling

Cell death can serve as a mechanism to eliminate intracellular pathogens before they complete their replication cycle. CVB possesses several mechanisms of delaying cell death, in order to counter the fact that CVB infection potently induces cell death pathways, as discussed in section 1.2. One such mechanism is through the manipulation the phosphatidylinositol 3-kinase (PI3K) signaling pathway, a pro-survival pathway activated by many viruses to delay or inhibit cell death [167]. CVB infection of HeLa cells leads to activation of PI3K and subsequent phosphorylation of downstream effector kinase, Akt (also known as protein kinase B). Inhibition of this pathway led to more apoptosis and decreased CVB release [168]. These data may be complicated by the additional role PI3K plays in regulating autophagy [169, 170], as effects on CVB release upon PI3K inhibition may additionally be due to inhibition of autophagy (section

1.7). One group showed that the PI3K/Akt pathways could be activated in CVB-infected HeLa cells through the action of interferon-γ-inducible GTPase (IGTP) [171], a protein upregulated in CVB-infected murine myocardial tissue [172]. Activating transcription factor 3 (ATF3) has been shown to sensitize HeLa cells to CVB-induced apoptosis, but CVB infection leads to an abrupt and significant reduction in ATF3 protein levels that serves to reduce cell death [173].

CVB-encoded proteases $2A^{pro}$ and $3C^{pro}$ can also directly target host proteins involved in cell death signaling for proteolytic cleavage and inactivation. For example, $3C^{pro}$ cleaves Toll/IL-1 receptor domain containing adaptor inducing interferon-beta (TRIF), a protein involved in apoptotic signaling, and inhibits its apoptotic functions [174]. Another example of a viral protein directly inhibiting cell death is the viral protein 2B. Expression of the CVB nonstructural protein 2B causes Ca^{2+} release through its ability to from pores in the ER membrane [175]. Because Ca^{2+} efflux from the ER and its subsequent influx into the mitochondria is known to cause apoptosis [176], it may seem that 2B would then be a pro-apoptotic protein. And indeed, in some cases viral proteins causing release of Ca^{2+} stores are pro-apoptotic [177]. However, 2B of CVB seems to prevent apoptosis through destruction of the Ca^{2+} gradients necessary for the cell to initiate intrinsic apoptosis [178, 179].

1.4.3 CVB and innate immune signaling

CVB targets both TLR and RLR signaling pathways for proteolytic cleavage upon infection. The CVB protease $3C^{pro}$ cleaves the TLR3 adaptor TRIF upon infection, as discussed in section 1.4.2, and the resultant TRIF fragments were non-functional [174]. MAVS is also targeted for cleavage

by $3C^{pro}$ and the cleavage fragments were functionally deficient in NF-κB and type I IFN signaling when compared to full-length MAVS, resulting in attenuation of IFNβ-signaling [174]. Finally, $3C^{pro}$ also targets the RLR signaling pathway through direct cleavage of focal adhesion kinase (FAK), which is recruited to mitochondria upon viral infection and potentiates MAVS signaling by an as-yet-undefined mechanism [180].

1.5 UNC93B AND TOLL-LIKE RECEPTOR TRAFFICKING

As introduced in section 1.3, TLRs are important PRRs involved in sensing both viral and bacterial infections. Tight regulation of TLR signaling is important, as aberrant TLR signaling, especially recognition of self-antigens, leads to a variety of disease states [181], including systemic lupus erythematosus (SLE) [182]. One key mechanism of regulation of TLR signaling is through the regulation of the subcellular localization of TLRs, as correct localization of TLRs can preclude the possibility of recognition of a self-antigen [183, 184]. Therefore, much work has been done to elucidate the mechanism of trafficking of TLRs. Here, the focus remains on trafficking of endosomal TLRs, those TLRs most relevant to the recognition of CVB infection (see section 1.3.1).

Upon initial synthesis, TLRs 3, 7, and 9 are inserted into the endoplasmic reticulum as transmembrane, full-length proteins [185-187]. In order for these TLRs to be functional, they must be both translocated to the endosome and proteolytically processed. This processing is carried out by acid-dependent proteases in the endolysosomal compartment [187-191]. Unlike

TLRs 7 and 9, which are primarily found in the ER in resting cells [185, 186], a significant pool of processed TLR3 is found in the endosome, ready to signal, in resting cells [187]. The mechanism for this differential regulation is not well understood.

The trafficking of these TLRs from the ER to the endosome, as well as the trafficking of TLR5 to the cell surface, is carried out by Unc93b, an ER-resident transmembrane protein [186, 192-195]. Unc93b serves as a chaperone, binding its client TLRs in the ER and trafficking them to their appropriate subcellular locations where they are then available to sense their cognate ligands [186, 196].

The function of Unc93b was initially discovered through a forward genetic screen in mice in which mice expressing a non-functional point mutant of Unc93b, (H412R), were shown to be sensitive to a diverse group of pathogens [192]. Unc93bH412R is incapable of binding its client TLRs [196] or exiting the ER [186, 197], resulting in cells that are not sensitive to endosomal TLR ligands.

The trafficking of TLR9 by Unc93b has been best studied. While it is likely that Unc93b traffics its other client TLRs using a similar mechanism, there is data to show that Unc93b is capable of discriminating between endosomal TLRs for trafficking purposes. For example, mutation of a single amino acid in the N-terminus of Unc93b favors trafficking of TLR7 over TLR9, suggesting selective trafficking by Unc93b [198, 199]. In the case of TLRs 3, 7, or 9, Unc93b binds its client TLR in the ER and mediates its transit from the ER to the Golgi compartment in coat protein II (COPII) vesicles [197]. From the Golgi, Unc93b-TLR9 complexes travel to the cell surface through an unspecified mechanism where a C-terminal Yxxϕ motif in Unc93b is necessary to recruit AP2, which serves to trigger endocytosis of the Unc93b-

TLR9 complex and results in endosomal TLR9 localization [197, 200]. Surprisingly, this AP2 recruitment was not necessary for TLR7 trafficking. Instead TLR7 itself seems to recruit AP4 directly while it is in the Golgi and uses this to traffic directly to the endosomal compartment [197]. TLR3 trafficking past the Golgi is not yet understood in any detail.

Unc93b function is important for the control of several important pathogens, including CVB. Mice expressing a non-functional Unc93b mutant were much more susceptible to CVB-induced myocarditis, for example [201]. By controlling the subcellular localization of endosomal TLRs, Unc93b sits at an important nexus of innate immune control, balancing the promotion of pathogen recognition with the prevention of self-antigen recognition.

1.6 RIP3-DEPENDENT NECROPTOSIS

A living cell may become a non-living cell in one of two ways—(1) the cell may be subject to such extreme mechanical or chemical forces that its internal architecture collapses in a completely non-regulated process, or (2) the cell may, through sensing of some component of its environment, initiate cell death utilizing genetically encoded pathways whose purpose is to end the life of the cell. The first type of cell death is considered ‘accidental cell death’, in contrast to the second type of cell death, known as ‘programmed cell death’ [202]. The concept of programmed cell death was tangentially introduced in section 1.2. Here, the focus is directly on the idea of programmed cell death, specifically necrotic programmed cell death. Death by apoptosis is the classical form of programmed cell death, which occurs by well-characterized,

tightly controlled signaling pathways [86, 203]. In contrast, necrosis was long considered to be a form of accidental cell death, with cell swelling leading to membrane rupture and an inflammatory spillage of cellular contents. However, in the past 15 years, evidence began to emerge that necrosis may be programmed, with genetically encoded pathways serving to execute necrotic death functions [204, 205]. Investigation into this hypothesis led to the discovery of receptor interacting protein kinase 3 (RIP3), the central kinase in programmed necrotic cell death, now referred to as necroptosis [202, 206-209]. Here, the role of RIP3 in necroptosis is introduced.

1.6.1 Cellular mechanisms of necroptosis

1.6.1.1 Activation of necroptosis. Necroptosis is defined as a RIP3-dependent form of regulated necrosis, which is sometimes also dependent on fellow receptor interacting protein kinase family member, RIP1 [202, 209]. Activation of necroptosis depends on phosphorylation of RIP3 and assembly of RIP3 into a signaling complex with either RIP1 or other partners. Here, the various mechanisms by which this process is known to be initiated are discussed.

Necroptosis was originally observed as a consequence of ligation of death receptor family members such as TNFR1 [205-208]. Though it is now understood that a variety of upstream triggers can lead to necroptosis, necroptotic signaling is still best characterized in the context of death receptor ligation. The ligation of TNFR1 by TNFα can result in three distinct outcomes for the cell. First, ligation of TNFR1 can lead to pro-survival, pro-inflammatory NF-κB signaling. Second, it can lead to apoptosis. Third, it can lead to necroptosis. This diversity of outcomes is

achieved by a series of signaling complexes whose assembly is dependent on cellular context. Upon ligation, TNFR1, a transmembrane cell surface receptor, recruits what is known as Complex-I, the core of which consists of the proteins TRADD (tumor necrosis factor receptor type 1-associated DEATH domain protein) [210], RIP1 [211], and TRAF2 (tumor necrosis factor receptor associated factor 2) [212, 213]. In Complex-I, RIP1 is in a ubiquitinated state [214] and this serves to initiate NF-κB signaling [215, 216]. The ubiquitination of RIP1 is carried out by cIAPs (cellular inhibitor of apoptosis proteins) [217-219]. The deubiquitination of RIP1 [220], which is carried out by the deubiquitinase CYLD (cylindromatosis) [221, 222], favors the disassembly of Complex-I and the assembly of Complex-II, which serves to initiate apoptotic signaling. This entails the dissociation of Complex-I from TNFR and the subsequent recruitment of FADD (Fas-associated protein with death domain) and caspase 8 to Complex-I [215]. Finally, inhibition of apoptosis through caspase inhibition leads to recruitment of RIP3 to Complex-II, which is now known as the necrosome or Complex-IIb, and the initiation of necroptosis [206-208].

Subsequent work showed that a necroptotic signaling complex can form in the absence of TNFR1 signaling. This spontaneously assembling complex, termed the ripoptosome, consists of RIP1, FADD, and caspase 8, much like Complex II. However, this complex forms in the absence of TNF signaling and instead requires depletion of cIAPs, which occurs during genotoxic stress, among other conditions. RIP3 can be recruited into this complex and this results in the initiation of necroptosis [223, 224].

Necroptosis has also been shown to occur downstream of a variety of pattern recognition receptors, with the term ripoptosome or necrosome also being applied to the necroptotic

signaling complex assembling downstream of these PRRs. TLR3 and TLR4 both utilize the adaptor protein TRIF to transduce their signals. TRIF can recruit RIP3 in a RIP1-independent manner, and this TRIF-RIP3 complex can induce necroptotic signaling [225, 226]. The cytoplasmic DNA sensor DAI is also capable of recruiting RIP3 in a RIP1-indepenent manner, resulting in necroptosis [227]. There is also some evidence showing that T cell receptor ligation on T cells may lead to necroptosis, though this is not as yet a well-developed area of research [228, 229].

Both type I IFN and type II IFN signaling can lead to necroptosis. Type I or II IFN signaling in MEFs and Type II IFN signaling in murine macrophages resulted in formation of the RIP1-RIP3 necrosome and subsequent necroptosis, though in MEFs necroptosis required destabilization of the FADD-RIP1 complex or caspase inhibition. Surprisingly, activation of the necrosome relied on phosphorylation of RIP1 by PKR [230]. A separate study also showed that type I IFN signaling resulted in necroptosis in murine macrophages, but in contrast to the previous study, this necroptosis was independent of PKR [231]. The mechanisms for IFN induced necroptosis remain to be clarified.

Finally, an interesting new study has shown that ER stress results in necroptosis dependent on both RIP1 and RIP3, though the mechanism for this induction is not clear [232].

Taken together, these data support a model by which a variety of stimuli converge on a single RIP3-dependent pathway to induce necroptosis.

1.6.1.2 Negative regulation of necroptosis. A number of studies in mouse models have shown that loss of proteins involved in extrinsic apoptosis leads to uncontrolled RIP3-dependent

necroptosis *in vivo*. This suggests that constitutive negative regulation of necroptosis is necessary for prevention of aberrant cell death.

The best characterized negative regulator of necroptosis is caspase 8 [233]. As detailed above, caspase 8 is recruited to Complex-II upon TNFR ligation, and is involved in the execution of apoptosis through cleavage of downstream effector caspases 3 and 7 [234, 235]. Recently it has been found that caspase 8 also cleaves RIP1 [218], RIP3 [236], and CYLD [237] to negatively regulate necroptosis [233]. Caspase 8 is itself regulated by cFLIP (cellular FLICE-inhibitory protein), which exists in two isoforms, $cFLIP_S$ and $cFLIP_L$ [238]. Both $cFLIP_S$ and $cFLIP_L$ inhibit caspase-8 mediated initiation of apoptosis through formation of a heterodimer with caspase 8, preventing the caspase 8 homodimerization that is necessary for autoprocessing and apoptosis activation [238]. The $cFLIP_S$-caspase 8 heterodimer is also incapable of disabling the necroptotic pathway. However, the $cFLIP_L$-caspase 8 heterodimer is still competent to proteolyze local substrates, such as RIP1, RIP3 and CYLD, an event that does not require autoprocessing of caspase 8 [233, 239, 240]. Together, these data suggest a complex situation of regulation in which caspase 8, through its proteolytic activity, negatively regulates necroptosis, and the presence of cFLIP isoforms regulates the proteolytic activity of caspase 8.

The importance of caspase 8 in restricting necroptosis is underlined in evidence from mouse models lacking caspase 8 or its fellow Complex-II proteins, FADD and cFLIP. Caspase $8^{-/-}$ mice are not viable and experience massive necrotic cell death during embryogenesis, but caspase-$8^{-/-}$/$RIP3^{-/-}$ mice are viable [241]. Similarly, mice lacking FADD in their intestinal epithelial cells ($FADD^{IEC\text{-}KO}$) exhibit spontaneous pathologies in the colon due to necrotic cell death of the epithelium, but $FADD^{IEC\text{-}KO}$/$RIP3^{-/-}$ mice do not exhibit such pathologies [242]. This

does not seem to be a cell-type specific phenomenon, as mice lacking FADD in their epidermal keratinocytes exhibit similar RIP3-dependent necroptotic phenotypes in those cells [243].

IAP family members cIAP1, cIAP2, and XIAP (X-linked IAP) also negatively regulate necroptosis [223, 224, 244]. While these proteins are known to ubiquitinate RIP1, recent evidence has shown that they may also ubiquitinate RIP3 in order to repress necroptosis [245].

Surprisingly, recent evidence has emerged that RIP1 negatively regulates necroptosis under certain circumstances, though RIP1 is required for and positively regulates TNFα-mediated necroptosis, as discussed above. $RIP1^{-/-}$ mice die soon after parturition, as do $RIP1^{-/-}$/caspase $8^{-/-}$ and $RIP1^{-/-}/RIP3^{-/-}$ mice, but it was observed that $RIP1^{-/-}/RIP3^{-/-}$/caspase $8^{-/-}$ mice are viable [246-248]. This observation led to further characterization of the role of RIP1, and it was found that while RIP1 kinase activity is indeed required for TNFα-mediated necroptosis, RIP1 has an alternate, kinase-independent function of inhibiting TRIF-mediated, IFN-mediated, and spontaneous necroptosis [246, 247, 249].

Recently, Ppm1b, a phosphatase that dephosphorylates RIP3 to negatively regulate necroptosis, was discovered [250]. Loss of Ppm1b led to spontaneous necroptosis [250], and $Ppm1b^{-/-}$ mice are not viable [251] indicating that Ppm1b regulates RIP3 under resting conditions.

1.6.1.3 Necroptosis signaling. The diversity of RIP3-containing complexes detailed above necessitates an explanation of how such diverse complexes are all capable of initiating necroptosis. One key to activation of necroptosis is the structure of the RIP3 complexes formed. RIP3 contains a RIP homotypic interaction motif (RHIM) domain, a protein-protein interaction

motif capable of associating with other RHIM domains [252]. RIP1, TRIF, and DAI, all of which are capable of complexing with RIP3 to induce necroptosis, all also contain RHIM domains [252-255]. RIP1 and RIP3 form RHIM domain dependent amyloid filamentous complexes containing many RIP1-RIP3 heterodimers [256]. RIP3 in these amyloid fibrils further recruits free RIP3 molecules and autophosphorylation of RIP3 then serves to potentiate signaling [257].

Once RIP3 is activated by phosphorylation of Ser-227 [258] within necrosomes [256], it physically associates with the pseudokinase mixed lineage kinase domain-like protein (MLKL) [259]. RIP3 then phosphorylates MLKL at Thr-357 and Ser-358 [258]. The interaction between RIP3 and MLKL is necessary for the prevention of accumulation of non-functional RIP3 aggregates as well as translocation of the necrosome to the mitochondria-associated membrane (MAM), from whence it potentiates its signaling [260]. The formation of this RIP3-MLKL complex is key to downstream events, as blocking its formation inhibits necroptosis [258].

1.6.1.4 Necroptosis effector mechanisms. It was initially thought that cell death upon necroptosis was mediated by the generation of reactive oxygen species (ROS) with activation of MLKL being a secondary mechanism. However, data showing that $MLKL^{-/-}$ mice were completely resistant to TNFα-induced necroptosis established MLKL activation as the key effector mechanism of necroptosis [261, 262]. Later data showed that ROS production was not necessary for necroptosis but often accompanies it [263]. Instead, death is effected during necroptosis by clustering of activated MLKL into tetramers or trimers which then translocate to lipid rafts of the plasma membrane through a domain that interacts with phosphatidyl inositol phosphates [264-266]. Phosphorylation of MLKL serves to effect a structural rearrangement of

MLKL, allowing the formation of a pore through which uncontrolled ion efflux can lead to plasma membrane rupture [267, 268]. There is also some evidence that MLKL oligomers may interact with the Ca^{2+} channel protein transient receptor potential cation channel, subfamily M, member 7 (TRPM7) to lead to Ca^{2+} influx [265]. The importance of MLKL-mediated necroptosis was confirmed *in vivo*; animal models have suggested that necroptosis is a key pathway in drug-induced liver injury [269], and liver biopsies of human patients suffering from drug-induced liver injury showed significant increases in phosphorylated MLKL by immunohistochemistry [270]. The best-characterized mechanisms of RIP3-dependent necroptosis are summarized in Figure 3.

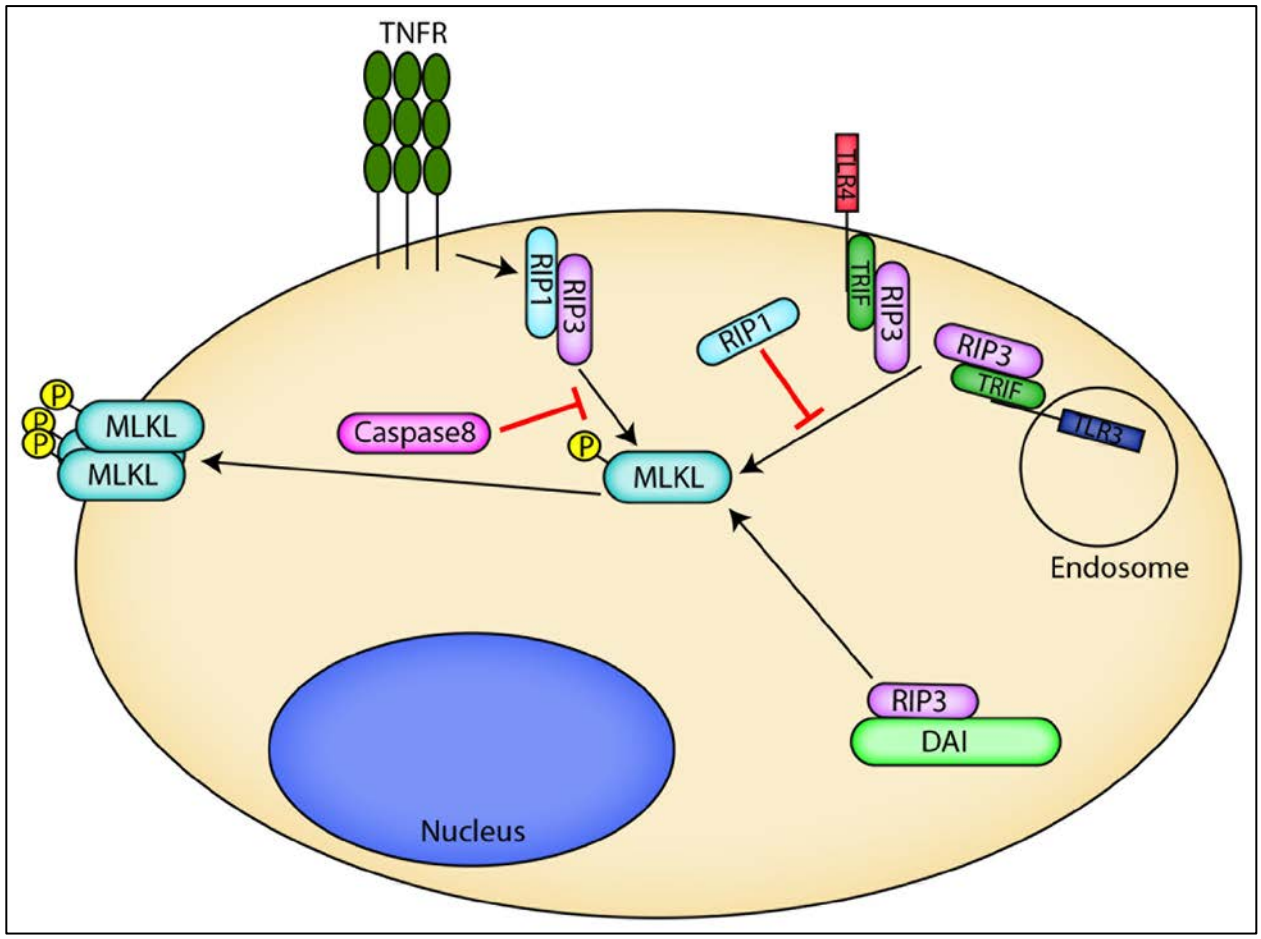

Figure 3. Cellular Mechanisms of Necroptosis

RIP3 mediates necroptosis downstream of diverse stimuli, including ligation of TNFR, TLR3, TLR4, and DAI. This results in phosphorylation of MLKL and translocation of trimerized or tetramerized MLKL to the plasma membrane where it forms a pore, facilitates ion dysregulation, and leads to compromise of the plasma membrane. The yellow-circled P represents a phosphate group.

1.6.2 Necroptosis and microbial infections

Cell death pathways are a key part of host defense against pathogens, and, accordingly, necroptosis has been shown to play an important role in many microbial infections. However, work in this field has been complicated by the discovery of an alternative RIP1-RIP3 pathway, which leads not to necroptosis but instead to inflammasome activation. This pathway is activated by various stimuli, including RNA virus infection, and is effected by the RIP1 substrate DRP1 (dynamin related protein 1) through a mechanism involving mitochondrial damage and ROS generation [271]. This could explain early data suggesting that necroptosis was effected by ROS generation; it is possible this alternative pathway was being activated concurrently with necroptosis in those cases.

Despite this complication, it is clear that necroptosis itself is also important in the control of several pathogen infections. The best developed line of evidence for this has to do with murine cytomegalovirus infections (mCMV). mCMV encodes a structural protein, known as M45 or vIRA (viral inhibitor of RIP activation), that contains a RHIM domain and can interact with with RIP1 and RIP3 [272]. Upon infection, mCMV triggers a necroptotic pathway that is dependent on DAI and RIP3 [227]; however, this pathway is inhibited by vIRA interaction with RIP3 through its RHIM domain [273]. Necroptosis seems to be key to control of mCMV

infection, as mice infected with mCMV expressing vIRA with a mutated RHIM domain that cannot inhibit necroptosis completely control infection, whereas $RIP3^{-/-}$ mice infected with mutant mCMV cannot control the infection [227]. Human CMV infections also inhibit necroptosis through a distinct mechanism that acts at an unknown point downstream of MLKL activation [274].

HSV-1 infection in mice also induces necroptosis. In this case, infected cell protein 6 (ICP6), a RHIM-domain containing viral protein, binds directly to RIP3 to assemble a signaling complex and drive necroptosis [275]. However, in humans, ICP6 also forms complexes with RIP3, but instead of driving necroptosis, this disrupts the formation of the necrosomes and prevents necroptosis [276, 277]. This fascinating difference between human and mouse necroptotic pathways underlines the need for use of appropriate models when studying this system.

There is also evidence that influenza infection is capable of triggering necroptosis in the respiratory epithelium, as $cIAP2^{-/-}$ mice died from sublethal doses of influenza due to necroptosis [278].

Necroptosis is also important in the control of vaccinia virus (VV) infection. $RIP3^{-/-}$ mice exhibited reduced inflammation and higher viral titers in response to VV infection, eventually succumbing to a sublethal dose [208]. Interestingly, VV encodes a caspase inhibitor [279]; this may explain one mechanism by which necroptosis is induced.

There is also evidence of necroptosis during bacterial infections. *Salmonella* typhimurium induces type I IFN dependent necroptosis in macrophages upon infections; this actually leads to impaired control of the infection, as interferon α/β receptor $(IFNAR)^{-/-}$ mice

exhibited better control of infection [280]. β-toxin produced by *Clostridium perfringens* also is able to induce a form of cell death that is likely necroptosis [281].

1.6.3 Necroptosis in human physiology

Since the delineation of necroptotic signaling, it has been shown that necroptosis plays an important role in diverse human pathologies involving aberrant tissue death. Many diseases of the eye involving cell death are mediated by necroptosis. Cone cell degeneration during retinitis pigmentosa (RP) is caused by necroptosis, as a $RIP3^{-/-}$ mouse model of RP did not show signs of cone cell death [282]. Cell culture models have also shown that oxidative stress induced cell death of retinal pigment epithelial cells, characteristic of late-stage age-related macular degeneration, is necroptotic in nature [283].

There is also evidence of intestinal pathologies caused by necroptosis. Mouse models show that loss of caspase 8 in intestinal epithelial cells leads to high susceptibility to colitis due to enhanced necroptosis [284]. Additionally, biopsies of the terminal ileum of patients with Crohn's disease showed increased necroptosis of Paneth cells [284] and children with irritable bowel disease show increased protein levels of RIP3 and MLKL and decreased levels of caspase 8 [285].

In addition to these pathologies, there is considerable evidence that other organs experience necroptotic cell death that contributes to disease or injury, including the liver [269, 270, 286] and the skin [287, 288]. Systemic TNFα-mediated shock is also dependent on necroptosis [289, 290].

Taken together, the current literature suggests that RIP3-mediated necroptotic cell death is a pathway activated downstream of diverse stimuli, including death receptor ligation, PRR signaling, and IFN signaling. It is constitutively negatively regulated by caspase 8 and RIP1, and release of these regulations can result in spontaneous necroptosis. Mechanistically, necroptosis results in phosphorylation of MLKL and insertion of MLKL into membranes to form pores, resulting in eventual membrane rupture. This process is relevant in the control of a variety of microbial infections, and is active in diverse pathologies involving aberrant cell and/or tissue death.

1.7 AUTOPHAGY

Macroautophagy (hereafter, autophagy) is an evolutionarily conserved process by which cytoplasmic contents are degraded and their components recycled for reuse by the cell [291]. Here the mechanisms of autophagic initiation and flux are detailed, the data regarding the source of autophagic membranes are explored, and the methods by which autophagy is measured experimentally are discussed. Additionally, data surrounding the role of autophagy during pathogen infection, specifically CVB infection, are discussed.

1.7.1 Mechanisms of Autophagy

Autophagy can be categorized into selective and non-selective forms, characterized by degradation of bulk cytoplasmic contents or targeted degradation of specific organelles and cytoplasmic contents, respectively [292]. Selective autophagy is further subdivided into categories based on the identity of what is selectively degraded, including mitophagy (mitochondria) [293], pexophagy (peroxisomes) [294], and xenophagy (intracellular pathogens) [295]. This process has been thoroughly studied in yeast model systems, and many of the autophagy related proteins are conserved in mammalian systems [296].

Constitutive autophagy is important in the maintenance of cell health, and maintenance of basal levels of autophagy appears to be especially important in neurons [297]. Additionally, the induction of autophagy is an important response to a variety of cell stressors. Starvation is the classical stimulus of autophagy, with both glucose starvation [298] and amino acid starvation [299] resulting in rapid activation of autophagy through distinct mechanisms. Additional circumstances can also lead to the induction of autophagy, including oxidative stress [300], ER stress [301], or organellar damage [302].

In brief, the autophagic process consists of the formation of a phagophore, a double-membraned structure, which then expands and engulfs cytoplasmic contents. This structure, now known as an autophagosome, fuses with a lysosome, a degradative compartment, to effect the degradation of its contents. There is a core autophagy machinery that is required for the initiation of all subtypes of autophagy. This machinery consists of the unc-51 like kinase (ULK) complex, a regulatory complex involved in initiation, the autophagosome-related 9 (Atg9) complex,

required for membrane recruitment, the PI3K complex, required for nucleation of the phagophore, and ubiquitin-like (Ubl) conjugation systems, required for expansion of the phagophore [303]. The source of the membranes that form the phagophore is a key question in the field of autophagy research. Much focus has been placed on the ER as a source of autophagosome membranes, with mounting evidence that the ER, including ER-mitochondria contact points, ER exit sites, and the ER-Golgi intermediate complex (ERGIC), is a major source of membranes [304]. However, there is also evidence that other sources, including the Golgi and recycling endosomes, may play a role [305]. Once the autophagosome has been established, it must then fuse with a degradative compartment, the lysosome. This fusion is mediated by a soluble NSF attachment protein (SNAP)- SNAP receptor (SNARE) system [306] requiring the interaction of syntaxin 17 on the autophagosome [307] and vesicle-associated membrane protein 8 (VAMP8) on lysosomes [308].

The recruitment of specific cargo into autophagosomes to carry out selective autophagy is primarily accomplished through the action of p62, otherwise known as sequestosome 1 (SQSTM1) [309]. p62/SQSTM1 physically interacts with both ubiquitinated proteins destined for autophagosomal degradation and the autophagosomal-membrane associated protein light chain 3 B (LC3B) [310]. Other cargo can be targeted to the autophagosome by a similar method utilizing different adaptor proteins.

There are a number of experimental methods by which autophagy can be detected and measured. The initiation of autophagy results in the lipidation of LC3B, allowing its association with the autophagosomal membrane [311]. This lipidation can be detected by immunoblotting the results of a reducing polyacrylamide gel electrophoresis (SDS-PAGE), as non-lipidated

LC3B (LC3B-I) is detected at ~18 kD whereas lipidated LC3B (LC3B-II) is detected at ~16 kD [312]. Additionally, autophagy can be detected by electron microscopy due to the appearance of characteristic double-membraned vesicles [312]. Autophagy can also be detected by measuring the accumulation of autophagosomes by immunofluorescence microscopy to detect LC3B or p62/SQSTM1 punctae [312]. Finally, autophagic flux, or completion of the autophagic pathway, can be detected by the degradation of p62/SQSTM1; this can be measured by examining protein levels by immunoblot [312]. Proper application of these techniques is key to productive study of autophagic pathways.

1.7.2 Autophagy and CVB infection

Autophagy is largely considered an antimicrobial process. Innate immune signaling can induce autophagy, and diverse intracellular pathogens are shuttled to autophagosomes for degradation in a process known as xenophagy [295]. However, there are certain pathogens, particularly RNA viruses, which have evolved to take advantage of autophagy and utilize it to aid in their own replication [313]. Here, the ways in which CVB is known to interact with autophagic pathways are discussed.

Blocking autophagy *in vitro* [314] or *in vivo* [315] reduces CVB replication. There has been much research into the ways in which autophagy is subverted by CVB for its replication. It has long been noted that enteroviral replication occurs on membranous structures [316], and that enteroviral infection results in massive rearrangement of host membranes to form these structures [317]. It has been proposed that autophagic pathways provide the membranes for these

viral replication complexes [318, 319], explaining the requirement of autophagy by CVB. Whether CVB requires only autophagic initiation or benefits from autophagic flux remains unclear. Studies in non-polarized cells have suggested that whereas autophagosome formation and initiation of the autophagic pathway is utilized by CVB for replication, autolysosomal fusion is dispensable [314]. However, recent studies from our laboratory have shown that in polarized endothelial cells, complete flux through the autophagic pathway may be beneficial for CVB infection [320]. It is clear, however, that induction of autophagy benefits CVB replication.

2.0 UNC93B INDUCES CELL DEATH AND IS CLEAVED BY CASPASES AND AN ENTEROVIRAL PROTEASE

2.1 INTRODUCTION

Unc93b is an ER-resident transmembrane protein that is required for signaling from endosomally localized TLRs as well as TLR5, a cell surface receptor [192-195]. The importance of Unc93b and its client TLRs in initiating immune responses to viral infections was underscored when it was discovered that children inheriting two autosomal recessive mutant alleles of Unc93b that produce a non-functional, truncated version of the protein developed Herpes Simplex Encephalitis (HSE), a rare but serious viral encephalopathy, after Herpes Simplex Virus-1 (HSV-1) infection [321]. An increased risk of HSE after HSV-1 infection is also seen in children with autosomal dominant mutations in TLR3 [322], suggesting that the trafficking of TLR3 by Unc93b is crucial for the control of HSV-1 infection. Additionally, it was shown that patients with SLE had higher levels of Unc93b expressed in immune cells than in healthy control patients, suggesting that high levels of Unc93b are responsible for the dysregulated TLR signaling known to be associated with SLE pathogenesis [323]. Thus, Unc93b is important in

both innate immune defense against pathogens and in the development of autoimmunity in humans.

In addition to TLR-mediated signaling, the induction of cell death is a powerful innate immune pathway by which host cells protect themselves from microbial infections. Indeed, many components of TLR-mediated signaling also participate in the induction of pro-apoptotic signaling in response to viral infections, underscoring the importance of these pathways in host defense. For example, TRIF, the TLR3/4 adaptor, potently induces apoptosis via its RHIM domain located in its C-terminus [253, 324].

TLR3 is considered to be the critical TLR in sensing the presence of CVB, an enterovirus that is a leading cause of myocarditis. Humans who develop myocarditis after enteroviral infections have increased frequencies of SNPs in TLR3 that render them less responsive to TLR3 ligands [149], and $TLR3^{-/-}$ mice show increased mortality and myocarditis in response to CVB infection [147]. These data suggest that TLR3 senses the dsRNA intermediate produced during CVB replication, and that this sensing and subsequent activation of innate immune signaling is key to the control of CVB infection. Indeed, recent work has shown that $Unc93b1^{LETR/LETR}$ mice, which have a loss of function mutation in the gene encoding Unc93b, exhibit increased mortality upon CVB-induced myocarditis due to higher viral titers and dysregulation of inflammation in these mice [201].

CVB utilizes cell death-mediated destruction of the host cell membrane for its egress. However, the virus must balance cell death induction precisely during its replication as activating cell death prematurely, or by alternative pathways, could inhibit replication and/or induce inflammatory signaling. CVB commonly induces apoptosis in many cell types to facilitate its

egress [93, 110, 325]. The mechanisms by which CVB modulates cell death signaling are likely complex and involve the alteration of many components associated with this pathway. CVB commonly alters host cell signaling, including TLR and cell death signaling, by the direct cleavage of host proteins by the $2A^{pro}$ and $3C^{pro}$ virally encoded cysteine proteases [104, 174].

Interestingly, analysis of microarray data [201] using the database for annotation, visualization and integraded discovery (DAVID), a bioinformatics tool from the National Institute of Allergy and Infectious Diseases (NIAID) [326, 327], from cardiac tissue of wild-type mice found that there was a significant enrichment in expression of genes involved in cell death as compared to $Unc93b1^{LETR/LETR}$ mice ($p=0.0051$). Given that Unc93b is directly linked to CVB-induced pathogenesis *in vivo*, we examined whether Unc93b was involved in cell death signaling during infection. We found that ectopic expression of Unc93b robustly induced apoptosis, and that this induction required its exit from the ER as the H412R mutant of Unc93b lacking this function was incapable of inducing cell death. In addition, we found that caspases activated by TNFα signaling, or by the induction of TRIF-mediated TLR3 signaling, cleaved Unc93b at a single site (position D27) located within its N-terminus. Additionally, we found that the CVB-encoded protease $3C^{pro}$ also cleaved Unc93b at a single site within 10 amino acids of the caspase cleavage site (position Q17). Collectively, these studies point to a previously uncharacterized role for Unc93b in the initiation of apoptosis during TLR3 signaling and suggest that both host and viral proteases target the N-terminus of Unc93b to alter some aspect of its function.

2.2 RESULTS

2.2.1 Expression of Unc93b induces cell death

The overexpression of several components associated with innate immune signaling, including the TLR3 adaptor TRIF, potently induces apoptosis [253, 328, 329]. We found that ectopic expression of Unc93b in 293T cells consistently induced significant morphological changes in transfected cells, resulting in cell rounding, disruption of cell monolayers, and other signs of cell stress/death (**Figure 4A**). To further investigate these morphological changes, we measured cell viability based on quantitation of ATP through a luminescent detection method (Cell Titer Glo) and found that Unc93b overexpression significantly decreased cell viability (**Figure 4B**). Additionally, we found that Unc93b expression also enhanced cell death induced upon treatment with staurosporine, an apoptosis inducer (**Figure 4B**). To identify the cell death pathway(s) initiated by Unc93b, we determined the impact of Unc93b overexpression on propidium iodide (PI) uptake and Annexin V binding by flow cytometry. We found that Unc93b specifically induced apoptotic cell death and led to an ~3-fold increase in the levels of PI- and Annexin V-positive cells. (**Figure 4C, 4D**). Additionally, we found that the induction of cell death was partially sensitive to caspase inhibition, as treatment of cells with the pan-caspase inhibitor zVAD-fmk was sufficient to block Unc93b induced morphological changes associated with cell death and caused a mild reduction in PI- and Annexin V-positive cells that did not reach statistical significance (**Figure 4F, 4G, 4H**). Of note, the frequency of PI-positive cells was not

reduced by zVAD-fmk treatment, suggesting that upon blockage of caspase-dependent pathways, alternative pathways may be activated (data not shown).

The H412R mutant of Unc93b has been well characterized for its inability to bind TLRs [196], facilitate TLR signaling [192], or traffic out of the ER [186, 197]. To determine whether these functions were also required for the apoptosis-inducing properties of Unc93b, we determined the effect of Unc93b H412R expression on apoptosis using the assays described above. Importantly, we found that the H412R mutant of Unc93b did not induce morphological changes when overexpressed in 293T cells (**Figure 4A**), did not alter cellular ATP levels (**Figure 4B**), and did not induce apoptosis as assessed by flow cytometry, despite equivalent levels of expression (**Figure 4C, 4D, 4E**). Taken together, these data implicate a previously uncharacterized role for Unc93b in the induction of apoptosis and suggest that its ability to traffic from the ER is required for this function.

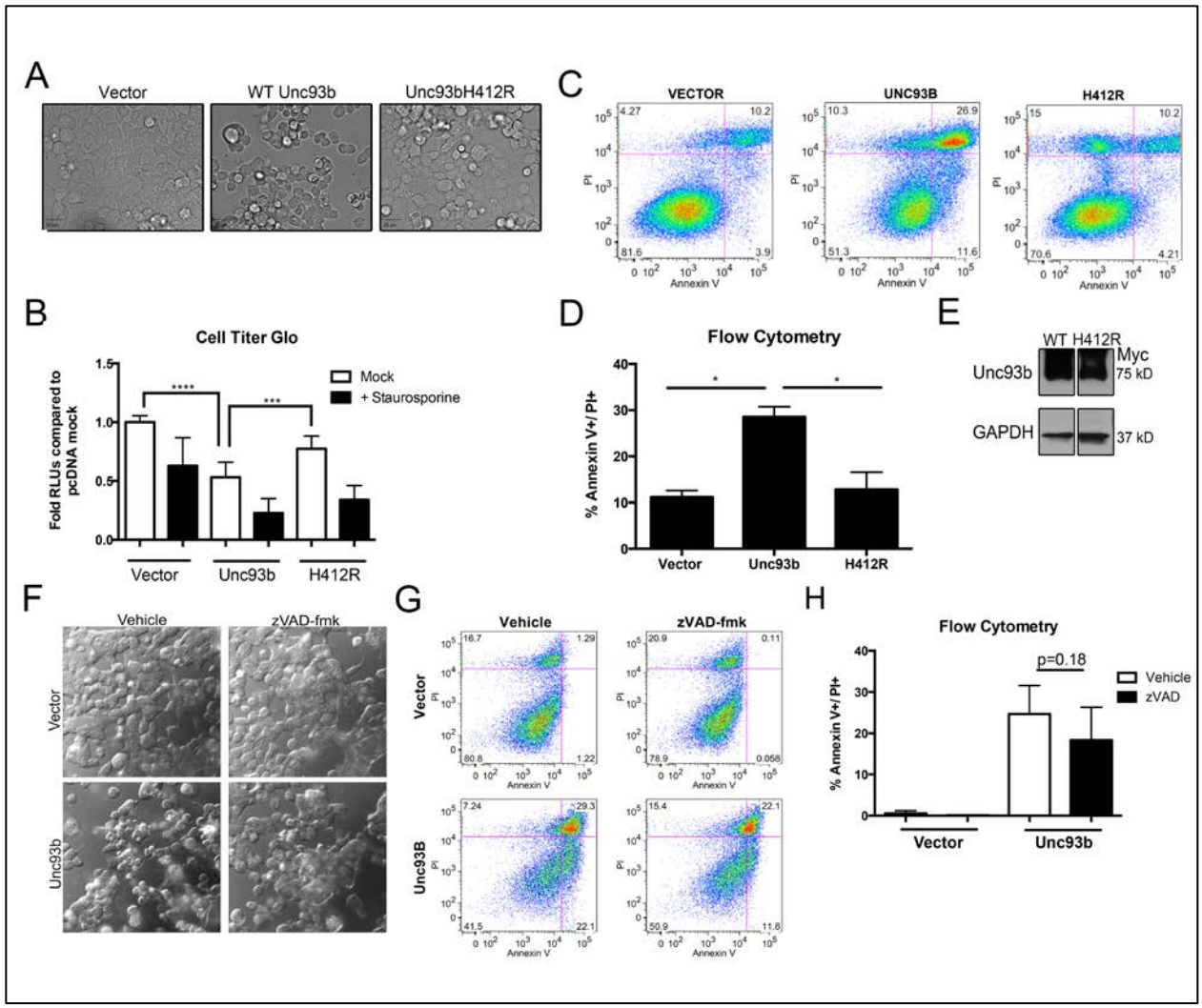

Figure 4. Unc93b expression induces apoptotic cell death.

(A-H) 293T cells were transfected with WT or H412R Unc93b containing a C-terminal Myc tag (A) 48 hours post-transfection, differential interference contrast (DIC) images were obtained from live cells. (B) 48 hours post-transfection, cells were treated with staurosporine for 24 hours and cell death was measured by Cell Titer Glo assay. Data shown is an average of 6 experiments. (C) 72 hours post-transfection, cells were stained with Annexin V and PI and analyzed by flow cytometry. Data shown are representative of 4 experiments. Cell population was determined by gating events on Forward Scatter (FSC) and Side Scatter (SSC). Cells were then gated based on Annexin V and PI staining intensities. (D) 48-72 hours post-transfection, cells were stained with Annexin V and PI and analyzed by flow cytometry as in 4C, and Annexin V+/PI+ populations were compared. Data shown are representative of 4 experiments (E) 293T cells were transfected in parallel with those shown in 4D, lysates were harvested and then subjected to immunoblotting with anti-Myc or -GAPDH antibodies. (F) Prior to transfection (1 hour) cells were treated with zVAD-fmk and then transfected with the indicated constructs for 48 hours (in zVAD-fmk-containing medium). Approximately 48 hours post-transfection, DIC images were obtained from live cells. (G-

H) Prior to transfection (1 hour) cells were treated with zVAD-fmk and then transfected with the indicated constructs for 72 hours (in zVAD-fmk-containing medium). 72 hours post-transfection cells were stained with Annexin V and PI and analyzed by flow cytometry as in 4C. Data shown are representative of 2 experiments (G) or average of 2 experiments (H).

2.2.2 Unc93b is cleaved by caspases

Because we observed a role for Unc93b in the induction of apoptosis, we next examined whether Unc93b is regulated by caspase-mediated cleavage during apoptotic cell death as a negative feedback mechanism to attenuate its function in cell death signaling. To do this, we activated caspases via TNFα treatment and determined whether this treatment led to the proteolytic cleavage of Unc93b. For these studies, we utilized an N-terminal EGFP fusion construct of Unc93b overexpressed in 293T cells. We found that activation of caspases through TNFα treatment induced the appearance of an ~33 kD N-terminal GFP-fused cleavage fragment of Unc93b when assessed by immunoblotting (**Figure 5A**). The quantity of this cleavage fragment was enhanced when cells were treated with TNFα in the presence of the NF-κB inhibitor JSH-23 (**Figure 5A**). By immunoblotting, Unc93b appears as a major species band and a high molecular weight 'smear', consistent with reports that Unc93b is ubiquitinated [330]. Importantly, Unc93b cleavage was inhibited by the addition of a pan-caspase inhibitor, zVAD-fmk, confirming the role of caspases in this cleavage event (**Figure 5A**). Caspase activation was confirmed by detection of cleaved poly ADP ribose polymerase (PARP), a classical caspase substrate [331] (**Figure 5A**). Using a caspase cleavage site detection algorithm [332], we identified two potential caspase cleavage sites (D21 and D27) within the N-terminus of Unc93b that would induce the appearance of the ~33kD N-terminal GFP-fused cleavage product by immunoblot. We found that

site-directed mutagenesis of D27 to alanine (D27A) completely inhibited the caspase-dependent cleavage of Unc93b (**Figure 5A**). Thus, we conclude that D27 is the only site within Unc93b targeted by caspases.

Sustained signaling through TLR3 can result in caspase-mediated cell death [333]. As Unc93b is necessary for TLR3 signaling, we postulated that TLR3-dependent caspase activation might also result in Unc93b cleavage via the activation of caspases. To test this, we overexpressed the TLR3 adaptor protein TRIF, which induces TLR3 signaling, and found that TRIF overexpression resulted in Unc93b cleavage in a caspase dependent manner at residue D27 (**Figure 5B**). TRIF-mediated caspase activation has been shown to be dependent on its C-terminal RHIM domain [253]. To determine whether this domain was required for the TRIF-induced cleavage of Unc93b, we expressed an N-terminal construct of TRIF lacking the RHIM domain (NT) or a C-terminal construct containing the RHIM domain (CT). We found that expression of the C-terminus of TRIF alone was sufficient to induce Unc93b cleavage and that this cleavage occurred at position D27 as cleavage was absent in the D27A mutant of Unc93B (**Figure 5C**). Collectively, these data show that Unc93b is targeted by cellular caspases at position D27 during apoptosis induced by TNFα and by TLR3-TRIF signaling.

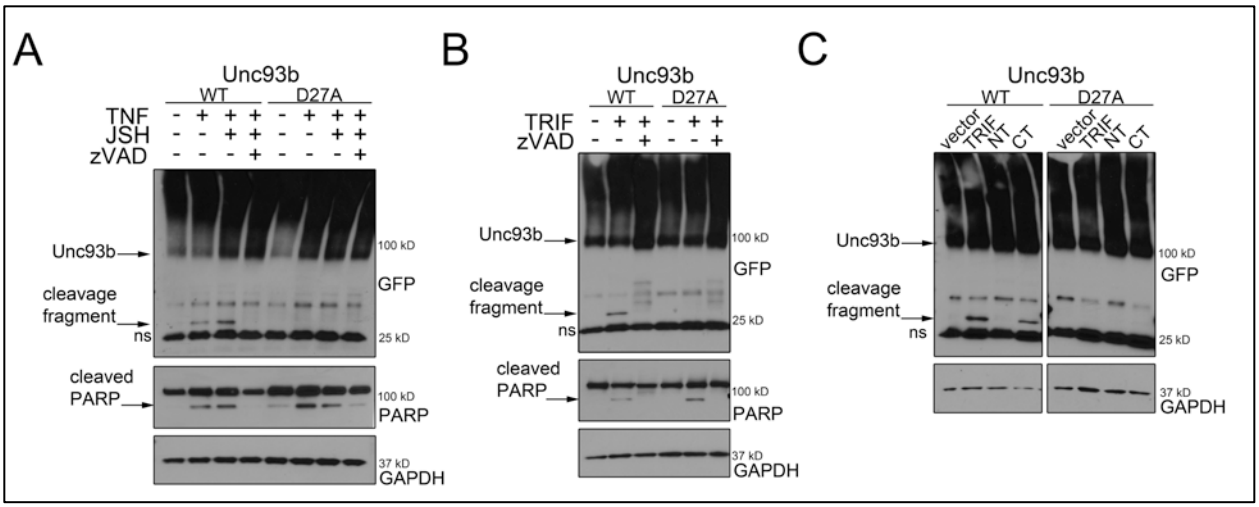

Figure 5. Unc93b is cleaved by caspases during apoptosis.

(**A**) 293T cells were transfected with the indicated eGFP-fused Unc93b construct and 48 hours post-transfection cells were treated with TNFα, JSH-23, and Z-VAD-FMK (or mock control) for 18 hours, lysates were harvested and subjected to immunoblotting with anti-GFP, -PARP, or -GAPDH antibodies. (**B**) 293T cells were transfected with the indicated eGFP-fused Unc93b constructs and HA- Flag dual-tagged TRIF and treated with zVAD-fmk 6 hours post-transfection. Lysates were harvested 48 hours post-transfection and subjected to immunoblotting with anti-GFP, -PARP, and –GAPDH antibodies. (**C)** 293T cells were transfected with the indicated eGFP-fused Unc93b and Flag-tagged TRIF constructs (Full-length, N-terminal or C-terminal); lysates were harvested 48 hours post-transfection and subjected to immunoblotting with anti-GFP and -GAPDH antibodies. In all panels, ns denotes nonspecific bands.

2.2.3 Unc93b is cleaved by the CVB virally-encoded protease $3C^{pro}$

Many viruses induce apoptosis during their infectious life cycles. In some cases, this induction is an innate immune response induced by the host cell in order to clear the viral infection whereas in other cases, viruses utilize the induction of cell death to promote their egress. Enteroviruses such as CVB often induce apoptosis to disrupt the host cell membrane to facilitate egress. Because we found that caspases cleaved Unc93b during apoptotic cell death in response to TNFα treatment and TRIF signaling, we next assessed whether this cleavage might also occur during

viral infection. Using 293T cells overexpressing N-terminal EGFP-fused Unc93b, we detected the appearance of an ~30 kD N-terminal GFP-fused cleavage fragment of Unc93b in CVB-infected cells by immunoblotting (**Figure 6A**). We found that the D27A mutant of Unc93b was not protected from CVB-induced cleavage, suggesting that other viral and/or cellular factors were responsible for cleavage of another site(s) within Unc93b (**Figure 6C**). CVB is known to utilize virally encoded proteases to target host proteins [107]. Using an algorithm designed to detect the semi-conserved consensus cleavage sites for the two CVB-encoded proteases $2A^{pro}$ and $3C^{pro}$ [334], we identified a putative $3C^{pro}$ cleavage site in Unc93b at residue Q17, which would be predicted to produce an N-terminal GFP-fused fragment consistent with that observed during CVB infection. In contrast, Unc93b did not contain any consensus $2A^{pro}$ cleavage sites. We found that overexpression of wild-type (WT) CVB $3C^{pro}$, but not a catalytically inactive mutant lacking protease activity (C147A), induced the appearance of the ~30kD N-terminal cleavage fragment of EGFP-fused Unc93b (**Figure 6B**). By performing site-directed mutagenesis, we found that $3C^{pro}$ specifically targeted residue Q17 in the N-terminus of Unc93b as a mutant of this site (Q17A) completely resisted cleavage (**Figure 6B**). We confirmed that Q17 was the sole site responsible for the cleavage of Unc93b during CVB infection by infecting 293T cells expressing either the Q17A or caspase-resistant D27A Unc93b mutants and assessing their cleavage sensitivity during infection. (**Figure 6C**). These data suggest that although caspases are activated during CVB infection, Unc93b is targeted for cleavage by the virally-encoded $3C^{pro}$ CVB protease.

As TLR3 signaling has been established as an important step in the initiating an immune response to CVB, we next assessed the possibility that $3C^{pro}$-mediated cleavage of Unc93b

effects its ability to facilitate TLR3 signaling. To do this, we generated a truncation mutant of Unc93b missing the first 17 N-terminal amino acids (Unc93bΔ17, schematic **Figure 7A**), which is representative of the C-terminal fragment of Unc93b that remains in the cell following cleavage by $3C^{pro}$. We determined the effect of expression of Unc93bΔ17 on IFNβ induction downstream of TLR3, an endosomal TLR entirely dependent on Unc93b for its endosomal trafficking [186, 196]**.** We treated HEK293 cells stably expressing TLR3, and transiently expressing a firefly luciferase construct downstream of the IFNβ promoter, with poly(I:C), a synthetic TLR3 ligand, and examined TLR3 activation in the presence or absence of WT-, Δ17-, or H412R-Unc93b by measuring luciferase levels. We found that expression of WT Unc93b enhanced TLR3 signaling, whereas Unc93bH412R did not. However, TLR3 signaling upon expression of Unc93bΔ17 was not significantly different than WT Unc93b (**Figure 6D**), indicating that the ability of Unc93b to facilitate TLR signaling is not affected by $3C^{pro-}$mediated cleavage. Although we observed that expression of Unc93bΔ17 trended towards a lower level of TLR3-mediated IFNβ induction than WT Unc93b, this effect was not statistically significant, suggesting that any defect in facilitating TLR3 signaling is mild and likely not biologically relevant.

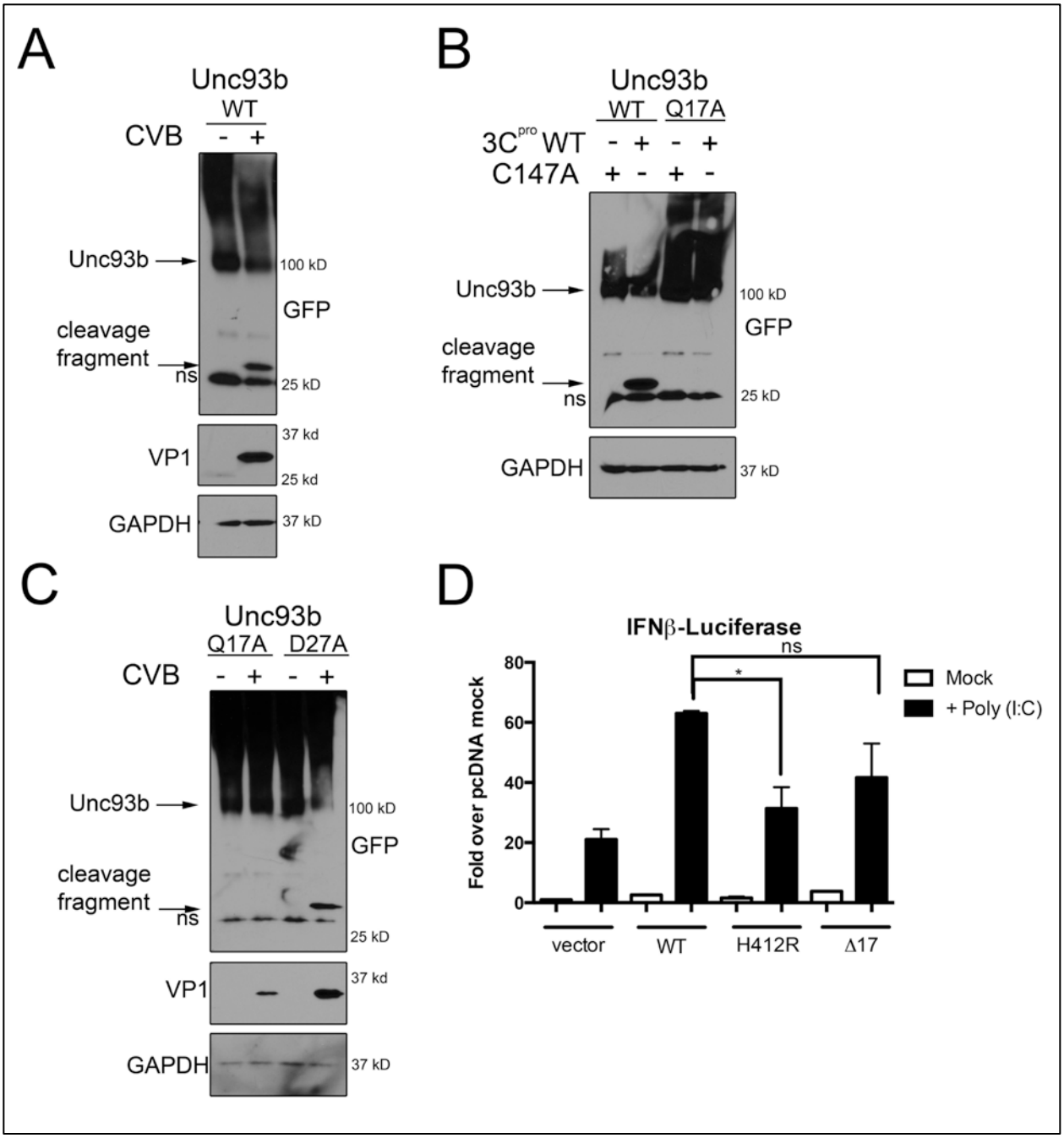

Figure 6. Unc93b is cleaved by 3C^{pro} during CVB infection.

(A) 293T cells transfected with eGFP-Unc93b were infected with CVB (MOI=1). Lysates were harvested 18 hours post-infection, then subjected to immunoblotting with anti-GFP, -VP1, and -GAPDH antibodies. (B) 293T cells were cotransfected with the indicated eGFP-fused Unc93b construct and Myc-tagged wild-type (WT) or catalytically inactive C147A 3C^{pro}. Lysates were harvested 48 hours post-transfection and subjected to

immunoblotting with anti-GFP and -GAPDH antibodies. (C) 293T cells transfected with the indicated eGFP-fused Unc93b construct were infected with CVB (MOI=1). Lysates were harvested 16 hours post-infection and subjected to immunoblotting with anti-GFP, -VP1, and –GAPDH antibodies. In all panels, ns denotes nonspecific bands. (D) HEK293-FlagTLR3 cells were co-transfected with the indicated Unc93b construct containing a C-terminal Myc tag and IFNβ luciferase reporter (pIFNβ-fluc) and control renilla (pRL-null) constructs. Approximately 24 hours post transfection, cells were treated with 100ng poly(I:C) for 16 hours. Luciferase levels were analyzed using the Dual Luciferase reporter assay system. Data shown are from a representative experiment. Firefly luciferase levels were normalized to renilla luciferase levels and then normalized to the vector transfected mock-treated condition.

2.2.4 Unc93b cleavage does not affect its localization or trafficking

We identified two distinct mechanisms of Unc93b cleavage—one dependent on a virally-encoded protease during viral infection and one induced by cellular caspases. Both of these cleavage events sever the N-terminal tail of Unc93b before its first transmembrane domain (schematic, **Figure 7B**). Given that two unrelated proteases cleave Unc93b, we next examined the effect of $3C^{pro}$- and caspase-mediated Unc93b cleavage on a hallmark Unc93b function: its ability to traffic through the secretory pathway. In addition to the Unc93bΔ17 truncation mutant described above, we also generated an Unc93b truncation mutant lacking the first 27 N-terminal amino acids (Unc93bΔ27, schematic **Figure 7A**), which is representative of the C-terminal fragment of Unc93b that remains in the cell following caspase cleavage. We overexpressed WT Unc93b, Unc93bΔ17, Unc93bΔ27, or Unc93bH412R in U2OS cells with EGFP-fused VSV-G, a glycoprotein from vesicular stomatitis virus widely used in the study of intracellular trafficking [335]. As expected, WT Unc93b efficiently trafficked through the secretory system, as indicated by its co-localization with VSV-G in punctate structures (**Figures 7C, 7D**). However, Unc93bH412R failed to localize to these VSV-G positive punctae (**Figures 7C, 7D**), supporting previously published data indicating that Unc93bH412R is incapable of exiting the ER [186,

197]. Similar to WT Unc93b, both Unc93bΔ17 and Unc93bΔ27 co-localized efficiently with the VSV-G positive punctae (**Figures 7C, 7D**), indicating that the trafficking of Unc93b is unaffected by $3C^{pro}$- and caspase-mediated N-terminal truncations.

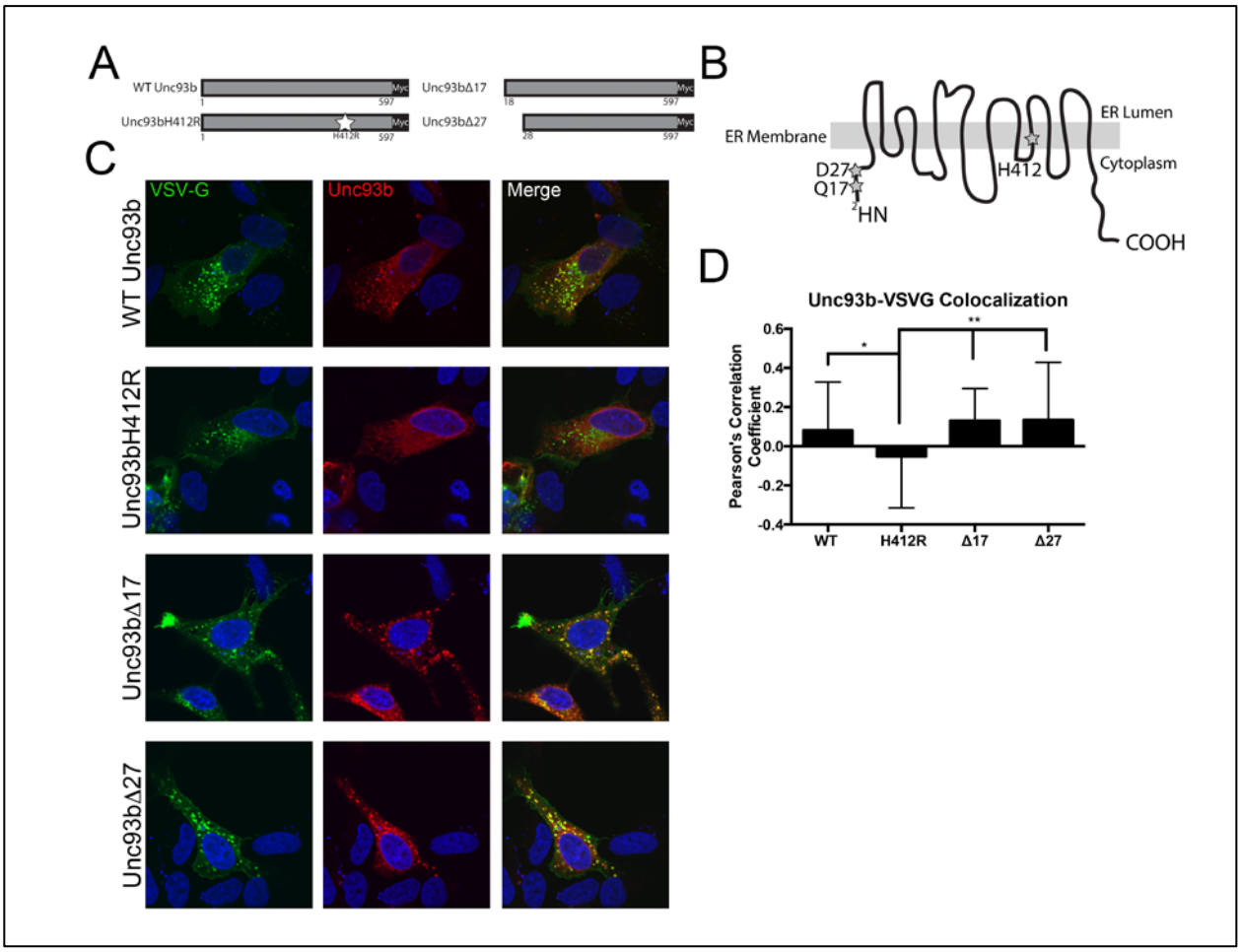

Figure 7. Unc93b cleavage does not affect trafficking to endosomes.

(A) Schematic of Unc93b truncation mutants. (B) Schematic of Unc93b cleavage events. (C,D) U2OS cells were co-transfected with Venus-fused VSV-G and the indicated Unc93b constructs containing a C-terminal Myc tag. Approximately 48-72 hours post-transfection, cells were fixed and then immunostained for Myc and confocal microscopy performed (C) and then images analyzed to obtain Pearson's correlation coefficients (D).

2.2.5 Unc93b cleavage does not affect its induction of cell death.

Because we found that ectopic expression of Unc93b induced apoptosis, we next assessed whether the $3C^{pro}$- and/or caspase-induced cleavage of Unc93b would ablate this function. We found that Unc93bΔ17 promoted apoptotic cell death at a level comparable to that of WT Unc93b as observed morphologically (**Figure 8A**) and measured by Cell Titer Glo and flow cytometric analysis as described previously (**Figures 8B-D**). In addition, an N-terminal truncation mutant lacking the first thirty amino acids (Δ30) of Unc93b also induced morphological changes consistent with apoptosis, suggesting that the N-terminal cleavage of Unc93b by caspases also does not affect this function (**Figure 8E**). Although the cells used in this study (293T) express low levels of endogenous Unc93b, it is unlikely that these endogenous levels are sufficient to mask the lack of functionality in the truncation mutants given that ectopic expression of Unc93bH412R did not induce apoptotic cell death.

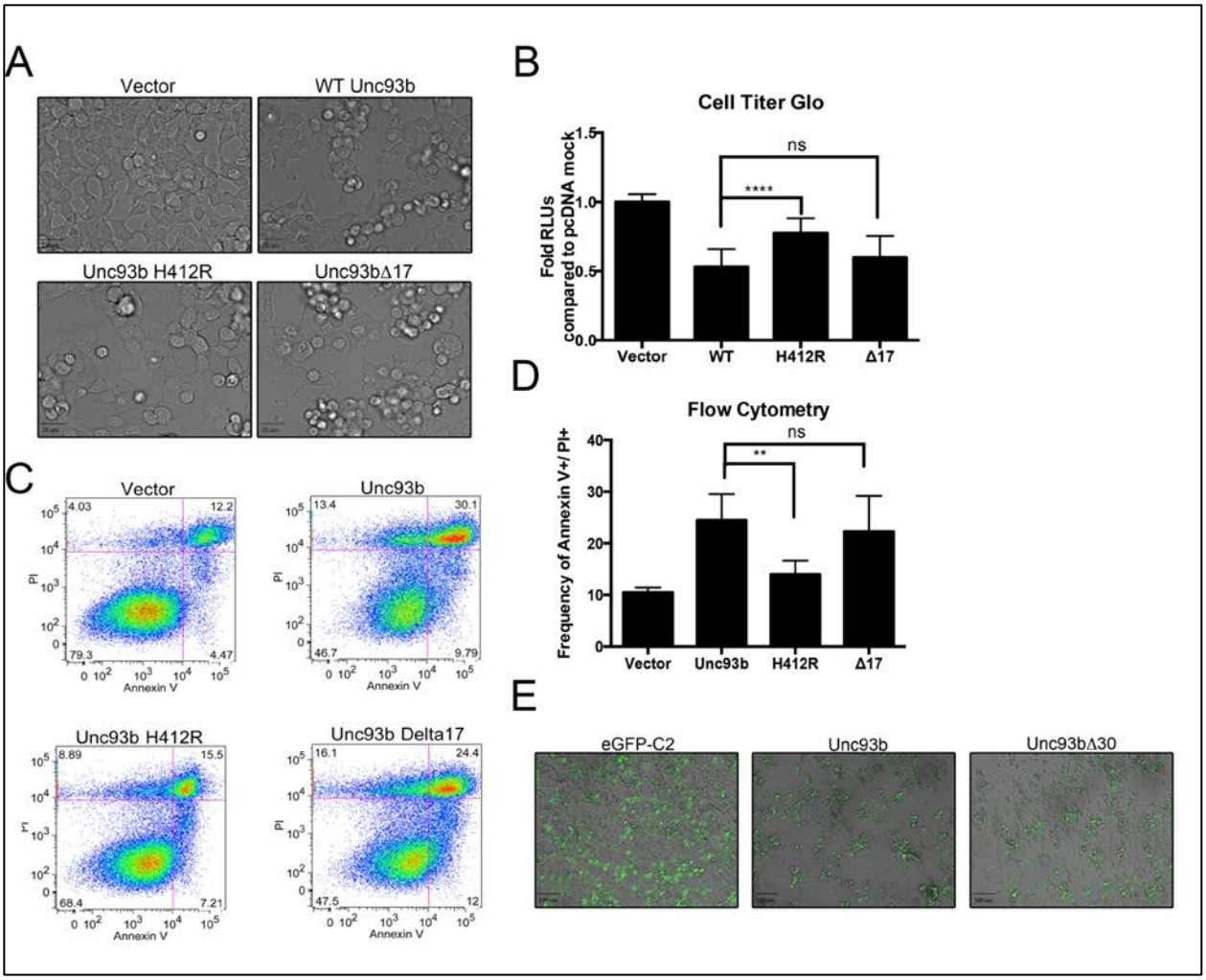

Figure 8. Unc93b cleavage does not affect its induction of cell death.

(A-D) 293T cells were transfected with the indicated Unc93b construct containing a C-terminal Myc tag. (A) 72 hours post-transfection, differential interference contrast (DIC) images were obtained from live cells. (B) 48 hours post-transfection, cell death was measured by Cell Titer Glo assay. Data shown is average of 6 experiments. (C) 72 hours post-transfection, cells were stained with Annexin V and PI and analyzed by flow cytometry. Data was analyzed as described in Figure 4C, gating events on FSC vs. SSC for cell population are not shown here. Data shown are representative of three experiments. (D) 48-72 hours post-transfection, cells were stained with Annexin V and PI and analyzed by flow cytometry. Data were analyzed as described in Figure 4C, and Annexin V+/PI+ populations were compared. Data shown are average of three separate experiments (E) 293T cells were transfected with eGFP-fused Unc93b constructs containing a C-terminal Myc tag. 48-72 hours post-transfection, DIC images were obtained from live cells.

2.3 DISCUSSION

Unc93b is critical for an effective immune response to diverse pathogens, including CVB, and has been associated with the development of autoimmune disease. Despite its important role in human health, its function has only recently been uncovered and, accordingly, our understanding of Unc93b function has been rapidly expanding in both breadth and depth. Here we show that CVB utilizes its virally-encoded $3C^{pro}$ cysteine protease to directly target the distal N-terminus of Unc93b. We also show that cellular caspases also target this region and cleave Unc93b within 10 amino acids from the site of $3C^{pro}$ cleavage. In addition, we further broaden the known role of Unc93b by describing its function in initiating apoptotic cell death pathways and find that the H412R mutant of Unc93b is unable to induce cell death.

Here, we discover a new and important function for Unc93b in the induction of apoptotic cell death. As it has been previously shown that genes known to be involved in cell death are downregulated in the cardiac tissue of mice expressing a non-functional Unc93b variant [201], it is likely that Unc93b is involved in the maintenance of a balance between cell death and cell survival under resting conditions. Additionally, cell death induction is critical in the response to many intracellular pathogens [336]. Thus, further understanding the role Unc93b is playing in cell death helps to broaden the understanding of Unc93b function during initiation of innate immune and cell death signaling. Although it remains unclear by what mechanism Unc93b initiates apoptosis, it is intriguing that Unc93bH412R is incapable of inducing this pathway. Unc93bH412R is incapable of binding TLRs, but the cell type used in our study (293T) does not express TLRs at significant levels [337]. Thus, the role Unc93b plays in inducing cell death is

most likely independent of its role in TLR trafficking and/or signaling. In addition to its inability to bind TLRs, Unc93bH412R also remains localized to the ER [197] and does not localize to endolysosomal vesicles. Given the lack of apoptosis induction by Unc93bH412R and its retention in the ER, it is possible that Unc93b may be involved in a more general trafficking pathway than previously appreciated, and serve to traffic components of apoptotic signaling out of the ER. Although the precise mechanism(s) by which Unc93b induces apoptosis remain to be determined, our work indicates that the effect is at least partially mediated by cellular caspases as the morphological changes associated with Unc93b-mediated apoptotic cell death are inhibited by the pan-caspase inhibitor zVAD-fmk.

The caspase-mediated cleavage of Unc93b discovered here serves to place Unc93b into the broader context of interactions between innate immune proteins and caspases. In recent years, caspases have been shown to be closely involved in the regulation of innate immune signaling through execution of specific cleavage events. For instance, innate immune signaling upon activation of RIG-I, a cytosolic RNA sensor, is dependent on recruitment of RIP1. Caspase 8 serves to cleave and disable RIP1, providing a negative feedback mechanism to control and down-regulate innate immune signaling [338]. Conversely, caspase activation has also been reported to be required for activation of innate immune signaling, as NF-κB activation can be dependent on caspase 8 activity in certain circumstances [339-341]. Clearly, the role of caspase-mediated cleavage events is crucial not only in the context of programmed cell death, but also in non-apoptotic functions associated with the regulation of intracellular innate immunity. Thus, it seems likely that the caspase-mediated cleavage of Unc93b serves to alter its role in some aspect of host innate immune and/or cell death signaling.

It is of special note that two evolutionarily independent proteases, the virally encoded $3C^{pro}$ cysteine protease of CVB and host caspases, target Unc93b for cleavage within the same 10 amino acid N-terminal region. As caspase activation results in the cleavage of Unc93b at residue D27, we initially suspected that this cleavage event would serve to modulate the proapoptotic signaling role of Unc93b. However, we found that Unc93bΔ30 was fully capable of inducing cell death under the conditions we tested. Although we found the truncated versions of Unc93b produced by both $3C^{pro}$ and caspases to be capable of performing the known functions of Unc93b, we suspect that this important and under-characterized protein has more functions than previously elucidated, and it is likely that these cleavage events serve to hinder one of those functions. We eagerly anticipate the advancement of the field of research surrounding Unc93b and expect that soon these cleavage events will be placed in their proper functional context.

3.0 RIP3 IS REQUIRED FOR CVB INFECTION

3.1 INTRODUCTION

Coxsackievirus B3 (CVB), a member of the enterovirus family, is transmitted via the fecal-oral route and encounters the polarized intestinal epithelial cells (IECs) lining the gastrointestinal tract early in infection. Despite serving as the primary cellular portal for CVB entry, very little is known regarding the specific molecular events that regulate CVB replication in and egress from the intestinal epithelium.

An important event in CVB pathogenesis is the induction of host cell death. CVB is a lytic virus and possesses few mechanisms for progeny release other than induction of cell death and subsequent destruction of the host cell membrane. The induction of cell death signaling by CVB in an infected cell must be precisely controlled as activating cell death prematurely or aberrantly could inhibit replication and/or induce inflammatory signaling. Whereas CVB induces apoptosis in non-polarized cells [93] we have shown that CVB-infected polarized IECs undergo calpain-mediated necrosis, which is required for viral egress [80]. These results suggest that the cellular factors that facilitate and/or restrict CVB replication in polarized IECs may be unique to these specialized cells.

In addition to direct lysis of an infected cell, CVB may also egress via microvesicles that are associated with markers of autophagy [81]. Autophagy is an evolutionarily conserved process that can be induced by a variety of cell stressors, including viral replication, to promote cell survival. Autophagy begins with the formation of an isolation membrane (which can be provided by an array of cellular organelles [305]) to form the characteristic double-membraned vesicle called the autophagosome (AP). Once formed, APs can fuse with endosomes to form amphisomes [342], and APs or amphisomes can fuse with lysosomes to form autolysosomes, wherein the degradation of many AP-associated components (and any factors they may interact with) by lysosomal hydrolases occurs. Completion of this process and degradation of any autophagosomal cargo is referred to as autophagic flux [312]. CVB replication is dependent on the induction of autophagy and the inhibition of this process both in vitro [314, 320] and in vivo [315] greatly reduces viral replication. Thus, CVB may rely on autophagy at two distinct stages of the viral life cycle—for the formation of double membrane replication organelles and possibly for viral egress in microvesicles. Whereas enteric bacterial pathogens are known to manipulate autophagy in polarized IECs [343], it is unknown whether CVB also manipulates the autophagic pathway in these cells.

In order to identify host cell factors that promote and/or restrict CVB replication, we previously performed genome-scale RNAi screening in polarized endothelial cells [152]. By applying this approach, we identified a number of previously uncharacterized host cell factors involved in various pathways involved in CVB replication [60, 344]. However, as this initial screening was conducted in polarized endothelial cells, it did not provide any information on the specific host cell factors involved in CVB replication in polarized IECs. In the current study, we

conducted additional RNAi screening to identify factors required for CVB replication in IECs. Together, these screens provide an unbiased comparison of the gene products necessary for CVB infection of both epithelial and endothelial barriers. In the current study, we performed RNAi screening in IECs and identified receptor-interacting serine/threonine-protein kinase 3 (RIP3) as a gene product whose depletion restricted CVB replication. RIP3 is a nonreceptor serine/threonine kinase required for necrotic cell death signaling downstream of tumor necrosis factor receptor (TNFR) and pattern recognition receptor ligation. However, although RIP3 has been associated with the induction of programmed necrosis ('necroptosis') in response to TNFα, we found that RIP3 regulates CVB replication independently of its role in cell death signaling and instead identify a previously uncharacterized role for RIP3 in the regulation of autophagy. We show that RIP3 expression is restricted to many polarized IEC cell lines and that RNAi-mediated silencing of its expression in these cells restricts an early post-entry event associated with CVB replication. In addition, we show that IECs lacking RIP3 exhibit defects in autophagy and autophagic flux and are unable to survive nutrient deprivation. Furthermore, RIP3 interacts with p62/SQSTM1, an adaptor protein that links cargo destined for degradation to APs, and is degraded upon serum starvation. Interestingly, we also show that the CVB virally-encoded cysteine protease $3C^{pro}$ proteolytically cleaves RIP3 to generate two RIP3 fragments, neither of which are capable of necrotic cell death signaling, but one of which retains its capacity to associate with p62/SQSTM1. Thus, our current study not only identifies RIP3 as a host cell factor specifically required for CVB replication in polarized IECs, but also points to a direct role for RIP3 in the regulation of autophagy.

3.2 RESULTS

3.2.1 RIP3 facilitates CVB infection in intestinal epithelial cells

In order to identify genes required for CVB infection of IECs, we performed a genome-scale RNAi screen in Caco-2 cells (schematic, **Figure 9A**). Pathway analysis of the gene products identified as required for CVB infection in IECs revealed enrichment of several pathways, including cell death and survival ($p=5x10^{-5}$), molecular transport ($p=9.5x10^{-5}$), protein trafficking ($p=9x10^{-5}$), and lipid metabolism ($p=5.6x10^{-4}$). Our screening identified RIP3 as a gene product whose depletion significantly reduced CVB replication (robust z score of -2.08), which was confirmed in secondary follow up studies (**Figure 9B**). In addition, we confirmed that RNAi-mediated knockdown of RIP3 reduced CVB infection in HT29 cells, an independently derived IEC line (**Figure 9C**), and also found that CVB replication was restricted in HT29 cells stably expressing an shRNA targeting RIP3 (HT29shRIP3) (**Figure 9D, 9E**). In contrast, vesicular stomatitis virus (VSV) infection was significantly enhanced in HT29shRIP3 cells, indicating that RIP3 may be an enterovirus or CVB specific pro-viral factor (**Figure 9D, 9E**). Notably, treatment of cells with the RIP1 inhibitor necrostatin-1 did not restrict CVB replication in HT29 cells, suggesting that RIP3 may be acting independently of RIP1 to positively regulate CVB infection (**Figure 9F**).

Because RNAi-mediated knockdown of RIP3 restricted CVB infection in IEC cells, but its silencing had no effect on CVB infection in polarized endothelial cells by RNAi screening [152], we next examined the expression of RIP3, as well as RIP1, in a panel of cell lines by

immunoblotting. We found that every IEC cell line tested (Caco-2 (subclone BBE or ATCC), HCT116, HT-29, and T84) expressed RIP3, whereas a diverse panel of non-IEC lines (human brain microvascular endothelial cells (HBMEC), HEK293, HeLa, HT1080, and U2OS) did not (**Figures 9G, 9H**). In contrast, all cell lines expressed RIP1. Because we found that silencing of RIP3 in IECs restricted CVB replication, we next determined whether overexpression of RIP3 in HeLa cells, which do not endogenously express RIP3 (**Figure 9G**), would alter CVB replication. We found that induction of RIP3 in HeLa cells stably expressing a tetracycline inducible RIP3 expression vector had little effect on CVB replication (**Figure 9I**), although we did observe a significant reduction in RIP3 expression levels upon CVB infection (**Figure 9I**, inset).

Taken together, these data imply that RIP3 is a specific regulator of CVB replication in polarized IECs.

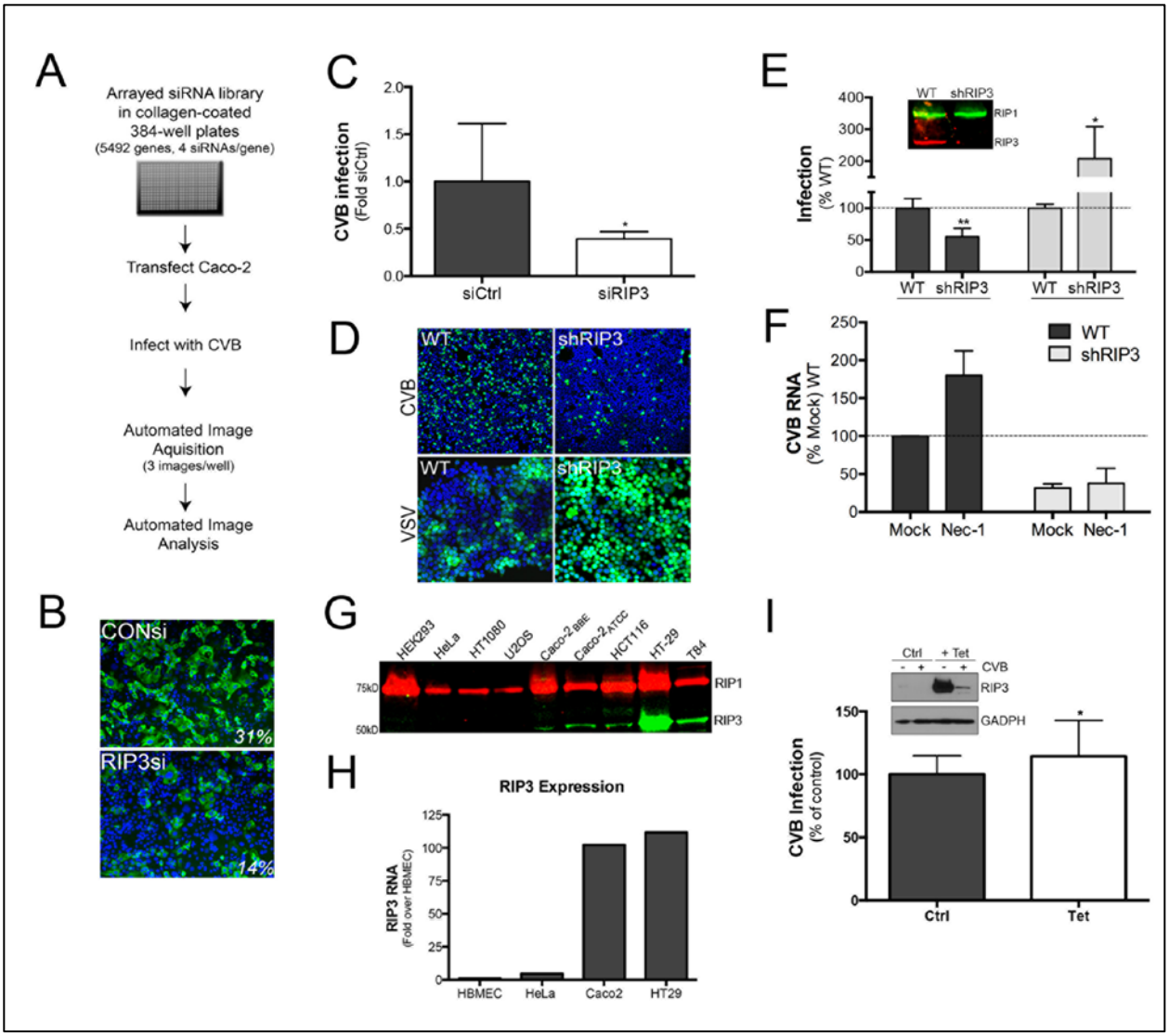

Figure 9. RIP3 facilitates CVB Infection in intestinal epithelial cells.

(A) Schematic depicting genome-scale RNAi screening in Caco-2 cells. (B) Caco-2 cells transfected with siRNA targeting RIP3 (RIP3si) and a control scrambled sequence (CONsi) were infected with CVB (5 PFU/cell) for ~8 hours and then immunostained for VP1 (green). DAPI-stained nuclei are shown in blue. Infection (%) is shown in white text at low right. Representative images from four independent experiments are shown. (C) HT29 cells transfected with siRNA targeting RIP3 or a control scrambled sequence were infected with CVB (0.5 PFU/cell) for 24 hours. Shown are viral RNA levels as assessed by RT-qPCR and averaged from three independent experiments. (D-E) WT HT29 or HT29shRIP3 cells infected with CVB (3 PFU/cell) or GFP-VSV (1 PFU/cell) for ~16hrs. Infected cells were analyzed for infection by either immunofluorescence microscopy to detect CVB VP1 or GFP-tagged VSV (D) or RT-qPCR to detect viral RNA (E). Inset in panel (E) shows immunoblotting for RIP1 (in green) and RIP3 (in red) in wild-type HT29 or HT29shRIP3 cells. Data shown are representative of at least 3 independent experiments. (F) Wild-type or shRIP3 HT29 cells were infected with CVB (1 PFU/cell) for ~16 hrs in the absence (mock) or presence of necrostatin-1 (Nec-1) and viral RNA levels were measured by RT-qPCR. (G-H) The indicated

cell lines were grown to confluence, then lysed and analyzed for RIP1 and RIP3 expression by immunoblotting (G), RIP1 is shown in red and RIP3 is shown in green, or RT-qPCR (H), data are shown as fold over RIP3 expression in HBMEC. (I) HeLa-RIP3 Tet-Inducible cells with or without tetracycline were infected with CVB (0.5 PFU/cell) for 8 hours followed by immunofluorescence microscopy to detect CVB VP1. Shown is the percent infection normalized to untreated control cells. Data shown are an average of 3 independent experiments. Inset, HeLa-RIP3 Tet-Inducible cells with or without tetracycline were lysed and immunoblotted for RIP3 expression performed to confirm RIP3 protein expression upon tetracycline treatment. GAPDH (bottom) is included as a loading control.

3.2.2 RIP3 silencing reduces CVB replication prior to viral egress

We previously showed that polarized IECs undergo necrotic cell death in response to CVB infection whereas non-IECs undergo apoptosis and that necrotic cell death is required in IECs for viral egress [80]. Given that RIP3 expression has been associated with necrotic cell death in response to TNFα treatment [206-208], and was required for CVB replication in IECs, we next determined whether the decrease in CVB replication observed by RNAi silencing occurred early in the virus life cycle or could be attributed to deficiencies in viral egress due to alterations in necrotic cell death. To do this, we performed a time course of CVB infection and assessed the levels of vRNA in HT29 cells transfected with a control or RIP3 targeting siRNA. Surprisingly, we found that RNAi-mediated knockdown of RIP3 led to dramatic reductions of vRNA by as early as 4 hours post-infection (p.i.) (**Figure 10A**) suggesting that the reduction in vRNA could not be directly attributed to late stages of the viral life cycle (such as egress, which occurs between 8 and 12 hours p.i., **Figure 10B**).

3.2.3 RIP3 is not required for CVB entry into intestinal epithelial cells

Because we found that silencing of RIP3 expression impacted CVB vRNA levels early in infection (between 2-4hrs p.i.), we next directly tested whether RIP3 plays a role in CVB entry into IECs. In order to address this question, we performed a neutral red (NR) CVB infection assay. When propagated in the presence of NR (to generate NR-CVB), the virus becomes photosensitive due to damage of the viral RNA induced by photon emission from NR upon illumination, thus inhibiting further replication. However, once NR-CVB has entered the cell and uncoated, the virus becomes light insensitive due to dilution of the neutral red dye in the cytoplasmic compartment, thus preventing photon-mediated damage (schematic, **Figure 10C**) [345]. HT29 cells transfected with a control or RIP3 siRNA were infected with NR-CVB under dark and illuminated (light) conditions. As expected, we found that both control siRNA- and RIP3 siRNA-transfected-cells exposed to light at 0hrs p.i. (prior to entry and uncoating), were extremely photosensitive and exhibited very low levels of CVB replication (**Figure 10D**). In addition, we found that cells transfected with RIP3 siRNA and infected in the dark exhibited a reduction in CVB vRNA levels, confirming the role of RIP3 as a positive regulator of CVB infection (**Figure 10D**). Importantly, we found that light exposure at 2hr p.i. (allowing sufficient time for entry and uncoating to occur) did not further reduce CVB infection levels in cells transfected with siRIP3 compared to cells infected in the dark (**Figures 10D**), indicating that entry of CVB in IECs was not delayed or restricted by RNAi-mediated RIP3 knockdown.

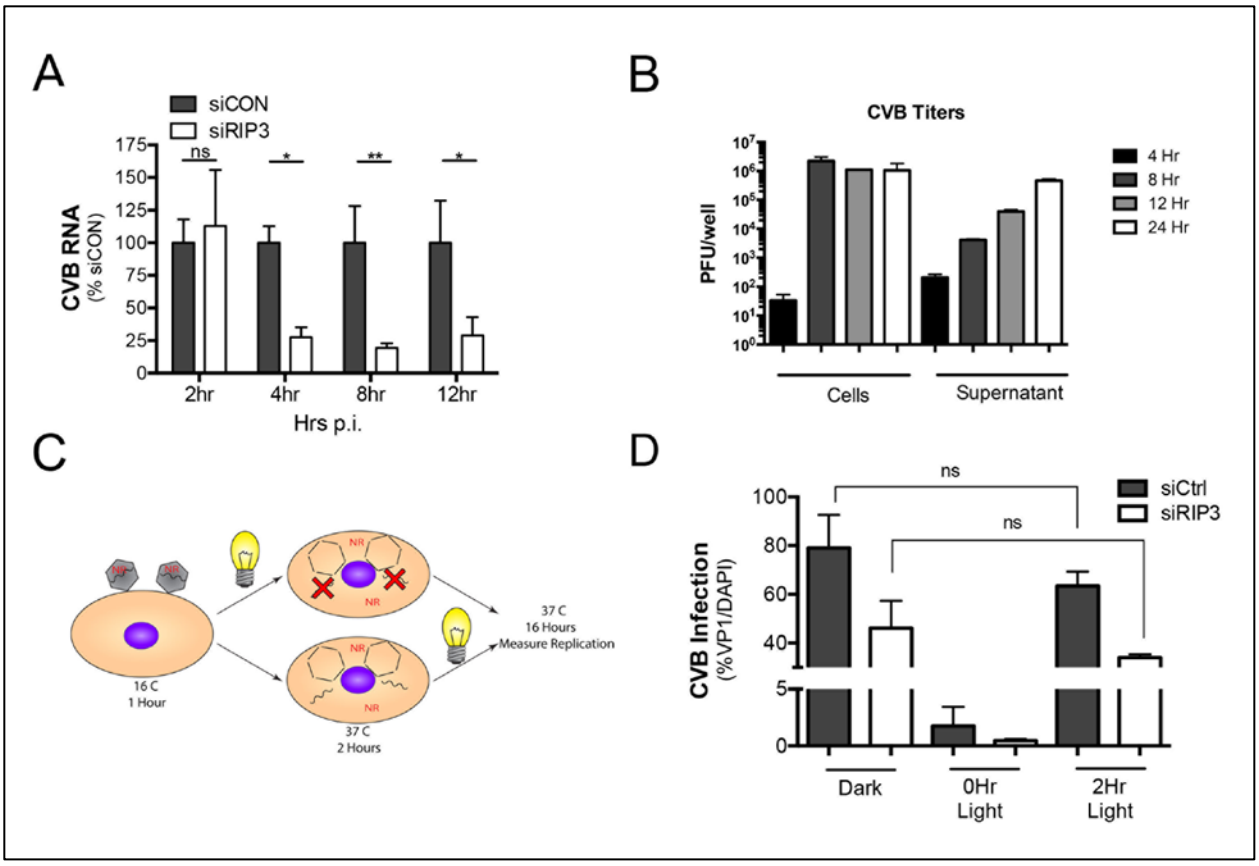

Figure 10. RIP3 silencing restricts CVB replication prior to viral egress but is not required for viral entry.

(A) HT29 cells transfected with siRNA targeting RIP3 or a control scrambled sequence were infected with CVB (0.5 PFU/cell) for 2-12 hours and viral RNA levels determined by RT-qPCR at the indicated times. Data shown are representative of 3 independent experiments (4-12 hours p.i.) or average of 3 independent experiments (2 hours p.i.) (B) HT29 cells transfected with siRNA targeting a control scrambled sequence were infected with CVB (0.5 PFU/cell) for 4-24 hours followed by assessment of viral titres by plaque assay. (C) Schematic depicting NR-CVB replication assay. (D) HT29 cells transfected with siRNAs targeting RIP3 or a control scrambled sequence were infected with NR-CVB (10 PFU/cell) as described in (C) and infection determined by immunofluorescence microscopy to detect VP1. Data shown are displayed as percent infection and are representative of 3 independent experiments.

3.2.4 RIP3 regulates autophagy in intestinal epithelial cells

As RIP3 was not required for CVB entry into IECs, we reasoned that RIP3 must be required for a viral and/or cellular event that takes place between 2 and 4hrs p.i., as we found similar levels of

CVB vRNA at 2hrs p.i., but alterations in vRNA by 4hrs p.i. (**Figure 10A**). CVB, like many positive-stranded RNA viruses, assembles viral replication complexes on scavenged host-cell membranes. These host-cell membranes can be derived from diverse locations within the cell, but there is evidence to support a prominent role for autophagy in the generation of CVB viral replication complexes [318]. Given that our data suggested a role for RIP3 in an early post-entry event associated with CVB replication, we examined whether RNAi-mediated knockdown of RIP3 impacted nutrient depletion-induced autophagy and/or interfered with CVB-induced autophagy. First, we investigated the impact of RIP3 silencing in IECs under basal states and in cells subjected to serum starvation, which induces the canonical form of autophagy (macroautophagy). We observed a pronounced loss of cell viability in HT29shRIP3 cells subjected to serum starvation compared to wild-type controls, suggesting that these cells are unable to survive periods of starvation due to alterations in autophagy (**Figures 11A, Appendix B1A**). In addition, we found that knockdown of RIP3 increased the basal levels of p62 as assessed by immunoblotting (**Figures 11B, 11C**) and led to an accumulation of large p62-positive punctae as assessed by immunofluorescence microscopy (**Figures 11D, 11E**), but no change in the number of punctae (**Appendix B1B**). Additionally, we noted an accumulation of amphisome-like compartments in untreated HT29shRIP3 cells when compared to wild-type HT29 cells by transmission electron microscopy (TEM) that resembled the accumulation observed in wild-type HT29 cells treated with Bafilomycin-A1 (BafA1) (**Figures 11F, 11G, Appendix B1C**), which prevents the maturation of autolysosomes and thereby the degradation of any contents therein. These data suggest that RIP3 may regulate an aspect of autophagic flux that occurs following initiation/induction. In support of this, silencing of RIP3 expression did not

block conversion of LC3B-I to LC3B-II, a hallmark of autophagy initiation, upon serum starvation (**Appendix B1D**).

Next, we determined whether loss of RIP3 impacted CVB-induced autophagy. We found that RIP3 knockdown in IECs did not prevent conversion of LC3B-I to LC3B-II in response to CVB infection, but inhibited the degradation of p62/SQSTM1, an LC3B-binding protein that becomes degraded upon flux through the autophagic pathway (**Figure 11H**). To prevent the degradation of LC3B via autophagic flux, cells were also treated with BafA1. Interestingly, LC3B-II levels were enhanced upon RIP3 knockdown, suggesting a defect in post-initiation autophagic flux in the absence of RIP3 (**Figure 11H**). We also observed the accumulation of LC3B-II during the course of CVB infection in HT29shRIP3 cells when compared to WT HT29 cells (**Appendix B1E**). Collectively, these data support a direct role for RIP3 in the regulation of a post-initiation step of autophagic flux in IECs and suggest that the decrease in CVB replication in IECs lacking RIP3 may be related to alterations in this pathway.

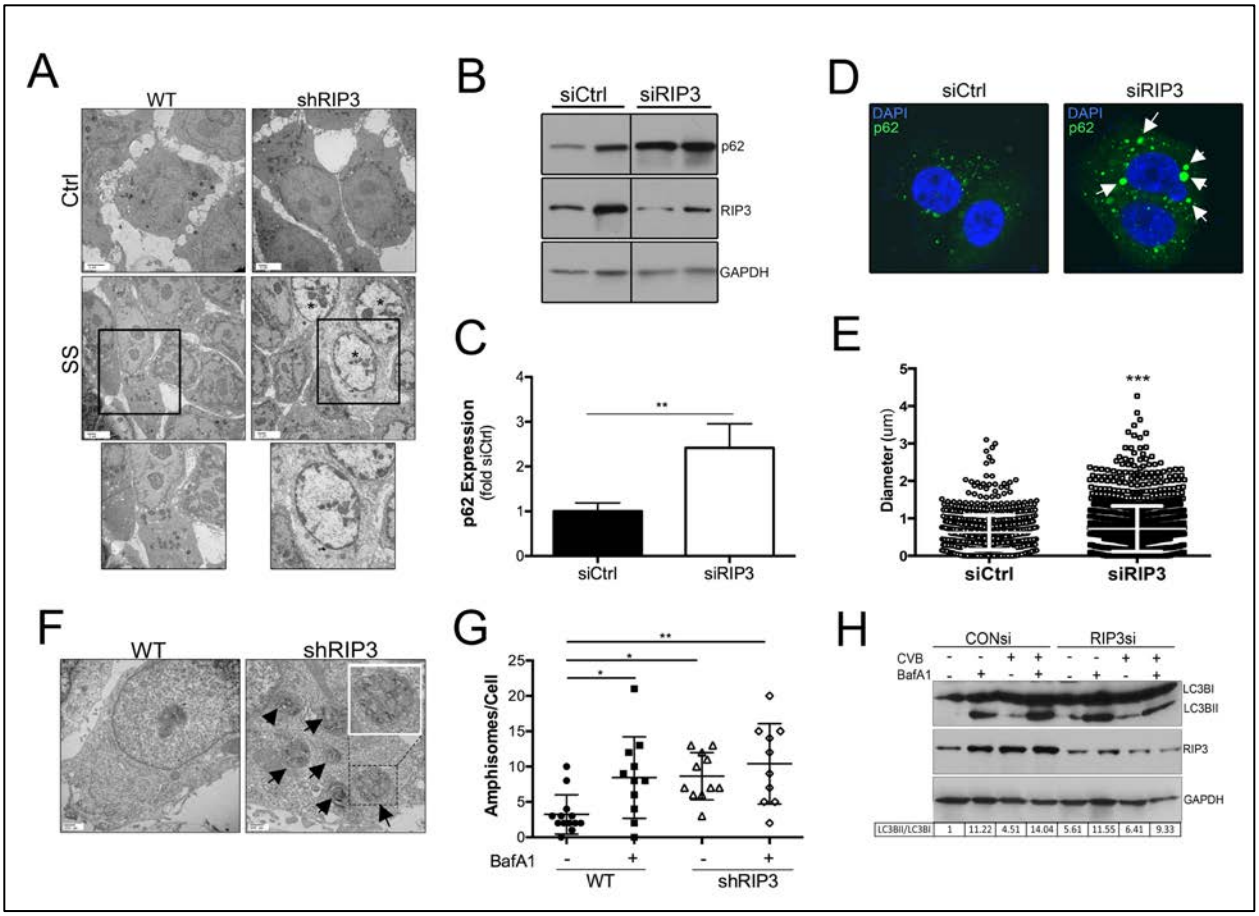

Figure 11. RIP3 is required for autophagic flux in intestinal epithelial cells.

(A) Transmission electron micrographs of WT HT29 or HT29shRIP3 cells grown to confluence in 12 well plates were subjected to serum starvation (SS) in Hank's Buffered Saline Solution for 9 hours. Black square denotes zoomed image shown below. * indicates nuclei of nonviable cells. (B-C) HT29 cells were transfected with siRNAs targeting RIP3 or a control scrambled sequence and immunoblotted for p62 (top) and RIP3 (middle). GAPDH (bottom) is included as a loading control. Shown are two replicates immunoblotted in parallel, non-adjacent lanes from the same gel are separated with a black bar (B). Densitometry was performed and averaged from three independent experiments and is shown as the fold change in p62 expression normalized to control siRNA (C). (D-E) HT29 cells transfected with siRNA targeting RIP3 or a control scrambled sequence were analyzed by immunofluorescence microscopy for p62. Representative images are shown (D) and punctae size was quantified from at least 28 individual cells per condition (E). (F-G) Transmission electron micrographs of WT HT29 or HT29shRIP3 cells are shown, black arrows denote amphisomes, hatched box denotes zoomed image shown in inset (F). Number of amphisomes per cell under mock or Bafilomycin A1-treated conditions for 5 hours were quantified (G). (H) HT29 cells transfected with siRNAs targeting RIP3 or a control scrambled sequence were infected with CVB for 7 hours. 2 hours p.i. cells were mock- or Bafilomycin A1-treated. Following infection (with or without BafilomycinA1 treatment), cells were lysed and immunoblotted for LC3B (top) and RIP3 (middle). GAPDH (bottom) is included as a loading control. Densitometry was performed to obtain a ratio of LC3B-II/LC3B-I and is shown below.

3.2.5 RIP3 interacts with p62

p62 associates with LC3B, is localized in the internal compartment of the autophagosome, and is thus degraded by autophagic flux [310]. p62- and other LC3B-associated proteins can bind to cargo proteins that become internalized into APs and are degraded by autophagic flux [346]. Surprisingly, we found that similar to p62, RIP3 protein levels were diminished upon serum starvation of IECs (**Figures 12A, 12B**), suggesting that RIP3 may be incorporated into APs through a physical association with a component of the autophagic pathway such as p62. Indeed, we found that ectopically expressed RIP3 co-immunoprecipitated with endogenous p62 in 293T cells (**Figure 12C**), which do not express any endogenous RIP3 (**Figure 12A**). This association was not disrupted by mRFP-LC3B, suggesting that RIP3 does not compete with LC3B for p62 association **(Figure 12C).** These findings are consistent with a recent publication that suggested an association between RIP3 and p62 [347]. Additionally, we found that endogenous RIP3 co-immunoprecipitated with endogenous p62 in HT29 IECs (**Figure 12D**). Taken together, these data suggest that RIP3 is required for autophagy in IECs, and this role may be facilitated by its physical association with p62.

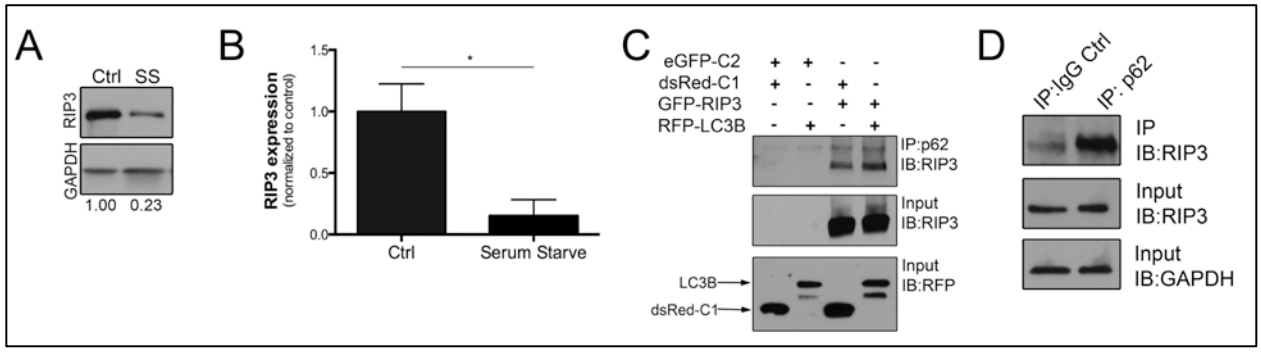

Figure 12. RIP3 associates with p62.

(A-B) HT29 cells in nutrient rich (Ctrl) or depleted (SS) conditions for 12 hours were immunoblotted for RIP3. Control lysates are also immunoblotted in Figure 11B. (A). Densitometry was performed and is representative of eight independent experiments (B). (C) 293T cells ectopically expressing GFP-tagged RIP3 and/or RFP-tagged LC3B were lysed, subjected to immunoprecipitation for p62, and then immunoblotted for RIP3 (top). In parallel, whole cell lysates were immunoblotted for RIP3 (middle) and RFP (bottom) to control for protein loading and transfection efficiency. (D) HT29 cells grown to confluence were lysed, subjected to immunoprecipitation for p62, and then immunoblotted for RIP3 (top). In parallel, whole cell lysates were immunoblotted for RIP3 (middle) and GAPDH (bottom) to control for protein loading. Data shown are representative of 3 experiments.

3.2.6 The CVB-encoded cysteine protease $3C^{pro}$ cleaves RIP3

CVB is known to extensively interact with host cell pathways to antagonize them through various mechanisms [107, 348]. One way in which CVB alters its host cell environment is through the activity of two virally-encoded proteases, $2A^{pro}$ and $3C^{pro}$. These proteases are required for both processing the viral polypeptide and cleaving a wide variety of host proteins to manipulate diverse processes from translation to innate immune signaling to cell death pathways [107, 348]. Although we found that RIP3 was involved in the facilitation of CVB replication in IECs by promoting autophagy, RIP3 is also a key component in the pro-inflammatory necrotic cell death pathway, which may be detrimental to CVB replication. Additionally, we observed a reduction in RIP3 expression levels upon CVB infection in HeLa cells overexpressing RIP3 (**Figure 9G**). Therefore, we determined whether the loss of RIP3 expression in response to CVB infection was a direct result of CVB-mediated proteolytic cleavage. We analyzed the primary protein sequence of RIP3 for the presence of consensus cleavage sites for $2A^{pro}$ or $3C^{pro}$ [334] and found that there were two possible cleavage sites for $3C^{pro}$ located at Q134 and Q430 of RIP3 (schematic, **Figure 13A**). Indeed, CVB infection of 293T cells ectopically expressing RIP3 resulted in a cleavage of RIP3 as detected by immunoblotting (**Figure 13B**). Cleavage of RIP3 in

293T cells was also observed upon ectopic expression of $3C^{pro}$, but not when a catalytically inactive $3C^{pro}$ mutant ($3C^{pro}$ C147A) was expressed (**Figure 13C**), implicating $3C^{pro}$ in the cleavage of RIP3 during CVB infection. By mutating the consensus $3C^{pro}$ cleavage sites of RIP3, we found that mutation of residue Q430 resulted in complete blockage of CVB- and $3C^{pro}$ expression-mediated RIP3 cleavage (**Figures 13D, 13B**), indicating that $3C^{pro}$-mediated cleavage occurs exclusively after RIP3 Q430.

Interestingly, $3C^{pro}$-mediated cleavage of RIP3 after residue Q430 cleaves RIP3 in close proximity to its RHIM domain, a protein-protein interaction motif necessary for recruitment to cell death signaling complexes for the induction of necrosis (schematic, **Figure 13A**). Given this, we investigated the function of the CVB-induced cleavage fragments of RIP3 that contain either the kinase domain ($RIP3_{NT}$) or the RHIM domain ($RIP3_{CT}$). First, we assessed the localization of these fragments in U2OS cells, which do not express endogenous RIP3 (**Figure 9F**). Upon ectopic expression, we found that $RIP3_{NT}$ localized diffusely throughout the cytoplasm, whereas $RIP3_{CT}$ localized either to punctate structures that resembled those observed upon expression of full length RIP3 or to the nucleus (**Figure 13E**).

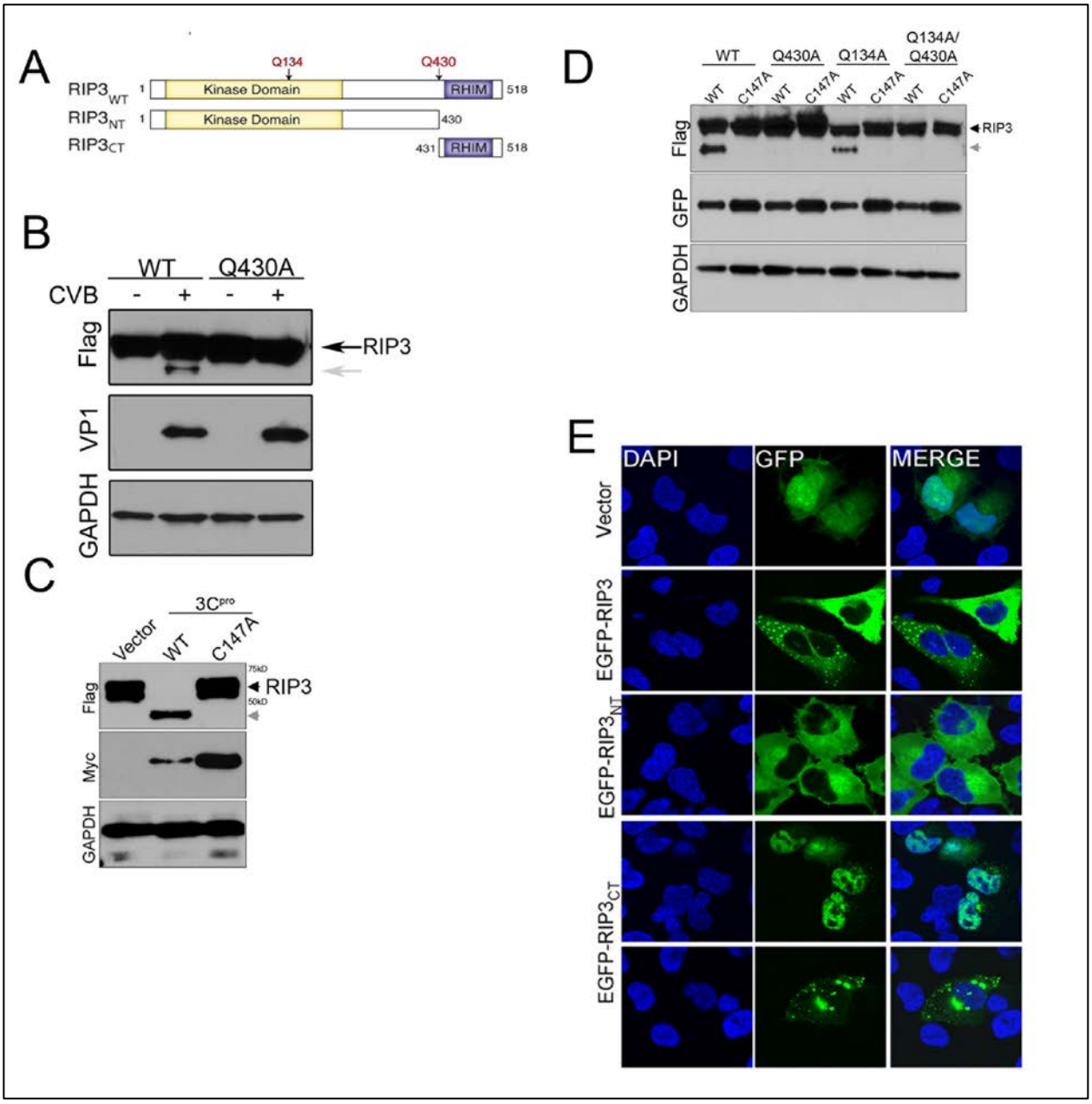

Figure 13. The CVB-encoded cysteine protease 3C^{pro} cleaves RIP3

(A) Schematic depicting RIP3 domains, consensus 3C^{pro} cleavage sites (in red), and fragments generated by CVB infection. (B) 293T cells ectopically expressing Flag-tagged WT or Q430A RIP3 were infected with CVB (2 PFU/cell) for 9 hours followed by immunoblotting for RIP3 (top), VP1 (middle), and GAPDH (bottom). (C) 293T cells ectopically expressing Flag-tagged RIP3 and Myc-tagged WT or C147A 3C^{pro} were lysed and lysates were immunoblotted for Flag(top), Myc (middle), and GAPDH (bottom). (D) 293T cells ectopically expressing Flag-tagged WT, Q430A, Q134A, or Q134A/Q430A RIP3 and GFP-tagged WT or C147A 3C^{pro} were lysed and lysates were immunoblotted for Flag (top), GFP (middle), and GAPDH (bottom). Grey arrow indicates RIP3 cleavage

fragment (B-D). (E) Confocal micrographs of U2OS cells transiently transfected with GFP-tagged RIP3, $RIP3_{NT}$, or $RIP3_{CT}$.

3.2.7 $3C^{pro}$-mediated cleavage fragments are incapable of inducing necrotic cell death

The formation of the RIP1-RIP3 complex (termed the 'necrosome') is mediated by the RHIM domains present in both molecules and is required for the induction of necroptosis downstream of TNFα [349]. Consistent with the RHIM-dependent role of RIP3 in the formation of RIP1/RIP3 necrosomes, we found that $RIP3_{CT}$ co-immunoprecipitated with RIP1, whereas $RIP3_{NT}$ did not (**Figure 14A**). In addition to its role in necrotic signaling, RIP1 is also an essential component of pro-survival NF-κB signaling. However, unlike RIP1, RIP3 acts a negative regulator of NF-κB signaling, which is attributed to the formation of a RIP1-RIP3 complex that interferes with the association of RIP1 with upstream signaling components [350]. Because we found that $RIP3_{CT}$ interacted with RIP1, we determined whether this fragment retained the ability of full-length RIP3 to suppress RIP1-mediated NF-κB signaling. Strikingly, we found that ectopic expression of $RIP3_{NT}$ and $RIP3_{CT}$ significantly increased RIP1-mediated NF-κB signaling in 293T cells as measured by a luciferase reporter fused to the NF-κB promoter (**Figure 14B**), suggesting that the $3C^{pro}$-generated fragments of RIP3 act as positive regulators of RIP1-mediated NF-κB signaling.

Given the role of RIP3 in necrotic signaling, we next assessed the ability of either $RIP3_{NT}$ or $RIP3_{CT}$ to mediate cell death signaling. Unlike full-length RIP3, we found that expression of $RIP3_{CT}$ was incapable of inducing necrosis as determined by the nuclear release of HMGB1 (**Figure 14C**) despite its localization into punctate structures and co-

immunoprecipitation with RIP1. Similarly, $RIP3_{NT}$ expression had no effect on HMGB1 nuclear release (**Figure 14C**). Although we found that expression of $RIP3_{NT}$ and $RIP3_{CT}$ did not induce necrosis, we noted that cells ectopically expressing $RIP3_{CT}$ exhibited classic signs of cell death and distress, including cell rounding and disruption of the cell monolayer (data not shown). Therefore, we examined levels of cell death in 293T cells ectopically expressing full length RIP3, $RIP3_{NT}$, or $RIP3_{CT}$ by propidium iodide (PI) uptake as measured by flow cytometry. We found that ectopic expression of full-length RIP3 and $RIP3_{CT}$, but not $RIP3_{NT}$, led to the enhanced uptake of PI, consistent with an induction of cell death (**Figure 14D**). Thus, although $RIP3_{CT}$ is incapable of inducing necrotic cell death, these results suggest that this fragment potently induces a non-necrotic form of cell death. Taken together, these data suggest that the cleavage of RIP3 by $3C^{pro}$ directly alters the ability of RIP3 to induce necrotic cell death signaling while promoting an alternative non-necrotic cell death pathway as well as enhanced NF-κB signaling. This suggests that CVB actively manipulates the balance of cell death and cell survival signaling pathways in infected host cells through the cleavage of RIP3.

3.2.8 The C-terminal fragment of RIP3 generated by $3C^{pro}$ cleavage retains its ability to bind p62

Our data implicate RIP3 as both a pro-viral regulator of CVB replication due to its involvement in autophagy and an antiviral regulator given its role in necrosis and targeting by $3C^{pro}$. We found that the targeting of RIP3 by $3C^{pro}$ inhibited its ability to function in necrotic cell death signaling. To determine whether this cleavage would also impact its ability to function in

autophagy, we determined whether $3C^{pro}$-generated RIP3 fragments were still capable of associating with p62. We found that $RIP3_{CT}$ interacted with p62 to similar levels as full-length RIP3, whereas $RIP3_{NT}$ exhibited little to no association (**Figure 14E**). Interestingly, we also found that a kinase inactive RIP3 mutant described previously (RIP3K50A) [351] also associated with p62, and appeared to do so more efficiently than did wild-type RIP3 (**Figure 14E**), suggesting that the association of RIP3 with p62 may be transient and may be mediated by a RIP3-dependent phosphorylation event. These data suggest that the $3C^{pro}$-mediated cleavage of RIP3 abrogates its ability to function in necrotic cell death signaling, but likely does not impact its ability to mediate autophagic flux.

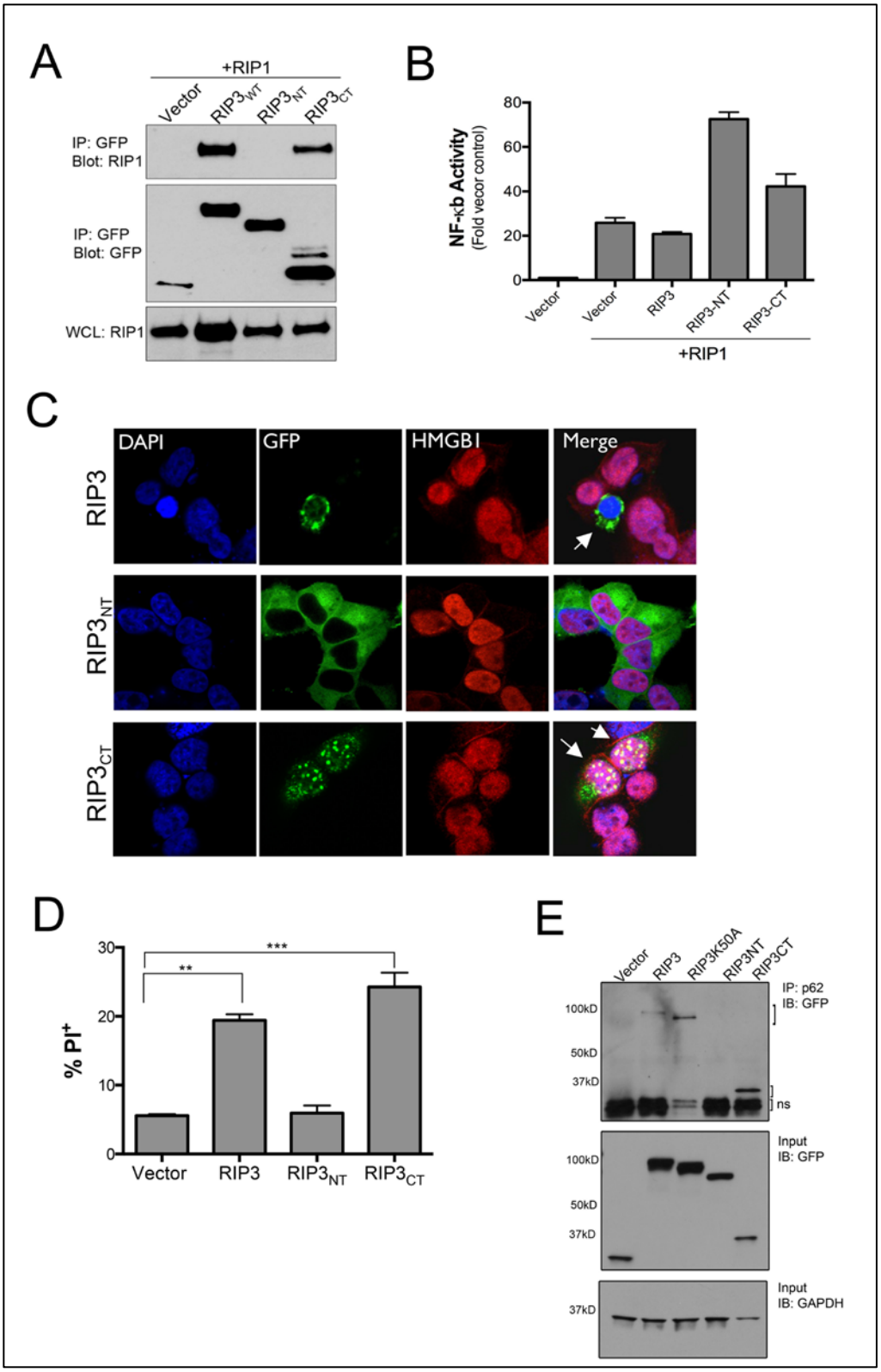
A
+RIP1
Vector
RIP3WT
RIP3NT
RIP3CT
IP: GFP
Blot: RIP1
IP: GFP
Blot: GFP
WCL: RIP1
B
NF-κb Activity
(Fold vecor control)
80
60
40
20
0
Vector
Vector
RIP3
RIP3-NT
RIP3-CT
+RIP1
C
DAPI
GFP
HMGB1
Merge
RIP3
RIP3NT
RIP3CT
D
% PI+
30
20
10
0
***
**
Vector
RIP3
RIP3NT
RIP3CT
E
Vector
RIP3
RIP3K50A
RIP3NT
RIP3CT
IP: p62
IB: GFP
100kD
50kD
37kD
ns
Input
IB: GFP
100kD
50kD
37kD
Input
IB: GAPDH
37kD

Figure 14. $3C^{pro}$-mediated cleavage of RIP3 alters host cell signaling pathways.

(A) 293T cells transfected with vector or GFP-tagged RIP3, $RIP3_{NT}$, or $RIP3_{CT}$ and HA-tagged RIP1 were lysed, subjected to immunoprecipitation for GFP, and immunoblotted for RIP1 (top) or GFP (middle). In parallel, whole cell lysates were immunoblotted for RIP1 to control for protein loading. (B) 293T cells were co-transfected with HA-tagged RIP1, GFP-tagged RIP3, $RIP3_{NT}$, or $RIP3_{CT}$, NF-κB promoted firefly luciferase, and a control renilla luciferase. Luciferase activity was assessed with the dual luciferase reporter kit. Data shown are representative of 3 independent experiments. (C) HeLa cells transfected with GFP-tagged RIP3, $RIP3_{NT}$, or $RIP3_{CT}$ were fixed, permeabilized, and HMGB1 localization was determined by immunofluorescence microscopy. White arrows indicate nuclei of interest. (D) 293T cells transfected with GFP-tagged RIP3, $RIP3_{NT}$, or $RIP3_{CT}$ were analyzed for propidium iodide (PI) uptake by flow cytometry. Data shown are representative of 3 experiments. (E) 293T cells transfected with GFP-tagged RIP3, RIP3K50A, $RIP3_{NT}$, or $RIP3_{CT}$ were lysed and subjected to immunoprecipitation for p62, then immunoblotted GFP (top). In parallel, whole cell lysates were subjected to immunoblotting for GFP (middle) and GAPDH (bottom) to control for protein loading; ns=non-specific band.

3.3 DISCUSSION

Here we show that RIP3 positively regulates CVB infection. Our data suggest that RIP3 contributes to the formation of CVB replication organelles via its IEC-specific regulation of autophagy. Strikingly, we also found that once CVB establishes its replication and produces significant levels of $3C^{pro}$, the protease directly targets RIP3 for proteolytic cleavage. The CVB-mediated cleavage of RIP3 dampens its ability to promote necrotic cell death while driving pro-survival NF-κB signaling. Additionally the C-terminal fragment of RIP3 remains associated with p62/SQSTM1. In this way, CVB manipulates the function of RIP3 in a targeted way to enhance its own replication at both early and late stages of the viral life cycle (schematic, **Figure 15**).

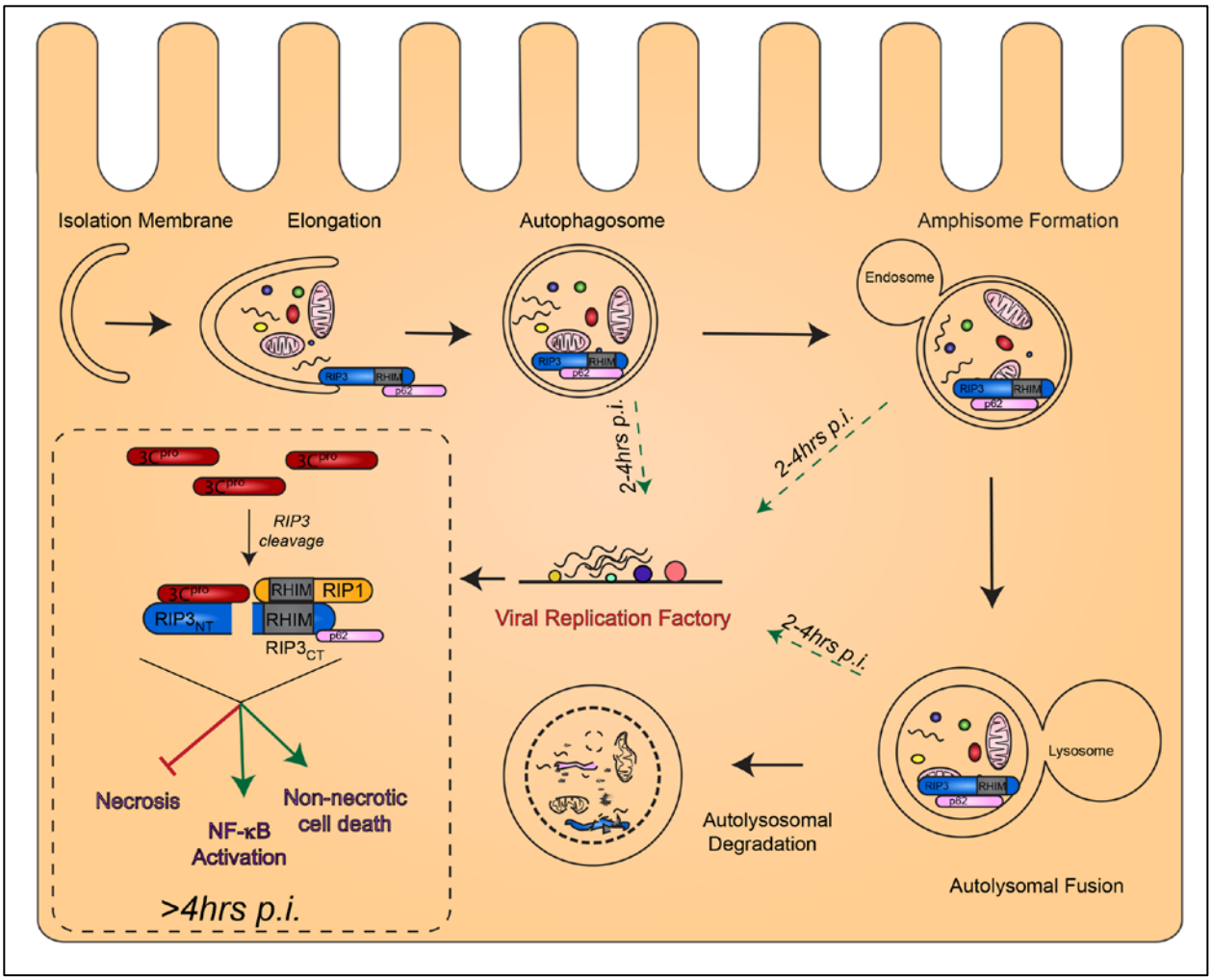

Figure 15. Schematic depicting the role of RIP3 during CVB infection.

Approximately 2-4 hours post-infection, RIP3 contributes to the establishment of viral replication factories (green dashed arrows) through its role as a positive regulator of autophagy. Later in infection (>4hrs p.i., black dashed box), large amounts of the viral protease $3C^{pro}$ are produced, leading to the cleavage of RIP3 into two distinct cleavage fragments, $RIP3_{NT}$ and $RIP3_{CT}$. These fragments are incapable of inducing necrosis, but do enhance RIP1-mediated NF-κB signaling, and $RIP3_{CT}$ retains its ability to associate with RIP1 and p62/SQSTM1 and leads to a non-necrotic form of cell death.

Since the identification of RIP3 as a key regulator of necrotic cell death, RIP3 has been implicated in myriad disease processes. RIP3-mediated necrotic cell death is responsible for the destruction of cone cells in retinitis pigmentosa [282], hepatocyte toxicity in acetaminophen

overdose [269], and is linked to the destruction of the polarized intestinal epithelium experienced in inflammatory bowel disease [242, 285]. Additionally, RIP3-mediated necrosis is responsible for cell death upon infection with several DNA viruses including herpes simplex virus 1 [275], vaccinia virus [208], and murine cytomegalovirus [227], as well as bacterial infections [280]. We have shown previously that necrotic cell death pathways are activated in polarized IECs upon CVB infection [80]. Our data now show a positive correlation between necrotic cell death upon CVB infection and RIP3 expression. However, further investigation is required to conclusively delineate what role RIP3 may play, if any, in the induction of CVB-induced necrotic signaling in IECs.

Our findings suggest a functional link between RIP3 and autophagy. Autophagy is a cellular pathway that serves to promote cell survival upon conditions of cellular stress including starvation and organelle damage. Indeed, inhibition of autophagy upon nutrient depletion leads to accelerated cell death [352]. However, there have been many reports of high levels of autophagy accompanying cell death [353], and a subset of cases in which cell death is actually dependent upon autophagy [354-356]. One such case is blockade of caspase-8, which induces autophagic cell death in L929 cells [356]. Additionally, loss of cell viability upon caspase-8 inhibition in L929 cells was later shown to be dependent on RIP3 [241]. Though this loss of viability was initially assumed to be due to the role of RIP3 in necroptotic cell death, it is possible that inhibition of caspase 8, a known negative regulator of RIP3, in these scenarios may cause an increase in RIP3-dependent autophagic flux, resulting in autophagic cell death.

The relationship between host cell autophagy and viral pathogens is complex. Autophagy can serve as an antiviral defense for the host cell, degrading intracellular pathogens and

preventing establishment of an infection [357]. Indeed, here we note that depletion of RIP3, which we show to be a positive regulator of autophagy, enhances VSV infection in IECs, a virus whose replication can be restricted by autophagy [358]. In contrast, autophagy is conducive to enterovirus replication, possibly through the provision of membranes for the assembly of viral replication complexes. Whether flux through the autophagic pathway is necessary or autophagic initiation alone is sufficient to promote CVB replication remains unclear. Here, our data suggest that a post-initiation and RIP3-regulated step of autophagic flux may be involved in the regulation of CVB infection in polarized IECs, consistent with the notion that complete autophagic flux promotes CVB replication.

Recently it was reported that exogenously expressed RIP3 and p62 associated in 293T cells, a line that does not express any endogenous RIP3 [347]. Here, we show that endogenous RIP3 exists in complex with endogenous p62 in IECs under resting conditions. As p62 is necessary for selective autophagy through its role in binding to both the autophagic membrane associated protein LC3B and cellular components destined for degradation [359], it is likely that the endogenous association of RIP3 with p62 serves to recruit RIP3 to the inside of APs, where it acts to promote flux. Consistent with this, we found that RIP3 is degraded during autophagy, likely due to its localization within the AP.

We propose that RIP3 may be a tissue-specific regulator of autophagy. It is known that autophagy is an especially important pathway in IECs for maintaining intestinal homeostasis. Genome wide association studies have identified a role for autophagy related genes in inflammatory bowel disease [360] and autophagy is known to be important for the maintenance of the intestinal epithelium as a barrier against intestinal pathogens [361]. Thus, RIP3 may

function as an IEC-specific regulator of autophagy. In support of this, we found that ectopic expression of RIP3 in HeLa cells had little impact on CVB replication. Additionally, autophagy is known to play a key role in embryonic development and mice deficient in various genes required for autophagy display embryonic lethality [362]. As RIP3 deficient mice do not exhibit such defects [363], and RIP3 is expressed in tissue-specific patterns [364], it is unlikely that RIP3 is globally required for autophagy.

The function of RIP3 in necrosis is conserved between mice and humans. However, residue Q430 in human RIP3, which is targeted by CVB $3C^{pro}$, is not conserved in mouse RIP3 (**Figure 16A)**. Interestingly, sequence comparisons of RIP3 from several primates revealed that RIP3 in Old World and New World monkeys contains a Histidine at position 430, whereas the evolution of a Glutamine at position 430 arose in the common ancestor of the apes. (**Figure 16A**). Indeed, we found that neither African Green Monkey nor Colobus Monkey RIP3 constructs were targeted by $3C^{pro}$ for cleavage (**Figure 16B**). The viral protease $3C^{pro}$ is well-conserved among all enteroviruses. The ubiquity of these viruses suggests extensive co-evolution of enteroviruses with their hosts, perhaps made possible in part by their ability to take advantage of the newly evolved cleavage site in RIP3 of ancestral apes. Indeed, limiting necrotic cell death through cleavage of RIP3 at residue Q430 by $3C^{pro}$ could serve to lessen the damaging inflammatory effects of intestinal necrosis; such attenuations of pathogenic effects of infection are common in viral pathogens that are well-adapted to their hosts [365].

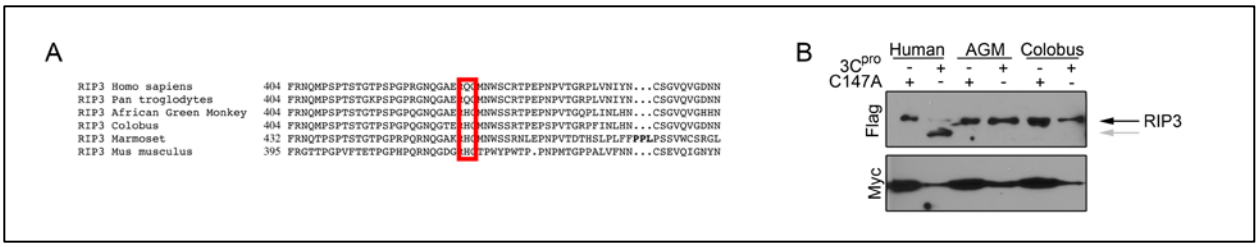

Figure 16. RIP3 residue Q430 is conserved in the common ancestor of the apes.

(A) Sequence alignments of RIP3 from the Homonidae family (*Homo sapiens* and *Pan troglodytes*), the Old World Monkeys (African green monkey and Colobus monkey), the New World Monkeys (Marmoset) and *Mus musculus* are shown. Red box indicates position Q430 in *Homo sapiens* and aligned positions in other sequences. Sequence alignments were made using SNAP [366] (B) 293T cells ectopically expressing Flag-tagged human, African green monkey (AGM), or Colobus monkey RIP3 with Myc-tagged WT or C147A CVB $3C^{pro}$ were immunoblotted for Flag (top) or Myc (bottom). Grey arrow indicates RIP3 cleavage fragment.

Here, we show that RIP3 serves as a specific pro-viral regulator of CVB replication in polarized IECs via its role in the regulation of autophagy. Although the polarized intestinal epithelium is likely to be the primary cell type targeted by CVB during host invasion, the mechanisms by which CVB establishes its infection in these cells have remained elusive. Our findings thus advance our understanding of intestinal epithelial cell pathways that specifically facilitate CVB replication and the pathways used by the virus to attenuate these defenses and promote intestinal infection.

4.0 CONCLUSIONS

Through the work presented here, we have identified two independent host cell pathways that are modified by CVB infection. CVB, a virus that contains only 7 kB of genetic material, must use this limited genetic real estate efficiently in order to effectively replicate in and transmit from a host. Replication and transmission is thereby accomplished through extensive remodeling of host cell pathways by a limited number of viral proteins. The long evolutionary history of enteroviruses with their human hosts has resulted in a finely tuned set of interactions between virus and host whose study is both fascinating and useful. Here, we have uncovered previously unappreciated roles of two proteins, Unc93b and RIP3, in apoptosis and autophagy, respectively. Additionally, we have furthered the understanding of CVB pathogenesis by delineating the ways in which CVB infection alters these proteins. This work underlines the importance of viruses as tools for probing the functions of the host cell as well as emphasizing the need for understanding the ways in which a host and pathogen interact in order to fully understand the pathogenesis of an infectious agent.

4.1 UNC93B AND CELL DEATH

In Chapter 2, we presented work that significantly contributes to the field of Unc93b research. We have shown that Unc93b, which previously was known only to serve as an accessory to TLR trafficking, also has a role in the induction of apoptotic cell death (**Figure 4**). As the ability of Unc93b to induce cell death was dependent on its ability to leave the ER (**Figure 4**), it is possible that Unc93b serves to traffic some component of apoptotic cell death machinery. Additionally, we show that Unc93b is targeted for proteolysis by both CVB and host cell caspases in the same 10 amino acid region (**Figures 5, 6**). Though we find that these cleavage events do not alter the role of Unc93b in cell death or in TLR trafficking (**Figures 6, 7, 8**), this work provides a foundation for future studies of Unc93b function, and is the first report to our knowledge of any proteolytic processing of Unc93b.

4.2 RIP3 AND CVB INFECTION

In Chapter 3, we examine the role of RIP3 in CVB infection. RIP3 was identified in an RNAi screen in IECs as a gene product that facilitates CVB infection (**Figure 9**). Previously known to be involved in necroptotic signaling and inflammasome activation, here we provide evidence that RIP3 also positively regulates autophagy in IECs (**Figure 11**), and suggest that it is this role that facilitates CVB infection (**Figure 10**). Further, we show that during CVB infection, $3C^{pro}$ targets RIP3 for cleavage (**Figure 13**). This cleavage event inhibits the role of RIP3 in necroptotic

signaling (**Figure 14**). Interestingly, the amino acid residue targeted by $3C^{pro}$ for proteolytic processing is conserved among the great apes, but is not conserved in old world or new world monkeys (**Figure 16**). Taken together, this work greatly advances the knowledge of RIP3, provides a connection between necroptosis and autophagy, and identifies an IEC-specific factor necessary for CVB replication.

4.3 CONCLUDING REMARKS

In conclusion, the work presented here has identified two proteins, Unc93b and RIP3, that are both targeted for cleavage during CVB infection by the virally-encoded protease $3C^{pro}$. In investigating the roles of these proteins in CVB infection, we discovered previously unappreciated aspects of the basic biology of each of them—that Unc93b is involved in apoptotic signaling and that RIP3 positively regulates autophagy in IECs. Understanding the ways in which innate immune signaling, cell death, and autophagy relate to one another in the context of viral infection is key to further developing the field of host-pathogen interaction. Here, we contribute to the understanding of each of these pathways, which have deep and pervasive impacts on diverse aspects of human health.

5.0 MATERIALS AND METHODS

Cells and Viruses.

Human kidney 293T cells stably expressing Flag-tagged TLR3 (293T-TLR3) were kindly provided by Dr. Saumendra Sarkar (University of Pittsburgh). HT29 cells stably expressing an shRNA vector targeting RIP3 and HeLa cells stably expressing a tetracycline-inducible RIP3 construct (HeLa-RIP3TetOn) were kindly provided by Dr. Xiaodong Wang (National Institute of Biological Sciences, Beijing), as previously described [207, 258]. HeLa-RIP3TetOn cells were treated with 1 ug/ml Tetracycline to induce RIP3 expression.

Human kidney 293T cells, 293T-TLR3, HeLa-RIP3TetOn, and human osteosarcoma U2OS cells were cultured in DMEM supplemented to contain 10% FBS. HeLa 7B cells were cultured in MEM supplemented with 5% FBS and nonessential amino acids. Human colorectal adenocarcinoma Caco-2 cells (ATCC HTB-37) were cultured in minimal essential media (MEM) supplemented with 20% fetal bovine serum (FBS), sodium pyruvate, and nonessential amino acids. Human colorectal adenocarcinoma HT29 cells (ATCC HTB-38) were cultured in McCoy's 5A (modified) media supplemented with 10% FBS.

Media for all cell lines was supplemented with penicillin-streptomycin and all cells were grown at 37°C, 5% CO_2.

Experiments were performed with CVB3-RD or VSV-GFP (Indiana), as previously described [56]. Neutral red-labeled CVB3-RD was prepared as previously described [58]. For time courses of infection, CVB was pre-adsorbed to cells for 1 hr at 16^{o}C to synchronize infection.

Plasmids.

WT Unc93b constructs were constructed by amplification of Unc93B1 pCR4-TOPO purchased from Harvard PlasmID (clone ID: HsCD00341813) with primers encoding a C-terminal Myc tag followed by insertion into the HindIII and KpnI sites of eGFP-C2 (NT-GFP, CT-Myc construct) or pcDNA3.1(+) (CT-Myc construct). Truncated Unc93b constructs were constructed by amplification of Unc93B1 pCR4-TOPO using primers encoding a C-terminal Myc tag and beginning amplification at residues 18 or 28 for Δ17 or Δ27, respectively, followed by insertion into the HindIII and KpnI sites of pcDNA3.1(+). Unc93bΔ30 was constructed by amplification of Unc93B1 pCR4-TOPO using primers encoding a C-terminal Myc tag and beginning amplification at residue 31 followed by insertion into the HindII and KpnI sites of eGFP-C2. Point mutations producing alanine substitutions in residues Q17 and D27 or an arginine substitution in residue H412 were generated by splice overlap extension, as previously described [367]. NT-GFP, CT-Myc Unc93bQ17A or Unc93bD27A were then constructed by amplification using primers encoding a C-terminal Myc tag followed by insertion in the HindIII and KpnI sites of eGFP-C2. CT-Myc Unc93bH412R was then constructed by amplification using primers encoding a C-terminal Myc tag followed by insertion into the HindIII and KpnI sites of pcDNA3.1(+).

GFP tagged RIP3 was constructed by amplification of RIP3 cDNA followed by insertion into the HindIII/KpnI sites of eGFP-C2 (Clontech). Flag-tagged RIP3 was constructed by amplification of RIP3 cDNA using primers encoding an N-terminal Flag tag followed by insertion into the HindIII/XhoI sites of pcDNA3.1(+). Point mutations in RIP3 to produce alanine substitutions at residue K50 was generated using splice overlap extension mutagenesis, as previously described [367], whereas those at Q134 and Q430 were generated using Stratagene Quikchange mutagenesis according to manufacturer's protocol. GFP tagged $RIP3_{NT}$ or $RIP3_{CT}$ were generated by amplification of RIP3 cDNA using primers amplifying bases encoding for residues one through 430 or 431 through 518, respectively, followed by insertion into the HindIII/KpnI or EcoRI/BamHI sites of peGFP-C2, respectively.

HA-tagged RIP1 was constructed by amplification of purchased RIP1 cDNA with primers encoding an N-terminal HA tag followed by insertion into the XhoI/HindIII sites of pcDNA3.1(+).

GFP tagged and Myc-tagged CVB-$3C^{pro}$ and CVB-$3C^{pro}$C147A were generated as previously described [174, 180].

TRIF constructs were generated as previously described [174]; NT-TRIF contains residues 1-359, whereas CT-TRIF contains residues 360-712.

Venus VSV-G was purchased from Addgene (plasmid 11914, deposited by Dr. Jennifer Lippincott-Schwartz and described previously [335]).

RFP-tagged LC3B was purchased from Addgene (plasmid 21075, deposited by Dr. Tamotsu Yoshimori and described previously [368]).

Non-human primate RIP3 cDNA and primate RIP3 sequences were kindly provided by Dr. Harmit Malik (Fred Hutchinson Cancer Research Center). Flag-tagged non-human primate RIP3 constructs were generated through amplification of these cDNAs using primers encoding an N-terminal flag tag followed by insertion into the HindIII and XhoI sites of pcDNA3.1(+).

Reagents.

Necrostatin-1 was purchased from Calbiochem and used at a concentration of 5μM. Bafilomycin A1 was purchased from Sigma and used at a concentration of 100 nM. Poly(I:C) was purchased from GE Lifesciences. Poly(I:C) was used at 1μg/mL. zVAD-fmk was purchased from Calbiochem (Caspase Inhibitor VI), Invivogen (tlrl-vad), or ApexBio (A1902) and was used at 100 μM. TNFα was purchased from Sigma (H8916) and was used at 50 ng/mL. JSH-23 was purchased from Calbiochem (481408) and was used at 7.1 μM. Staurosporine was purchased from Sigma (S6942) and was used at 8 μM.

Plasmid transfections were performed with Xtreme Gene HP or Xtreme Gene 9 (Roche) and siRNA transfections were performed with Dharmafect-1 (GE Dharmacon) according to manufacturer's protocols

Buffers: Luciferase Cell Culture Lysis Reagent (CCLR; Promega; 25 mM Tris-phosphate pH 7.8, 2mM DTT, 2mM 1,2-diaminocyclohexane-N,N,N',N'-tetraacetic acid, 10% glycerol, 1% Triton X-100) was purchased from Promega. RIPA Buffer (50 mM Tris-HCl (pH 7.4), 1% NP-40, 0.25% sodium deoxycholate, 150 mM NaCl, 1mM EDTA, 1 mM phenylmethanesulfonyl fluoride, protease inhibitor tablets (Pierce)), EBC Buffer (50 mM Tris, 120 mM Nacl, 0.5% NP-

40, ph 8.0, protease inhibitor tablets (Roche)), and NETN Buffer (900 mM NaCl, 1 mM EDTA, 20 mM Tris, 0.5% NP-40, pH 8.0), were all made in house.

Antibodies.

Mouse monoclonal antibody directed against enterovirus VP1 (NCL-ENTERO) was purchased from Novocastra Laboratories. Rabbit monoclonal antibody against PARP (46D11) was purchased from Cell Signaling Technology. Rabbit polyclonal antibody directed against RIP3 was purchased from Imgenex (Novus). Rabbit polyclonal anti-LC3B and mouse monoclonal antibodies against p62 and HMGB1 were purchased from Abcam. Rabbit polyclonal or mouse monoclonal antibodies against GAPDH, GFP, and Myc were purchased from Santa Cruz. Mouse monoclonal antibody against Flag (M2) was purchased from Sigma and mouse monoclonal antibody against RIP1 was purchased from BD-Biosciences. Alexa-Fluor conjugated secondary antibodies were purchased from Invitrogen, HRP-conjugated secondary antibodies were purchased from Santa Cruz and IRDye conjugated secondary antibodies were purchased from LI-COR Biosciences.

siRNAs.

siRNA targeting RIP3 was purchased from Sigma (sequence 5'-3': GGAAUGCCUACCAAAAACU). Control siRNAs were purchased from Ambion (AM4621) or Sigma (SIC-001).

RNAi Screen.

Using the Ambion druggable genome siRNA library (~7000 genes), four siRNAs targeted to a single gene product were arrayed in pairs in duplicate collagen-coated 384-well plates and reverse transfected into Caco-2 cells with Lipofectamine 2000 transfection reagent (Life Technologies) followed by infection with CVB (2 PFU/cell) for 6 hours. After fixation, infection levels were assessed by immunofluorescence staining with a primary antibody directed against VP1 and a fluorescein isothiocyanate (FITC) conjugated secondary antibody and cell number was assessed through the nuclear stain DAPI. The percentage of infected cells was determined through automated image acquisition (ImageXpressMicro Microscope) and analysis (MetaXpress). Percentage of cells ($DAPI^+$) infected with CVB ($VP1^+$) were log transformed and used to calculate the mean and interquartile ranges and these data were used to calculate robust Z scores. Genes associated with cell toxicity (robust Z score for $DAPI^+ \leq -2$) were eliminated, then genes were selected for which wells with identical siRNAs inhibited infection in duplicate assays (with robust Z-scores ≥ 2.0 or $- \leq 2.0$), or for which inhibition (with Z-scores ≥ 1.7 or ≤ -1.7) was seen in at least 3 of 4 wells These candidate genes were then subjected to a secondary screen in which 4 siRNAs, different from those used for the primary screen, were plated individually in duplicate 384-well plates. Transfection, infection, imaging, and image analysis were performed as in the primary screen. Genes whose targeting by at least one siRNA resulted in a robust Z score of ≥ 1.7 or ≤ -1.7 were considered hits**.**

Neutral Red CVB Entry Assay.

Confluent cell monolayers were grown in 8-well chamber slides (BD Biosciences) and then incubated with neutral red-labeled CVB3-RD (described above) (MOI=10) for one hour at 16°C

in semi-dark conditions in McCoy's 5A (modified) media supplemented with 20 mM HEPES. Monolayers were then washed in PBS and fresh media was added. Monolayers were incubated at 37°C, 5% CO_2 and illuminated for 20 minutes on a light box at 0 or 120 minutes p.i., or kept in semi-dark conditions. 16-18 hours post-infection, infection levels were assessed by immunofluorescence microscropy to detect VP1 as described above.

Immunoblotting

Confluent monolayers were grown in 24-well plates. Monolayers were lysed in in Luciferase Cell Culture Lysis Reagent (Chapter 2) or RIPA Buffer (Chapter 3 and Figure 4e). Lysates were briefly sonicated and nonsoluble cell debris was removed through centrifugation. Protein lysates in SDS containing sample buffer (Boston BioProducts) were heated at 95°C for 10 minutes, then electrophoresed in polyacrylamide gradient gels (4-20% or 10-20%, Bio-Rad). Protein was transferred onto nitrocellulose membranes and probed with indicated primary antibodies in 5% non-fat dry milk and the appropriate secondary antibodies conjugated to horseradish peroxidase (HRP, Santa Cruz) or infrared dyes (Li-Cor) and protein was detected using chemiluminescent HRP substrates (Pierce) or by the Odyssey CLx imaging system (Li-Cor).

Immunoprecipitation Assay.

Confluent monolayers were grown in 6-well plates. Monolayers were lysed in EBC Buffer. Nonsoluble cell debris was removed through centrifugation. A portion of the lysate was then incubated with primary antibody overnight at 4°C (for p62 immunoprecipitations) or 90 minutes at 4°C (for GFP immunoprecipitations), followed by incubation with Protein G agarose beads

(Pierce) for 60-90 minutes at 4°C. Protein G beads were then washed with NETN Buffer. Protein was eluted off beads in SDS containing sample buffer (Boston BioProducts) and heated at 95°C for 10 minutes followed by electrophoresis and immunoblotting as described above.

qRT-PCR.

Confluent monolayers were grown in 24-well plates, then total RNA was isolated using TRI Reagent (Sigma) according to manufacturer's protocol. Any contaminating genomic DNA was removed using RNase-free DNaseI (Qiagen), followed by ethanol precipitation of RNA. cDNA was produced from isolated RNA using an iScript cDNA synthesis kit (Bio-Rad) according to manufacturer's protocol. cDNA levels were quantified using quantitative PCR with iQ SYBR Green Supermix (Bio-Rad) in an Applied Biosystems StepOnePlus Real-Time PCR system. RNA levels were normalized to an internal standard (actin) and normalized to the indicated control. Primers to detect actin, CVB, and VSV have been described previously [369]. Primers to detect RIP3 were as follows: (Forward: 5'-TGCTGGAAGAGAAGTTGAGTTG; Reverse: 5'-CTGTTGCACACTGCTTCGTACAC)

Reporter Gene Assays.

Cells were co-transfected with a plasmid containing a renilla luciferase gene (pRL-null, Promega) and a plasmid containing a firefly luciferase gene under the control of an NF-κB responsive promoter (kindly provided by Saumendra Sarkar, University of Pittsburgh), or an IFNβ promoter (p125-luc) at a ratio of 1:30, renilla:firefly. Levels of firefly and renilla luciferase were quantified using the Dual-Luciferase Reporter Assay System (Promega) according to

manufacturer's protocol and a Synergy 2 luminescence plate reader (Bio-Tek). Firefly luciferase levels were normalized to renilla luciferase levels.

Flow Cytometry.

Cells were grown to confluence in 24-well plates, then stained with Annexin V and Propidium Iodide (PI) or PI alone using the AlexaFluor488 Annexin V/Dead Cell Apoptosis Kit (Invitrogen) according to the manufacturer's protocol and analyzed using a MACSQuant Analyzer (Miltenyi). Data analysis was performed using FlowJo software.

Microscopy.

Confluent monolayers grown in 8-well chamber slides (BD Biosciences) were fixed and permeabilized with an ice-cold mixture of 3:1 methanol:acetone or 4% paraformaldehyde followed by 0.1% Triton X-100. Cells were incubated with the indicated primary antibodies for 1 hour at RT, washed in PBS, then incubated in appropriate AlexaFluor-conjugated secondary antibodies for 30 minutes at RT, washed in PBS, and mounted in Vectashield containing DAPI (Vector Labs). Images were captured using a FV1000 confocal laser scanning microscope (Olympus). Image analysis was performed using Imaris (Bitplane) or ImageJ and contrasted and merged using Phostoshop (Adobe). For differential interference contrast (DIC) microscopy, confluent monolayers were grown in 35 mm glass-bottomed dishes (Mat Tek) and images were captured from living cells using IX81 or IX83 inverted microscopes (Olympus). Transmission electron microscopy was performed as described [369]. For measurements of amphisome size

and number by TEM, at least 40 individual amphisomes were measured using ImageJ from at least 10 unique cells.

Virus Titration.

Intracellular virus was prepared for titration by three successive freeze-thaw cycles. To titrate virus, HeLa 7B cells were cultured to confluence in 12-well plates. Cells were incubated for 1 hour at room temperature with serially diluted samples followed by overlay of cell culture media containing 0.4% agarose. 48 hours post-infection agarose overlays were removed and plaques were visualized through fixation and staining with a solution of ethanol and crystal violet.

Cell Viability Assays.

Cells to be analyzed by Cell Titer Glo Assay were grown to confluency in 96-well plates, then mock- or staurosporine-treated. Cell Titer Glo Luminescent Cell Viability Assays (Promega) were performed as described in manufacturer's protocol.

Statistical Analysis.

All statistical analysis was performed using GraphPad Prism. Students t-test or one-way ANOVA were performed as appropriate. * indicates $p<0.05$. ** indicates $p<0.01$. *** indicates $p<0.001$. **** indicates $p<0.0001$.

APPENDIX A

TABLE OF ABBREVIATIONS

5'-ppp – 5'-triphosphate group
AP – autophagosome
AP2 – assembly protein 2
AP4 – assembly protein 4
ATCC – American type culture collection
ATF3 – activating transcription factor 3
ATF6 – activating transcription factor 6
Atg9 – autophagosome-related 9
BafA1 – bafilomycin-A1
Bcl-2 – B-cell lymphoma 2
Bcl-XL – B-cell lymphoma extra large
C-terminus – carboxy terminus
CAR – coxsackievirus and adenovirus receptor
CCLR – cell culture lysis reagent
cDNA – complementary DNA
cFLIP – cellular FLICE-inhibitory protein
$cFLIP_L$ – cFLIP long isoform
$cFLIP_s$ – cFLIP short isoform
CHOP – C/EBP homologous protein
cIAP – cellular inhibitor of apoptosis
CMV – cytomegalovirus
CNS – central nervous system
COPII – coat protein II
CpG – unmethylated deoxycytidylate-phosphate-deoxyguanylate
CVB – coxsackievirus B3
CYLD – cylindromatosis

DAF – decay accelerating factor
DAI – DNA-dependent activator of IRFs
DAMP – damage associated molecular patterns
DAPI – 4',6-diamidino-2-phenylindole
DAVID – the database for annotation, visualization and integrated discovery
DC – dendritic cell
DIC – differential interference contrast
DMEM – dulbecco's modified eagle's medium
DNA – deoxyribonucleic acid
Drp1 – dynamin-related protein 1
dsRNA – double stranded RNA
ECHO – enteric cytopathic human orphan
eGFP – enhanced GFP
eIF-4G – eukaryotic initiation factor 4G
ER – endoplasmic reticulum
ERGIC – ER-Golgi intermediate compartment
FADD – Fas-associated protein with Death Domain
FAK – focal adhesion kinase
FBS – fetal bovine serum
FLICE – FADD-like ICE
FSC – forward-scatter light
GAPDH – glyceraldehyde 3-phosphate dehydrogenase
GFP – green fluorescent protein
GI – gastrointestinal
GTP – guanosine triphosphate
HBMEC – human brain microvascular endothelial cells
HMGB1 – high-mobility group protein B1
HSE – herpes simplex encephalitis
HSV-1 – herpes simplex virus 1
ICE – interleukin-1β-converting enzyme
ICP6 – infected cell protein 6
IEC – intestinal epithelial cell
IFN – interferon
IFNAR – interferon α/β receptor
IGTP – interferon γ induced GTP-ase
IL-12p40 – interleukin 12p40
IL-6 – interleukin 6
IRE1 – inositol requiring enzyme 1
IRES – internal ribosomal entry site
IRF – interferon regulatory factor
ISG – interferon stimulatory gene
JNK – c-Jun N-terminal kinase
kB – kilobase

kD – kiloDalton
LC3B – light chain 3 B
LGP2 – laboratory of genetics and physiology 2
LPS – lipopolysaccharide
MAM – mitochondria-associated membrane
MAVS – mitochondrial antiviral signaling
mCMV – murine CMV
MDA5 – melanoma differentiation associated 5
MEFs – murine embryonic fibroblast
MEM – minimal essential media
MLKL – mixed lineage kinase domain-like
MOI – multiplicity of infection
mRFP – modified RFP
N-terminus – amino terminus
Nec-1 – necrostatin-1
NF-κB – nuclear factor kappa light chain enchancer of activated B cells
NIAID – National Institute of Allergy and Infectious Disease
NR – neutral red
ns – non-specific
p.i. – post infection
p38MAPK – p38 mitogen-activated protein kinase
PABP – poly(A) binding protein
PAMP – pathogen associated molecular pattern
PARP – poly ADP ribose polymerase
PCR – polymerase chain reaction
pDC – plasmacytoid DC
PERK – PKR-like ER kinase
PI – propidium iodide
PI3K – phosphoinositide 3-kinase
PKR – protein kinase R
Poly(I:C) – polyinosinic:polycytidylic acid
PRR – pattern recognition receptor
RHIM – RIP homotypic interaction motif
RIG-I – retinoic acid-inducible gene 1
RIP1 – receptor interacting protein kinase 1
RIP3 – receptor interacting protein kinase 3
RIPA – radioimmunoprecipitation assay
RLR – RIG-I like receptor
RNA – ribonucleic acid
RNAi – RNA interference
ROS – reactive oxygen species
RP – retinitis pigmentosa
RT-qPCR – reverse transcription quantitative PCR

SAPK – stress activated protein kinase
SCID – severe combined immunodeficiency
SDS-PAGE – sodium dodecyl sulfate – polyacrylamide gel electrophoresis
Ser – serine
shRNA – small hairpin RNA
siRNA – small interfering RNA
SLE – systemic lupus erythematosus
SNAP – scalable nucleotide alignment program
SNAP – soluble NSF attachment protein
SNARE – SNAP receptor
SNP – single nucleotide polymorphism
SQSTM1 – sequestosome 1
SS – serum starve
SSC – side-scattered light
ssRNA – single stranded RNA
TBP – TATA binding protein
TEM – transmission electron microscopy
TFIIIC – transcription factor for polymerase III C
Thr - threonine
TLR – toll-like receptor
TNFR1 – TNFα receptor 1
TNFα – tumor necrosis factor α
TRADD – TNFR1 associated death domain protein
TRAF2 – TNFR1 associated factor 2
TRIF – TIR-domain-containing adapter-inducing IFNβ
TRPM7 – transient receptor potential cation channel, subfamily M, member 7
Ubl – ubiquitin-like
ULK – unc-51 like kinase
UPR – unfolded protein response
VAMP8 – vesicle-associated membrane protein 8
vIRA – viral inhibitor of RIP activation
VP1 – viral protein 1
VP2 – viral protein 2
VP4 – viral protein 4
VPg – viral protein genome linked
VRCs – viral replication complexes
vRNA – viral RNA
VSV-G – vesicular stomatitis virus glycoprotein
VV – vaccinia virus
WT – wild type

APPENDIX B

SUPPLEMENTAL DATA CHAPTER 4.0

Appendix B
Figure 1

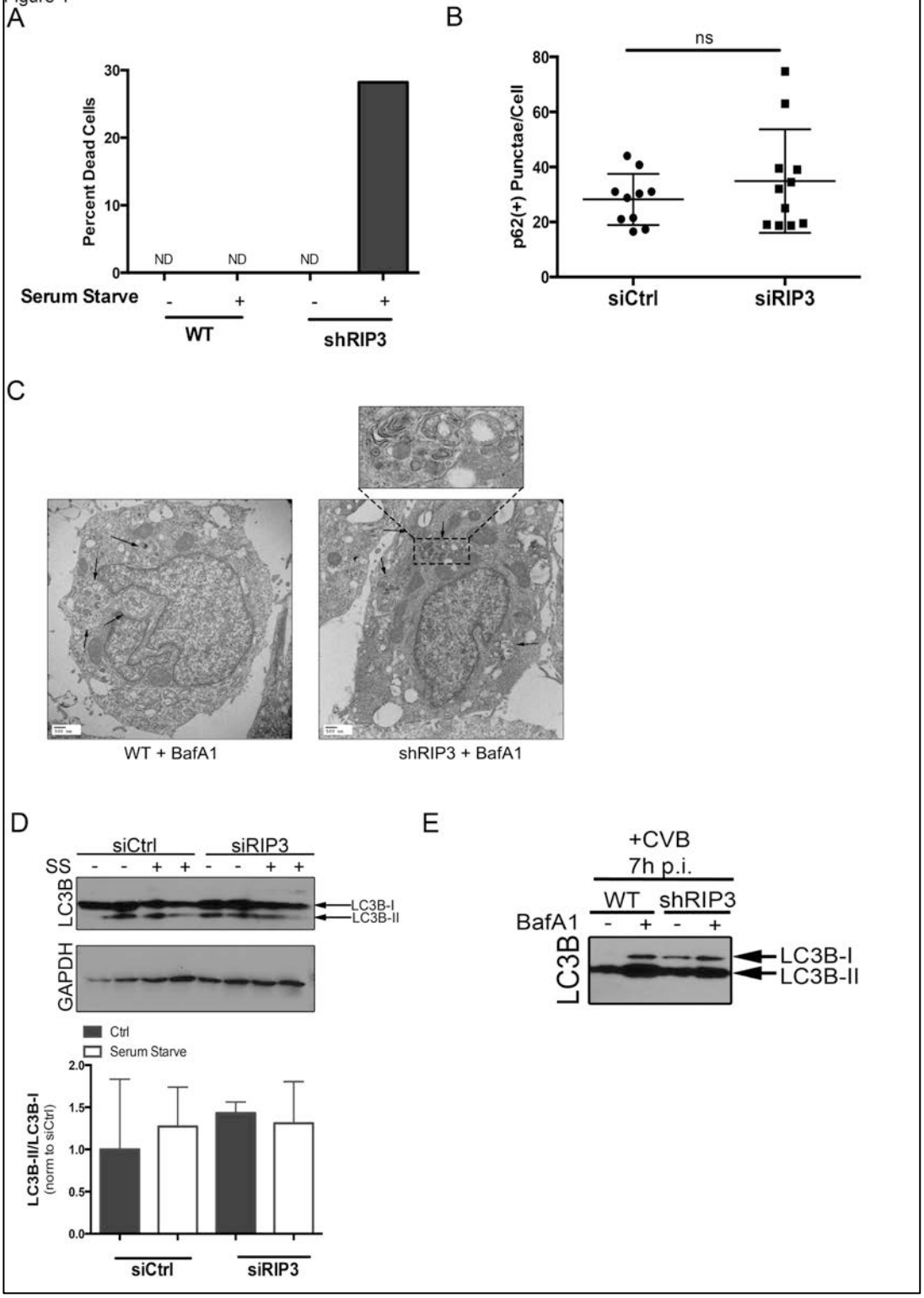

Appendix B 1. RIP3 is required for autophagic flux in intestinal epithelial cells.

(A) Transmission electron micrographs from Figure 11A were quantified for number of nonviable cells. At least 13 individual cells were observed per condition. (B) Immunofluorescence images from Figure 11C were quantified for number of p62 punctae using Imaris. At least 28 individual cells were quantified per condition. (C) Transmission electron micrographs of WT HT29 or HT29shRIP3 cells treated with BafA1 are shown, black arrows denote amphisomes, hatched box denotes zoomed image shown above. (D) HT29 cells transfected with siRNA targeting RIP3 or a control scrambled sequence in nutrient rich or depleted (SS) conditions for 12 hours then immunoblotted for LC3B (top) and GAPDH (bottom). Densitometry was performed and is shown below. Control lysates (nutrient rich) are the same lysates immunoblotted in Figure 11B. (E) WT HT29 or HT29shRIP3 cells were infected with CVB (5PFU/cell) for 7 hours then immunoblotted for LC3B.

BIBLIOGRAPHY

1. International Committee on Taxonomy of Viruses. (2012). Virus Taxonomy: 2012 Release (current).

2. Centers for Disease Control. (2015). Non-Polio Enterovirus Infections: http://www.cdc.gov/non-polio-enterovirus/index.html.

3. Dalldorf G and Sickles GM. (1948). An Unidentified, Filtrable Agent Isolated From the Feces of Children With Paralysis. *Science* **108,** 61-62.

4. Sturge WA. (1879). Three Cases of Acute Anterior Poliomyelitis (Acute Spinal Paralysis) in Adults. *Br Med J* **1,** 849-851.

5. Moore WW. (1881). Notes of Four Cases of Acute Anterior Poliomyelitis. *Br Med J* **2,** 111-113.

6. Russell J. (1870). A Case of Arrested Development in One Arm, the Result of Infantile Paralysis: Grouping of the Affected Muscles. *Br Med J* **1,** 405.

7. Eggers HJ. (1999). Milestones in early poliomyelitis research (1840 to 1949). *J Virol* **73,** 4533-4535.

8. Wickman I. (1911). Die akute Poliomyelitis bzw. Heine-Medinsche Krankheit. *Handbuch der Neurologie*.

9. Landsteiner K and Popper E. (1909). Uebertragung der Poliomyelitis acuta auf Affen. *Z. Immunitatsforsch* **2,** 377-390.

10. Flexner S and Lewis PA. (1910). Experimental Epidemic Poliomyelitis in Monkeys. *J Exp Med* **12,** 227-255.

11. Trask JD, Paul JR and Vignec AJ. (1940). I. Poliomyelitic Virus in Human Stools. *J Exp Med* **71,** 751-763.

12. Dalldorf G. (1949). The Coxsackie group of viruses. *Science* **110,** 594.

13. Dalldorf G. (1950). The Coxsackie viruses. *Am J Public Health Nations Health* **40,** 1508-1511.

14. Contreras G, Barnett VH and Melnick JL. (1952). Identification of Coxsackie viruses by immunological methods and their classification into 16 antigenically distinct types. *J Immunol* **69,** 395-414.

15. Committee on the Enteroviruses National Foundation for Infantile Paralysis. (1957). The Enteroviruses. *American Journal of Public Health and the Nations Health* **47,** 1556-1566.

16. Carpenter CM and Boak RA. (1952). Coxsackie viruses; a review of pathologic, epidemiologic, diagnostic and etiologic observations. *Calif Med* **77,** 127-130.

17. Stanley NF, Dorman DC and Ponsford J. (1953). Virus neutralizing antibodies in pooled human serum. *J Immunol* **71,** 402-409.

18. Walton M and Melnick JL. (1953). Coxsackie virus antibody and incidence of minor illness during the summer. *Public Health Rep* **68,** 1167-1178.

19. Dalldorf G. (1955). The Coxsackie viruses. *Annu Rev Microbiol* **9,** 277-296.

20. Glajchen D. (1961). Myocarditis due to Coxsackie virus infection in an adult. *Br Med J* **2,** 870-871.

21. Pappenheimer AM, Kunz LJ and Richardson S. (1951). Passage of Coxsackie virus (Connecticut-5 strain) in adult mice with production of pancreatic disease. *J Exp Med* **94,** 45-64.

22. Dalldorf G and Gifford R. (1952). Adaptation of Group B Coxsackie virus to adult mouse pancreas. *J Exp Med* **96,** 491-497.

23. Gamble DR, Kinsley ML, FitzGerald MG, Bolton R and Taylor KW. (1969). Viral antibodies in diabetes mellitus. *Br Med J* **3,** 627-630.

24. Craig ME, Nair S, Stein H and Rawlinson WD. (2013). Viruses and type 1 diabetes: a new look at an old story. *Pediatr Diabetes* **14,** 149-158.

25. Horstmann DM, Mc CR and Mascola AD. (1954). Viremia in human poliomyelitis. *J Exp Med* **99,** 355-369.

26. Bodian D. (1952). Pathogenesis of poliomyelitis. *Am J Public Health Nations Health* **42,** 1388-1402.

27. Pfeiffer JK. (2010). Innate host barriers to viral trafficking and population diversity: lessons learned from poliovirus. *Adv Virus Res* **77,** 85-118.

28. Rose NR and Kaya Z. (2014). 70. In *The Autoimmune Diseases* 1033-1048.

29. Tam PE. (2006). Coxsackievirus myocarditis: interplay between virus and host in the pathogenesis of heart disease. *Viral Immunol* **19,** 133-146.

30. Andreoletti L, Leveque N, Boulagnon C, Brasselet C and Fornes P. (2009). Viral causes of human myocarditis. *Arch Cardiovasc Dis* **102,** 559-568.

31. Martino T, Liu P, Petric M and Sole M. (1995). 14. In *Human Enterovirus Infections (*H. Rotbart, H. Rotbart)*,* 291-351. Washington, DC: American Society for Microbiology.

32. Herzum M, Ruppert V, Kuytz B, Jomaa H, Nakamura I and Maisch B. (1994). Coxsackievirus B3 infection leads to cell death of cardiac myocytes. *J Mol Cell Cardiol* **26,** 907-913.

33. Ahn J, Joo CH, Seo I, Kim D, Kim YK and Lee H. (2005). All CVB serotypes and clinical isolates induce irreversible cytopathic effects in primary cardiomyocytes. *J Med Virol* **75,** 290-294.

34. Claycomb WC, Lanson NA, Jr., Stallworth BS, Egeland DB, Delcarpio JB, Bahinski A and Izzo NJ, Jr. (1998). HL-1 cells: a cardiac muscle cell line that contracts and retains phenotypic characteristics of the adult cardiomyocyte. *Proc Natl Acad Sci U S A* **95,** 2979-2984.

35. Miteva K, Haag M, Peng J, Savvatis K, Becher PM, Seifert M, . . . Van Linthout S. (2011). Human cardiac-derived adherent proliferating cells reduce murine acute Coxsackievirus B3-induced myocarditis. *PLoS One* **6,** e28513.

36. Venteo L, Bourlet T, Renois F, Douche-Aourik F, Mosnier JF, Maison GL, . . . Andreoletti L. (2010). Enterovirus-related activation of the cardiomyocyte mitochondrial apoptotic pathway in patients with acute myocarditis. *Eur Heart J* **31,** 728-736.

37. Chow LH, Beisel KW and McManus BM. (1992). Enteroviral infection of mice with severe combined immunodeficiency. Evidence for direct viral pathogenesis of myocardial injury. *Lab Invest* **66,** 24-31.

38. Wolfgram LJ, Beisel KW and Rose NR. (1985). Heart-specific autoantibodies following murine coxsackievirus B3 myocarditis. *J Exp Med* **161,** 1112-1121.

39. Maisch B, Berg PA and Kochsiek K. (1980). Autoantibodies and serum inhibition factors (sif) in patients with myocarditis. *Klin Wochenschr* **58,** 219-225.

40. Rotbart H. (1995). 13. In *Human Enterovirus Infections (*H. Rotbart, H. Rotbart)*,* 271-289. American Society for Microbiology.

41. Lee CJ, Huang YC, Yang S, Tsao KC, Chen CJ, Hsieh YC, . . . Lin TY. (2014). Clinical features of coxsackievirus A4, B3 and B4 infections in children. *PLoS One* **9,** e87391.

42. Feuer R, Mena I, Pagarigan RR, Harkins S, Hassett DE and Whitton JL. (2003). Coxsackievirus B3 and the neonatal CNS: the roles of stem cells, developing neurons, and apoptosis in infection, viral dissemination, and disease. *Am J Pathol* **163,** 1379-1393.

43. Ruller CM, Tabor-Godwin JM, Van Deren DA, Jr., Robinson SM, Maciejewski S, Gluhm S, . . . Feuer R. (2012). Neural stem cell depletion and CNS developmental defects after enteroviral infection. *Am J Pathol* **180,** 1107-1120.

44. Kamei S, Hersch SM, Kurata T and Takei Y. (1990). Coxsackie B antigen in the central nervous system of a patient with fatal acute encephalitis: immunohistochemical studies of formalin-fixed paraffin-embedded tissue. *Acta Neuropathol* **80,** 216-221.

45. Swanson PA, 2nd and McGavern DB. (2015). Viral diseases of the central nervous system. *Curr Opin Virol* **11C,** 44-54.

46. Yeung WC, Rawlinson WD and Craig ME. (2011). Enterovirus infection and type 1 diabetes mellitus: systematic review and meta-analysis of observational molecular studies. *BMJ* **342,** d35.

47. Richardson SJ, Willcox A, Bone AJ, Foulis AK and Morgan NG. (2009). The prevalence of enteroviral capsid protein vp1 immunostaining in pancreatic islets in human type 1 diabetes. *Diabetologia* **52,** 1143-1151.

48. Yoon JW, Austin M, Onodera T and Notkins AL. (1979). Isolation of a virus from the pancreas of a child with diabetic ketoacidosis. *N Engl J Med* **300,** 1173-1179.

49. Dotta F, Censini S, van Halteren AG, Marselli L, Masini M, Dionisi S, . . . Marchetti P. (2007). Coxsackie B4 virus infection of beta cells and natural killer cell insulitis in recent-onset type 1 diabetic patients. *Proc Natl Acad Sci U S A* **104,** 5115-5120.

50. Vreugdenhil GR, Geluk A, Ottenhoff TH, Melchers WJ, Roep BO and Galama JM. (1998). Molecular mimicry in diabetes mellitus: the homologous domain in coxsackie B virus protein 2C and islet autoantigen GAD65 is highly conserved in the coxsackie B-like

enteroviruses and binds to the diabetes associated HLA-DR3 molecule. *Diabetologia* **41,** 40-46.

51. Bason C, Lorini R, Lunardi C, Dolcino M, Giannattasio A, d'Annunzio G, . . . Puccetti A. (2013). In type 1 diabetes a subset of anti-coxsackievirus B4 antibodies recognize autoantigens and induce apoptosis of pancreatic beta cells. *PLoS One* **8,** e57729.

52. Horwitz MS, Bradley LM, Harbertson J, Krahl T, Lee J and Sarvetnick N. (1998). Diabetes induced by Coxsackie virus: initiation by bystander damage and not molecular mimicry. *Nat Med* **4,** 781-785.

53. Bergelson JM, Cunningham JA, Droguett G, Kurt-Jones EA, Krithivas A, Hong JS, . . . Finberg RW. (1997). Isolation of a common receptor for Coxsackie B viruses and adenoviruses 2 and 5. *Science* **275,** 1320-1323.

54. He Y, Chipman PR, Howitt J, Bator CM, Whitt MA, Baker TS, . . . Rossmann MG. (2001). Interaction of coxsackievirus B3 with the full length coxsackievirus-adenovirus receptor. *Nat Struct Biol* **8,** 874-878.

55. Rossmann MG, Arnold E, Erickson JW, Frankenberger EA, Griffith JP, Hecht HJ, . . . et al. (1985). Structure of a human common cold virus and functional relationship to other picornaviruses. *Nature* **317,** 145-153.

56. Coyne CB and Bergelson JM. (2006). Virus-induced Abl and Fyn kinase signals permit coxsackievirus entry through epithelial tight junctions. *Cell* **124,** 119-131.

57. Milstone AM, Petrella J, Sanchez MD, Mahmud M, Whitbeck JC and Bergelson JM. (2005). Interaction with coxsackievirus and adenovirus receptor, but not with decay-accelerating factor (DAF), induces A-particle formation in a DAF-binding coxsackievirus B3 isolate. *J Virol* **79,** 655-660.

58. Delorme-Axford E, Sadovsky Y and Coyne CB. (2013). Lipid raft- and SRC family kinase-dependent entry of coxsackievirus B into human placental trophoblasts. *J Virol* **87,** 8569-8581.

59. Coyne CB, Shen L, Turner JR and Bergelson JM. (2007). Coxsackievirus entry across epithelial tight junctions requires occludin and the small GTPases Rab34 and Rab5. *Cell Host Microbe* **2,** 181-192.

60. Bozym RA, Morosky SA, Kim KS, Cherry S and Coyne CB. (2010). Release of intracellular calcium stores facilitates coxsackievirus entry into polarized endothelial cells. *PLoS Pathog* **6,** e1001135.

61. Patel KP, Coyne CB and Bergelson JM. (2009). Dynamin- and lipid raft-dependent entry of decay-accelerating factor (DAF)-binding and non-DAF-binding coxsackieviruses into nonpolarized cells. *J Virol* **83,** 11064-11077.

62. Shingler KL, Yoder JL, Carnegie MS, Ashley RE, Makhov AM, Conway JF and Hafenstein S. (2013). The enterovirus 71 A-particle forms a gateway to allow genome release: a cryoEM study of picornavirus uncoating. *PLoS Pathog* **9,** e1003240.

63. Fricks CE and Hogle JM. (1990). Cell-induced conformational change in poliovirus: externalization of the amino terminus of VP1 is responsible for liposome binding. *J Virol* **64,** 1934-1945.

64. Panjwani A, Strauss M, Gold S, Wenham H, Jackson T, Chou JJ, . . . Tuthill TJ. (2014). Capsid protein VP4 of human rhinovirus induces membrane permeability by the formation of a size-selective multimeric pore. *PLoS Pathog* **10,** e1004294.

65. Organtini LJ, Makhov AM, Conway JF, Hafenstein S and Carson SD. (2014). Kinetic and structural analysis of coxsackievirus B3 receptor interactions and formation of the A-particle. *J Virol* **88,** 5755-5765.

66. Brandenburg B, Lee LY, Lakadamyali M, Rust MJ, Zhuang X and Hogle JM. (2007). Imaging poliovirus entry in live cells. *PLoS Biol* **5,** e183.

67. Lee YF, Nomoto A, Detjen BM and Wimmer E. (1977). A protein covalently linked to poliovirus genome RNA. *Proc Natl Acad Sci U S A* **74,** 59-63.

68. Flanegan JB, Petterson RF, Ambros V, Hewlett NJ and Baltimore D. (1977). Covalent linkage of a protein to a defined nucleotide sequence at the 5'-terminus of virion and replicative intermediate RNAs of poliovirus. *Proc Natl Acad Sci U S A* **74,** 961-965.

69. Pelletier J and Sonenberg N. (1988). Internal initiation of translation of eukaryotic mRNA directed by a sequence derived from poliovirus RNA. *Nature* **334,** 320-325.

70. Yang D, Wilson JE, Anderson DR, Bohunek L, Cordeiro C, Kandolf R and McManus BM. (1997). In vitro mutational and inhibitory analysis of the cis-acting translational elements within the 5' untranslated region of coxsackievirus B3: potential targets for antiviral action of antisense oligomers. *Virology* **228,** 63-73.

71. Nicklin MJ, Krausslich HG, Toyoda H, Dunn JJ and Wimmer E. (1987). Poliovirus polypeptide precursors: expression in vitro and processing by exogenous 3C and 2A proteinases. *Proc Natl Acad Sci U S A* **84,** 4002-4006.

72. Hellen C and Wimmer E. (1995). 7. In *Human Enterovirus Infections (*H. Rotbart, H. Rotbart)*,* 155-174. Washington, D.C.: American Society for Microbiology.

73. Haller A and Semler B. (1995). 5. In *Human Enterovirus Infections (*H. Rotbart, H. Rotbart)*,* 113-133. Washington, D.C.: American Society for Microbiology.

74. Schlegel A and Kirkegaard K. (1995). 6. In *Human Enterovirus Infections (*H. Rotbart, H. Rotbart)*,* 135-154. Washington, D.C.: American Society for Microbiology.

75. Ogram SA and Flanegan JB. (2011). Non-template functions of viral RNA in picornavirus replication. *Curr Opin Virol* **1,** 339-346.

76. Nugent CI, Johnson KL, Sarnow P and Kirkegaard K. (1999). Functional coupling between replication and packaging of poliovirus replicon RNA. *J Virol* **73,** 427-435.

77. Nagy PD and Pogany J. (2012). The dependence of viral RNA replication on co-opted host factors. *Nat Rev Microbiol* **10,** 137-149.

78. Carthy CM, Yanagawa B, Luo H, Granville DJ, Yang D, Cheung P, . . . McManus BM. (2003). Bcl-2 and Bcl-xL overexpression inhibits cytochrome c release, activation of multiple caspases, and virus release following coxsackievirus B3 infection. *Virology* **313,** 147-157.

79. Kim SM, Park JH, Chung SK, Kim JY, Hwang HY, Chung KC, . . . Nam JH. (2004). Coxsackievirus B3 infection induces cyr61 activation via JNK to mediate cell death. *J Virol* **78,** 13479-13488.

80. Bozym RA, Patel K, White C, Cheung KH, Bergelson JM, Morosky SA and Coyne CB. (2011). Calcium signals and calpain-dependent necrosis are essential for release of coxsackievirus B from polarized intestinal epithelial cells. *Mol Biol Cell* **22,** 3010-3021.

81. Robinson SM, Tsueng G, Sin J, Mangale V, Rahawi S, McIntyre LL, . . . Feuer R. (2014). Coxsackievirus B exits the host cell in shed microvesicles displaying autophagosomal markers. *PLoS Pathog* **10,** e1004045.

82. Chen YH, Du W, Hagemeijer MC, Takvorian PM, Pau C, Cali A, . . . Altan-Bonnet N. (2015). Phosphatidylserine vesicles enable efficient en bloc transmission of enteroviruses. *Cell* **160,** 619-630.

83. Le X, Zonghui X, Xiaolin M, Feng H, Hailan Y and Zhewei L. (2014). Coxsackievirus B3 induces crosstalk between autophagy and apoptosis to benefit its release after replicating in autophagosomes through a mechanism involving caspase cleavage of autophagy-related proteins. *Infection, Genetics and Evolution* **26,** 95-102.

84. Ozoren N and El-Deiry WS. (2003). Cell surface Death Receptor signaling in normal and cancer cells. *Semin Cancer Biol* **13,** 135-147.

85. Zhao X, Ai M, Guo Y, Zhou X, Wang L, Li X and Yao C. (2012). Poly I:C-induced tumor cell apoptosis mediated by pattern-recognition receptors. *Cancer Biother Radiopharm* **27,** 530-534.

86. Kerr JF, Wyllie AH and Currie AR. (1972). Apoptosis: a basic biological phenomenon with wide-ranging implications in tissue kinetics. *Br J Cancer* **26,** 239-257.

87. Yuan J, Shaham S, Ledoux S, Ellis HM and Horvitz HR. (1993). The C. elegans cell death gene ced-3 encodes a protein similar to mammalian interleukin-1 beta-converting enzyme. *Cell* **75,** 641-652.

88. Salvesen GS and Dixit VM. (1997). Caspases: intracellular signaling by proteolysis. *Cell* **91,** 443-446.

89. Elmore S. (2007). Apoptosis: a review of programmed cell death. *Toxicol Pathol* **35,** 495-516.

90. de Almagro MC and Vucic D. (2015). Necroptosis: Pathway diversity and characteristics. *Semin Cell Dev Biol*.

91. Roos WP and Kaina B. (2006). DNA damage-induced cell death by apoptosis. *Trends Mol Med* **12,** 440-450.

92. Colli ML, Nogueira TC, Allagnat F, Cunha DA, Gurzov EN, Cardozo AK, . . . Eizirik DL. (2011). Exposure to the Viral By-Product dsRNA or Coxsackivirus B5 Triggers Pancreatic Beta Cell Apoptosis via a Bim/Mcl-1 Imbalance. *PLoS Pathog* **7,** e1002267.

93. Carthy CM, Granville DJ, Watson KA, Anderson DR, Wilson JE, Yang D, . . . McManus BM. (1998). Caspase activation and specific cleavage of substrates after coxsackievirus B3-induced cytopathic effect in HeLa cells. *J Virol* **72,** 7669-7675.

94. Gomes R, Guerra-Sa R and Arruda E. (2010). Coxsackievirus B5 induced apoptosis of HeLa cells: effects on p53 and SUMO. *Virology* **396,** 256-263.

95. Ron D and Walter P. (2007). Signal integration in the endoplasmic reticulum unfolded protein response. *Nat Rev Mol Cell Biol* **8,** 519-529.

96. Kim R, Emi M, Tanabe K and Murakami S. (2006). Role of the unfolded protein response in cell death. *Apoptosis* **11,** 5-13.

97. Zhang HM, Ye X, Su Y, Yuan J, Liu Z, Stein DA and Yang D. (2010). Coxsackievirus B3 infection activates the unfolded protein response and induces apoptosis through downregulation of p58IPK and activation of CHOP and SREBP1. *J Virol* **84,** 8446-8459.

98. Nakagawa T, Zhu H, Morishima N, Li E, Xu J, Yankner BA and Yuan J. (2000). Caspase-12 mediates endoplasmic-reticulum-specific apoptosis and cytotoxicity by amyloid-beta. *Nature* **403,** 98-103.

99. Oyadomari S and Mori M. (2004). Roles of CHOP/GADD153 in endoplasmic reticulum stress. *Cell Death Differ* **11,** 381-389.

100. Paul A, Wilson S, Belham CM, Robinson CJ, Scott PH, Gould GW and Plevin R. (1997). Stress-activated protein kinases: activation, regulation and function. *Cell Signal* **9,** 403-410.

101. Herr I, Wilhelm D, Meyer E, Jeremias I, Angel P and Debatin KM. (1999). JNK/SAPK activity contributes to TRAIL-induced apoptosis. *Cell Death Differ* **6,** 130-135.

102. Si X, Luo H, Morgan A, Zhang J, Wong J, Yuan J, . . . McManus BM. (2005). Stress-activated protein kinases are involved in coxsackievirus B3 viral progeny release. *J Virol* **79,** 13875-13881.

103. Jensen KJ, Garmaroudi FS, Zhang J, Lin J, Boroomand S, Zhang M, . . . Janes KA. (2013). An ERK-p38 subnetwork coordinates host cell apoptosis and necrosis during coxsackievirus B3 infection. *Cell Host Microbe* **13,** 67-76.

104. Chau DH, Yuan J, Zhang H, Cheung P, Lim T, Liu Z, . . . Yang D. (2007). Coxsackievirus B3 proteases 2A and 3C induce apoptotic cell death through mitochondrial injury and cleavage of eIF4GI but not DAP5/p97/NAT1. *Apoptosis* **12,** 513-524.

105. Li ML, Hsu TA, Chen TC, Chang SC, Lee JC, Chen CC, . . . Shih SR. (2002). The 3C protease activity of enterovirus 71 induces human neural cell apoptosis. *Virology* **293,** 386-395.

106. Alexopoulou L, Holt AC, Medzhitov R and Flavell RA. (2001). Recognition of double-stranded RNA and activation of NF-kappaB by Toll-like receptor 3. *Nature* **413,** 732-738.

107. Harris KG and Coyne CB. (2013). Enter at your own risk: How enteroviruses navigate the dangerous world of pattern recognition receptor signaling. *Cytokine* **63,** 230-236.

108. Ylipaasto P, Kutlu B, Rasilainen S, Rasschaert J, Salmela K, Teerijoki H, . . . Roivainen M. (2005). Global profiling of coxsackievirus- and cytokine-induced gene expression in human pancreatic islets. *Diabetologia* **48,** 1510-1522.

109. Henke A, Nestler M, Strunze S, Saluz HP, Hortschansky P, Menzel B, . . . Munder T. (2001). The apoptotic capability of coxsackievirus B3 is influenced by the efficient interaction between the capsid protein VP2 and the proapoptotic host protein Siva. *Virology* **289,** 15-22.

110. Henke A, Launhardt H, Klement K, Stelzner A, Zell R and Munder T. (2000). Apoptosis in coxsackievirus B3-caused diseases: interaction between the capsid protein VP2 and the proapoptotic protein siva. *J Virol* **74,** 4284-4290.

111. Chu F, Borthakur A, Sun X, Barkinge J, Gudi R, Hawkins S and Prasad KV. (2004). The Siva-1 putative amphipathic helical region (SAH) is sufficient to bind to BCL-XL and sensitize cells to UV radiation induced apoptosis. *Apoptosis* **9,** 83-95.

112. Rasilainen S, Ylipaasto P, Roivainen M, Lapatto R, Hovi T and Otonkoski T. (2004). Mechanisms of coxsackievirus B5 mediated beta-cell death depend on the multiplicity of infection. *J Med Virol* **72,** 586-596.

113. Medzhitov R and Janeway CA, Jr. (1997). Innate immunity: impact on the adaptive immune response. *Curr Opin Immunol* **9,** 4-9.

114. Medzhitov R, Preston-Hurlburt P and Janeway CA, Jr. (1997). A human homologue of the Drosophila Toll protein signals activation of adaptive immunity. *Nature* **388,** 394-397.

115. Janeway CA, Jr. (1989). Approaching the asymptote? Evolution and revolution in immunology. *Cold Spring Harb Symp Quant Biol* **54,** 1-13.

116. Seth RB, Sun L and Chen ZJ. (2006). Antiviral innate immunity pathways. *Cell Res* **16,** 141-147.

117. de Veer MJ, Holko M, Frevel M, Walker E, Der S, Paranjape JM, . . . Williams BR. (2001). Functional classification of interferon-stimulated genes identified using microarrays. *J Leukoc Biol* **69,** 912-920.

118. Lopez CB and Hermesh T. (2011). Systemic responses during local viral infections: type I IFNs sound the alarm. *Curr Opin Immunol* **23,** 495-499.

119. Taylor RT, Lubick KJ, Robertson SJ, Broughton JP, Bloom ME, Bresnahan WA and Best SM. (2011). TRIM79alpha, an interferon-stimulated gene product, restricts tick-borne

encephalitis virus replication by degrading the viral RNA polymerase. *Cell Host Microbe* **10,** 185-196.

120. Pahl HL. (1999). Activators and target genes of Rel/NF-kappaB transcription factors. *Oncogene* **18,** 6853-6866.

121. Balachandran S and Beg AA. (2011). Defining emerging roles for NF-kappaB in antivirus responses: revisiting the interferon-beta enhanceosome paradigm. *PLoS Pathog* **7,** e1002165.

122. Hoyos B, Ballard DW, Bohnlein E, Siekevitz M and Greene WC. (1989). Kappa B-specific DNA binding proteins: role in the regulation of human interleukin-2 gene expression. *Science* **244,** 457-460.

123. Li M, Shillinglaw W, Henzel WJ and Beg AA. (2001). The Rela(p65) subunit of NF-kappaB is essential for inhibiting double-stranded RNA-induced cytotoxicity. *J Biol Chem* **276,** 1185-1194.

124. Thanos D and Maniatis T. (1992). The high mobility group protein HMG I(Y) is required for NF-kappa B-dependent virus induction of the human IFN-beta gene. *Cell* **71,** 777-789.

125. Lund JM, Alexopoulou L, Sato A, Karow M, Adams NC, Gale NW, . . . Flavell RA. (2004). Recognition of single-stranded RNA viruses by Toll-like receptor 7. *Proc Natl Acad Sci U S A* **101,** 5598-5603.

126. Hemmi H, Kaisho T, Takeuchi O, Sato S, Sanjo H, Hoshino K, . . . Akira S. (2002). Small anti-viral compounds activate immune cells via the TLR7 MyD88-dependent signaling pathway. *Nat Immunol* **3,** 196-200.

127. Heil F, Hemmi H, Hochrein H, Ampenberger F, Kirschning C, Akira S, . . . Bauer S. (2004). Species-specific recognition of single-stranded RNA via toll-like receptor 7 and 8. *Science* **303,** 1526-1529.

128. Diebold SS, Kaisho T, Hemmi H, Akira S and Reis e Sousa C. (2004). Innate antiviral responses by means of TLR7-mediated recognition of single-stranded RNA. *Science* **303,** 1529-1531.

129. Bauer S, Kirschning CJ, Hacker H, Redecke V, Hausmann S, Akira S, . . . Lipford GB. (2001). Human TLR9 confers responsiveness to bacterial DNA via species-specific CpG motif recognition. *Proc Natl Acad Sci U S A* **98,** 9237-9242.

130. Hemmi H, Takeuchi O, Kawai T, Kaisho T, Sato S, Sanjo H, . . . Akira S. (2000). A Toll-like receptor recognizes bacterial DNA. *Nature* **408,** 740-745.

131. Hornung V, Ellegast J, Kim S, Brzozka K, Jung A, Kato H, . . . Hartmann G. (2006). 5'-Triphosphate RNA is the ligand for RIG-I. *Science* **314,** 994-997.

132. Kato H, Takeuchi O, Mikamo-Satoh E, Hirai R, Kawai T, Matsushita K, . . . Akira S. (2008). Length-dependent recognition of double-stranded ribonucleic acids by retinoic acid-inducible gene-I and melanoma differentiation-associated gene 5. *J Exp Med* **205,** 1601-1610.

133. Pichlmair A, Schulz O, Tan CP, Naslund TI, Liljestrom P, Weber F and Reis e Sousa C. (2006). RIG-I-mediated antiviral responses to single-stranded RNA bearing 5'-phosphates. *Science* **314,** 997-1001.

134. Yoneyama M, Kikuchi M, Natsukawa T, Shinobu N, Imaizumi T, Miyagishi M, . . . Fujita T. (2004). The RNA helicase RIG-I has an essential function in double-stranded RNA-induced innate antiviral responses. *Nat Immunol* **5,** 730-737.

135. Pichlmair A, Schulz O, Tan CP, Rehwinkel J, Kato H, Takeuchi O, . . . Reis e Sousa C. (2009). Activation of MDA5 requires higher-order RNA structures generated during virus infection. *J Virol* **83,** 10761-10769.

136. Peisley A, Lin C, Wu B, Orme-Johnson M, Liu M, Walz T and Hur S. (2011). Cooperative assembly and dynamic disassembly of MDA5 filaments for viral dsRNA recognition. *Proc Natl Acad Sci U S A* **108,** 21010-21015.

137. Berke IC, Yu X, Modis Y and Egelman EH. (2012). MDA5 assembles into a polar helical filament on dsRNA. *Proc Natl Acad Sci U S A* **109,** 18437-18441.

138. Berke IC and Modis Y. (2012). MDA5 cooperatively forms dimers and ATP-sensitive filaments upon binding double-stranded RNA. *EMBO J* **31,** 1714-1726.

139. Triantafilou K, Vakakis E, Kar S, Richer E, Evans GL and Triantafilou M. (2012). Visualisation of direct interaction of MDA5 and the dsRNA replicative intermediate form of positive strand RNA viruses. *J Cell Sci* **125,** 4761-4769.

140. Wu B, Peisley A, Richards C, Yao H, Zeng X, Lin C, . . . Hur S. (2013). Structural basis for dsRNA recognition, filament formation, and antiviral signal activation by MDA5. *Cell* **152,** 276-289.

141. Rothenfusser S, Goutagny N, DiPerna G, Gong M, Monks BG, Schoenemeyer A, . . . Fitzgerald KA. (2005). The RNA helicase Lgp2 inhibits TLR-independent sensing of viral replication by retinoic acid-inducible gene-I. *J Immunol* **175,** 5260-5268.

142. Komuro A and Horvath CM. (2006). RNA- and virus-independent inhibition of antiviral signaling by RNA helicase LGP2. *J Virol* **80,** 12332-12342.

143. Saito T, Hirai R, Loo YM, Owen D, Johnson CL, Sinha SC, . . . Gale M, Jr. (2007). Regulation of innate antiviral defenses through a shared repressor domain in RIG-I and LGP2. *Proc Natl Acad Sci U S A* **104,** 582-587.

144. Satoh T, Kato H, Kumagai Y, Yoneyama M, Sato S, Matsushita K, . . . Takeuchi O. (2010
). LGP2 is a positive regulator of RIG-I- and MDA5-mediated antiviral responses. *Proc Natl Acad Sci U S A* **107,** 1512-1517.

145. Liniger M, Summerfield A, Zimmer G, McCullough KC and Ruggli N. (2011). Chicken cells sense influenza A virus infection through MDA5 and CARDIF-signaling involving LGP2. *J Virol*.

146. Richer MJ, Lavallee DJ, Shanina I and Horwitz MS. (2009). Toll-like receptor 3 signaling on macrophages is required for survival following coxsackievirus B4 infection. *PLoS One* **4,** e4127.

147. Negishi H, Osawa T, Ogami K, Ouyang X, Sakaguchi S, Koshiba R, . . . Honda K. (2008). A critical link between Toll-like receptor 3 and type II interferon signaling pathways in antiviral innate immunity. *Proc Natl Acad Sci U S A* **105,** 20446-20451.

148. Riad A, Westermann D, Zietsch C, Savvatis K, Becher PM, Bereswill S, . . . Tschope C. (2011). TRIF is a critical survival factor in viral cardiomyopathy. *J Immunol* **186,** 2561-2570.

149. Gorbea C, Makar KA, Pauschinger M, Pratt G, Bersola JL, Varela J, . . . Bowles NE. (2010). A role for Toll-like receptor 3 variants in host susceptibility to enteroviral myocarditis and dilated cardiomyopathy. *J Biol Chem* **285,** 23208-23223.

150. Triantafilou K and Triantafilou M. (2004). Coxsackievirus B4-induced cytokine production in pancreatic cells is mediated through toll-like receptor 4. *J Virol* **78,** 11313-11320.

151. Satoh M, Nakamura M, Akatsu T, Shimoda Y, Segawa I and Hiramori K. (2004). Toll-like receptor 4 is expressed with enteroviral replication in myocardium from patients with dilated cardiomyopathy. *Lab Invest* **84,** 173-181.

152. Coyne CB, Bozym R, Morosky SA, Hanna SL, Mukherjee A, Tudor M, . . . Cherry S. (2011). Comparative RNAi screening reveals host factors involved in enterovirus infection of polarized endothelial monolayers. *Cell Host Microbe* **9,** 70-82.

153. Triantafilou K, Orthopoulos G, Vakakis E, Ahmed MA, Golenbock DT, Lepper PM and Triantafilou M. (2005). Human cardiac inflammatory responses triggered by Coxsackie B viruses are mainly Toll-like receptor (TLR) 8-dependent. *Cell Microbiol* **7,** 1117-1126.

154. Wang JP, Asher DR, Chan M, Kurt-Jones EA and Finberg RW. (2007). Cutting Edge: Antibody-mediated TLR7-dependent recognition of viral RNA. *J Immunol* **178,** 3363-3367.

155. Reizis B, Bunin A, Ghosh HS, Lewis KL and Sisirak V. (2011). Plasmacytoid dendritic cells: recent progress and open questions. *Annu Rev Immunol* **29,** 163-183.

156. Feng Q, Hato SV, Langereis MA, Zoll J, Virgen-Slane R, Peisley A, . . . van Kuppeveld FJ. (2012). MDA5 detects the double-stranded RNA replicative form in picornavirus-infected cells. *Cell Rep* **2,** 1187-1196.

157. Wang JP, Cerny A, Asher DR, Kurt-Jones EA, Bronson RT and Finberg RW. (2010). MDA5 and MAVS mediate type I interferon responses to coxsackie B virus. *J Virol* **84,** 254-260.

158. Huhn MH, McCartney SA, Lind K, Svedin E, Colonna M and Flodstrom-Tullberg M. (2010). Melanoma differentiation-associated protein-5 (MDA-5) limits early viral replication but is not essential for the induction of type 1 interferons after Coxsackievirus infection. *Virology* **401,** 42-48.

159. Imagawa A and Hanafusa T. (2006). Pathogenesis of fulminant type 1 diabetes. *Rev Diabet Stud* **3,** 169-177.

160. Aida K, Nishida Y, Tanaka S, Maruyama T, Shimada A, Awata T, . . . Kobayashi T. (2011). RIG-I- and MDA5-initiated innate immunity linked with adaptive immunity accelerates beta-cell death in fulminant type 1 diabetes. *Diabetes* **60,** 884-889.

161. Schneider RJ and Mohr I. (2003). Translation initiation and viral tricks. *Trends Biochem Sci* **28,** 130-136.

162. Liebig HD, Ziegler E, Yan R, Hartmuth K, Klump H, Kowalski H, . . . et al. (1993). Purification of two picornaviral 2A proteinases: interaction with eIF-4 gamma and influence on in vitro translation. *Biochemistry* **32,** 7581-7588.

163. Lamphear BJ, Yan R, Yang F, Waters D, Liebig HD, Klump H, . . . Rhoads RE. (1993). Mapping the cleavage site in protein synthesis initiation factor eIF-4 gamma of the 2A proteases from human Coxsackievirus and rhinovirus. *J Biol Chem* **268,** 19200-19203.

164. Kerekatte V, Keiper BD, Badorff C, Cai A, Knowlton KU and Rhoads RE. (1999). Cleavage of Poly(A)-binding protein by coxsackievirus 2A protease in vitro and in vivo: another mechanism for host protein synthesis shutoff? *J Virol* **73,** 709-717.

165. Clark ME, Hammerle T, Wimmer E and Dasgupta A. (1991). Poliovirus proteinase 3C converts an active form of transcription factor IIIC to an inactive form: a mechanism for inhibition of host cell polymerase III transcription by poliovirus. *EMBO J* **10,** 2941-2947.

166. Kundu P, Raychaudhuri S, Tsai W and Dasgupta A. (2005). Shutoff of RNA polymerase II transcription by poliovirus involves 3C protease-mediated cleavage of the TATA-binding protein at an alternative site: incomplete shutoff of transcription interferes with efficient viral replication. *J Virol* **79,** 9702-9713.

167. Cooray S. (2004). The pivotal role of phosphatidylinositol 3-kinase-Akt signal transduction in virus survival. *J Gen Virol* **85,** 1065-1076.

168. Esfandiarei M, Luo H, Yanagawa B, Suarez A, Dabiri D, Zhang J and McManus BM. (2004). Protein kinase B/Akt regulates coxsackievirus B3 replication through a mechanism which is not caspase dependent. *J Virol* **78,** 4289-4298.

169. Jaber N, Dou Z, Chen JS, Catanzaro J, Jiang YP, Ballou LM, . . . Zong WX. (2012). Class III PI3K Vps34 plays an essential role in autophagy and in heart and liver function. *Proc Natl Acad Sci U S A* **109,** 2003-2008.

170. Russell RC, Tian Y, Yuan H, Park HW, Chang YY, Kim J, . . . Guan KL. (2013). ULK1 induces autophagy by phosphorylating Beclin-1 and activating VPS34 lipid kinase. *Nat Cell Biol* **15,** 741-750.

171. Zhang HM, Yuan J, Cheung P, Luo H, Yanagawa B, Chau D, . . . Yang D. (2003). Overexpression of interferon-gamma-inducible GTPase inhibits coxsackievirus B3-induced apoptosis through the activation of the phosphatidylinositol 3-kinase/Akt pathway and inhibition of viral replication. *J Biol Chem* **278,** 33011-33019.

172. Yang D, Yu J, Luo Z, Carthy CM, Wilson JE, Liu Z and McManus BM. (1999). Viral myocarditis: identification of five differentially expressed genes in coxsackievirus B3-infected mouse heart. *Circ Res* **84,** 704-712.

173. Hwang HY, Kim JY, Lim JY, Chung SK, Nam JH and Park SI. (2007). Coxsackievirus B3 modulates cell death by downregulating activating transcription factor 3 in HeLa cells. *Virus Res* **130,** 10-17.

174. Mukherjee A, Morosky SA, Delorme-Axford E, Dybdahl-Sissoko N, Oberste MS, Wang T and Coyne CB. (2011). The coxsackievirus B 3C protease cleaves MAVS and TRIF to attenuate host type I interferon and apoptotic signaling. *PLoS Pathog* **7,** e1001311.

175. van Kuppeveld FJ, Hoenderop JG, Smeets RL, Willems PH, Dijkman HB, Galama JM and Melchers WJ. (1997). Coxsackievirus protein 2B modifies endoplasmic reticulum membrane and plasma membrane permeability and facilitates virus release. *EMBO J* **16,** 3519-3532.

176. Brisac C, Teoule F, Autret A, Pelletier I, Colbere-Garapin F, Brenner C, . . . Blondel B. (2010). Calcium flux between the endoplasmic reticulum and mitochondrion contributes to poliovirus-induced apoptosis. *J Virol* **84,** 12226-12235.

177. Madan V, Castello A and Carrasco L. (2008). Viroporins from RNA viruses induce caspase-dependent apoptosis. *Cell Microbiol* **10,** 437-451.

178. van Kuppeveld FJ, de Jong AS, Melchers WJ and Willems PH. (2005). Enterovirus protein 2B po(u)res out the calcium: a viral strategy to survive? *Trends Microbiol* **13,** 41-44.

179. Campanella M, de Jong AS, Lanke KW, Melchers WJ, Willems PH, Pinton P, . . . van Kuppeveld FJ. (2004). The coxsackievirus 2B protein suppresses apoptotic host cell responses by manipulating intracellular Ca2+ homeostasis. *J Biol Chem* **279,** 18440-18450.

180. Bozym RA, Delorme-Axford E, Harris K, Morosky S, Ikizler M, Dermody TS, . . . Coyne CB. (2012). Focal adhesion kinase is a component of antiviral RIG-I-like receptor signaling. *Cell Host Microbe* **11,** 153-166.

181. Marshak-Rothstein A. (2006). Toll-like receptors in systemic autoimmune disease. *Nat Rev Immunol* **6,** 823-835.

182. Celhar T, Magalhaes R and Fairhurst AM. (2012). TLR7 and TLR9 in SLE: when sensing self goes wrong. *Immunol Res* **53,** 58-77.

183. Lee BL and Barton GM. (2014). Trafficking of endosomal Toll-like receptors. *Trends Cell Biol* **24,** 360-369.

184. Barton GM, Kagan JC and Medzhitov R. (2006). Intracellular localization of Toll-like receptor 9 prevents recognition of self DNA but facilitates access to viral DNA. *Nat Immunol* **7,** 49-56.

185. Latz E, Schoenemeyer A, Visintin A, Fitzgerald KA, Monks BG, Knetter CF, . . . Golenbock DT. (2004). TLR9 signals after translocating from the ER to CpG DNA in the lysosome. *Nat Immunol* **5,** 190-198.

186. Kim YM, Brinkmann MM, Paquet ME and Ploegh HL. (2008). UNC93B1 delivers nucleotide-sensing toll-like receptors to endolysosomes. *Nature* **452,** 234-238.

187. Garcia-Cattaneo A, Gobert FX, Muller M, Toscano F, Flores M, Lescure A, . . . Benaroch P. (2012). Cleavage of Toll-like receptor 3 by cathepsins B and H is essential for signaling. *Proc Natl Acad Sci U S A* **109,** 9053-9058.

188. Ewald SE, Lee BL, Lau L, Wickliffe KE, Shi GP, Chapman HA and Barton GM. (2008). The ectodomain of Toll-like receptor 9 is cleaved to generate a functional receptor. *Nature* **456,** 658-662.

189. Ewald SE, Engel A, Lee J, Wang M, Bogyo M and Barton GM. (2011). Nucleic acid recognition by Toll-like receptors is coupled to stepwise processing by cathepsins and asparagine endopeptidase. *J Exp Med* **208,** 643-651.

190. Sepulveda FE, Maschalidi S, Colisson R, Heslop L, Ghirelli C, Sakka E, . . . Manoury B. (2009). Critical role for asparagine endopeptidase in endocytic Toll-like receptor signaling in dendritic cells. *Immunity* **31,** 737-748.

191. Park B, Brinkmann MM, Spooner E, Lee CC, Kim YM and Ploegh HL. (2008). Proteolytic cleavage in an endolysosomal compartment is required for activation of Toll-like receptor 9. *Nat Immunol* **9,** 1407-1414.

192. Tabeta K, Hoebe K, Janssen EM, Du X, Georgel P, Crozat K, . . . Beutler B. (2006). The Unc93b1 mutation 3d disrupts exogenous antigen presentation and signaling via Toll-like receptors 3, 7 and 9. *Nat Immunol* **7,** 156-164.

193. Itoh H, Tatematsu M, Watanabe A, Iwano K, Funami K, Seya T and Matsumoto M. (2011). UNC93B1 physically associates with human TLR8 and regulates TLR8-mediated signaling. *PLoS One* **6,** e28500.

194. Pifer R, Benson A, Sturge CR and Yarovinsky F. (2011). UNC93B1 is essential for TLR11 activation and IL-12-dependent host resistance to Toxoplasma gondii. *J Biol Chem* **286,** 3307-3314.

195. Huh JW, Shibata T, Hwang M, Kwon EH, Jang MS, Fukui R, . . . Kim YM. (2014). UNC93B1 is essential for the plasma membrane localization and signaling of Toll-like receptor 5. *Proc Natl Acad Sci U S A.*

196. Brinkmann MM, Spooner E, Hoebe K, Beutler B, Ploegh HL and Kim YM. (2007). The interaction between the ER membrane protein UNC93B and TLR3, 7, and 9 is crucial for TLR signaling. *J Cell Biol* **177,** 265-275.

197. Lee BL, Moon JE, Shu JH, Yuan L, Newman ZR, Schekman R and Barton GM. (2013). UNC93B1 mediates differential trafficking of endosomal TLRs. *Elife* **2,** e00291.

198. Fukui R, Saitoh S, Matsumoto F, Kozuka-Hata H, Oyama M, Tabeta K, . . . Miyake K. (2009). Unc93B1 biases Toll-like receptor responses to nucleic acid in dendritic cells toward DNA- but against RNA-sensing. *J Exp Med* **206,** 1339-1350.

199. Fukui R, Saitoh S, Kanno A, Onji M, Shibata T, Ito A, . . . Miyake K. (2011). Unc93B1 restricts systemic lethal inflammation by orchestrating Toll-like receptor 7 and 9 trafficking. *Immunity* **35,** 69-81.

200. Pelka K, Phulphagar K, Zimmermann J, Stahl R, Schmid-Burgk JL, Schmidt T, . . . Latz E. (2014). Cutting edge: the UNC93B1 tyrosine-based motif regulates trafficking and TLR responses via separate mechanisms. *J Immunol* **193,** 3257-3261.

201. Lafferty EI, Wiltshire SA, Angers I, Vidal SM and Qureshi ST. (2015). Unc93b1 - Dependent Endosomal Toll-Like Receptor Signaling Regulates Inflammation and Mortality during Coxsackievirus B3 Infection. *J Innate Immun*.

202. Galluzzi L, Bravo-San Pedro JM, Vitale I, Aaronson SA, Abrams JM, Adam D, . . . Kroemer G. (2015). Essential versus accessory aspects of cell death: recommendations of the NCCD 2015. *Cell Death Differ* **22,** 58-73.

203. Hengartner MO. (2000). The biochemistry of apoptosis. *Nature* **407,** 770-776.

204. Golstein P and Kroemer G. (2007). Cell death by necrosis: towards a molecular definition. *Trends Biochem Sci* **32,** 37-43.

205. Hitomi J, Christofferson DE, Ng A, Yao J, Degterev A, Xavier RJ and Yuan J. (2008). Identification of a molecular signaling network that regulates a cellular necrotic cell death pathway. *Cell* **135,** 1311-1323.

206. Zhang DW, Shao J, Lin J, Zhang N, Lu BJ, Lin SC, . . . Han J. (2009). RIP3, an energy metabolism regulator that switches TNF-induced cell death from apoptosis to necrosis. *Science* **325,** 332-336.

207. He S, Wang L, Miao L, Wang T, Du F, Zhao L and Wang X. (2009). Receptor interacting protein kinase-3 determines cellular necrotic response to TNF-alpha. *Cell* **137,** 1100-1111.

208. Cho YS, Challa S, Moquin D, Genga R, Ray TD, Guildford M and Chan FK. (2009). Phosphorylation-driven assembly of the RIP1-RIP3 complex regulates programmed necrosis and virus-induced inflammation. *Cell* **137,** 1112-1123.

209. Galluzzi L, Vitale I, Abrams JM, Alnemri ES, Baehrecke EH, Blagosklonny MV, . . . Kroemer G. (2012). Molecular definitions of cell death subroutines: recommendations of the Nomenclature Committee on Cell Death 2012. *Cell Death Differ* **19,** 107-120.

210. Hsu H, Xiong J and Goeddel DV. (1995). The TNF receptor 1-associated protein TRADD signals cell death and NF-kappa B activation. *Cell* **81,** 495-504.

211. Hsu H, Huang J, Shu HB, Baichwal V and Goeddel DV. (1996). TNF-dependent recruitment of the protein kinase RIP to the TNF receptor-1 signaling complex. *Immunity* **4,** 387-396.

212. Rothe M, Wong SC, Henzel WJ and Goeddel DV. (1994). A novel family of putative signal transducers associated with the cytoplasmic domain of the 75 kDa tumor necrosis factor receptor. *Cell* **78,** 681-692.

213. Hsu H, Shu HB, Pan MG and Goeddel DV. (1996). TRADD-TRAF2 and TRADD-FADD interactions define two distinct TNF receptor 1 signal transduction pathways. *Cell* **84,** 299-308.

214. Ea CK, Deng L, Xia ZP, Pineda G and Chen ZJ. (2006). Activation of IKK by TNFalpha requires site-specific ubiquitination of RIP1 and polyubiquitin binding by NEMO. *Mol Cell* **22,** 245-257.

215. Micheau O and Tschopp J. (2003). Induction of TNF receptor I-mediated apoptosis via two sequential signaling complexes. *Cell* **114,** 181-190.

216. Kelliher MA, Grimm S, Ishida Y, Kuo F, Stanger BZ and Leder P. (1998). The death domain kinase RIP mediates the TNF-induced NF-kappaB signal. *Immunity* **8,** 297-303.

217. Bertrand MJ, Milutinovic S, Dickson KM, Ho WC, Boudreault A, Durkin J, . . . Barker PA. (2008). cIAP1 and cIAP2 facilitate cancer cell survival by functioning as E3 ligases that promote RIP1 ubiquitination. *Mol Cell* **30,** 689-700.

218. Mahoney DJ, Cheung HH, Mrad RL, Plenchette S, Simard C, Enwere E, . . . Korneluk RG. (2008). Both cIAP1 and cIAP2 regulate TNFalpha-mediated NF-kappaB activation. *Proc Natl Acad Sci U S A* **105,** 11778-11783.

219. Varfolomeev E, Goncharov T, Fedorova AV, Dynek JN, Zobel K, Deshayes K, . . . Vucic D. (2008). c-IAP1 and c-IAP2 are critical mediators of tumor necrosis factor alpha (TNFalpha)-induced NF-kappaB activation. *J Biol Chem* **283,** 24295-24299.

220. O'Donnell MA and Ting AT. (2010). Chronicles of a death foretold: dual sequential cell death checkpoints in TNF signaling. *Cell Cycle* **9,** 1065-1071.

221. Wang L, Du F and Wang X. (2008). TNF-alpha induces two distinct caspase-8 activation pathways. *Cell* **133,** 693-703.

222. Vanlangenakker N, Vanden Berghe T, Bogaert P, Laukens B, Zobel K, Deshayes K, . . . Bertrand MJ. (2011). cIAP1 and TAK1 protect cells from TNF-induced necrosis by preventing RIP1/RIP3-dependent reactive oxygen species production. *Cell Death Differ* **18,** 656-665.

223. Feoktistova M, Geserick P, Kellert B, Dimitrova DP, Langlais C, Hupe M, . . . Leverkus M. (2011). cIAPs block Ripoptosome formation, a RIP1/caspase-8 containing intracellular cell death complex differentially regulated by cFLIP isoforms. *Mol Cell* **43,** 449-463.

224. Tenev T, Bianchi K, Darding M, Broemer M, Langlais C, Wallberg F, . . . Meier P. (2011). The Ripoptosome, a signaling platform that assembles in response to genotoxic stress and loss of IAPs. *Mol Cell* **43,** 432-448.

225. Kaiser WJ, Sridharan H, Huang C, Mandal P, Upton JW, Gough PJ, . . . Mocarski ES. (2013). Toll-like receptor 3-mediated necrosis via TRIF, RIP3, and MLKL. *J Biol Chem* **288,** 31268-31279.

226. He S, Liang Y, Shao F and Wang X. (2011). Toll-like receptors activate programmed necrosis in macrophages through a receptor-interacting kinase-3-mediated pathway. *Proc Natl Acad Sci U S A* **108,** 20054-20059.

227. Upton JW, Kaiser WJ and Mocarski ES. (2012). DAI/ZBP1/DLM-1 complexes with RIP3 to mediate virus-induced programmed necrosis that is targeted by murine cytomegalovirus vIRA. *Cell Host Microbe* **11,** 290-297.

228. He MX and He YW. (2013). A role for c-FLIP(L) in the regulation of apoptosis, autophagy, and necroptosis in T lymphocytes. *Cell Death Differ* **20,** 188-197.

229. Lu JV, Weist BM, van Raam BJ, Marro BS, Nguyen LV, Srinivas P, . . . Walsh CM. (2011). Complementary roles of Fas-associated death domain (FADD) and receptor interacting protein kinase-3 (RIPK3) in T-cell homeostasis and antiviral immunity. *Proc Natl Acad Sci U S A* **108,** 15312-15317.

230. Thapa RJ, Nogusa S, Chen P, Maki JL, Lerro A, Andrake M, . . . Balachandran S. (2013). Interferon-induced RIP1/RIP3-mediated necrosis requires PKR and is licensed by FADD and caspases. *Proc Natl Acad Sci U S A* **110,** E3109-3118.

231. McComb S, Cessford E, Alturki NA, Joseph J, Shutinoski B, Startek JB, . . . Sad S. (2014). Type-I interferon signaling through ISGF3 complex is required for sustained Rip3 activation and necroptosis in macrophages. *Proc Natl Acad Sci U S A* **111,** E3206-3213.

232. Saveljeva S, Mc Laughlin SL, Vandenabeele P, Samali A and Bertrand MJ. (2015). Endoplasmic reticulum stress induces ligand-independent TNFR1-mediated necroptosis in L929 cells. *Cell Death Dis* **6,** e1587.

233. Oberst A, Dillon CP, Weinlich R, McCormick LL, Fitzgerald P, Pop C, . . . Green DR. (2011). Catalytic activity of the caspase-8-FLIP(L) complex inhibits RIPK3-dependent necrosis. *Nature* **471,** 363-367.

234. Srinivasula SM, Ahmad M, Fernandes-Alnemri T, Litwack G and Alnemri ES. (1996). Molecular ordering of the Fas-apoptotic pathway: the Fas/APO-1 protease Mch5 is a CrmA-inhibitable protease that activates multiple Ced-3/ICE-like cysteine proteases. *Proc Natl Acad Sci U S A* **93,** 14486-14491.

235. Fernandes-Alnemri T, Armstrong RC, Krebs J, Srinivasula SM, Wang L, Bullrich F, . . . Alnemri ES. (1996). In vitro activation of CPP32 and Mch3 by Mch4, a novel human apoptotic cysteine protease containing two FADD-like domains. *Proc Natl Acad Sci U S A* **93,** 7464-7469.

236. Feng S, Yang Y, Mei Y, Ma L, Zhu DE, Hoti N, . . . Wu M. (2007). Cleavage of RIP3 inactivates its caspase-independent apoptosis pathway by removal of kinase domain. *Cell Signal* **19,** 2056-2067.

237. O'Donnell MA, Perez-Jimenez E, Oberst A, Ng A, Massoumi R, Xavier R, . . . Ting AT. (2011). Caspase 8 inhibits programmed necrosis by processing CYLD. *Nat Cell Biol* **13,** 1437-1442.

238. Irmler M, Thome M, Hahne M, Schneider P, Hofmann K, Steiner V, . . . Tschopp J. (1997). Inhibition of death receptor signals by cellular FLIP. *Nature* **388,** 190-195.

239. Boatright KM, Deis C, Denault JB, Sutherlin DP and Salvesen GS. (2004). Activation of caspases-8 and -10 by FLIP(L). *Biochem J* **382,** 651-657.

240. Micheau O, Thome M, Schneider P, Holler N, Tschopp J, Nicholson DW, . . . Grutter MG. (2002). The long form of FLIP is an activator of caspase-8 at the Fas death-inducing signaling complex. *J Biol Chem* **277,** 45162-45171.

241. Kaiser WJ, Upton JW, Long AB, Livingston-Rosanoff D, Daley-Bauer LP, Hakem R, . . . Mocarski ES. (2011). RIP3 mediates the embryonic lethality of caspase-8-deficient mice. *Nature* **471,** 368-372.

242. Welz PS, Wullaert A, Vlantis K, Kondylis V, Fernandez-Majada V, Ermolaeva M, . . . Pasparakis M. (2011). FADD prevents RIP3-mediated epithelial cell necrosis and chronic intestinal inflammation. *Nature* **477,** 330-334.

243. Bonnet MC, Preukschat D, Welz PS, van Loo G, Ermolaeva MA, Bloch W, . . . Pasparakis M. (2011). The adaptor protein FADD protects epidermal keratinocytes from necroptosis in vivo and prevents skin inflammation. *Immunity* **35,** 572-582.

244. Yabal M, Muller N, Adler H, Knies N, Gross CJ, Damgaard RB, . . . Jost PJ. (2014). XIAP restricts TNF- and RIP3-dependent cell death and inflammasome activation. *Cell Rep* **7,** 1796-1808.

245. Lawlor KE, Khan N, Mildenhall A, Gerlic M, Croker BA, D'Cruz AA, . . . Vince JE. (2015). RIPK3 promotes cell death and NLRP3 inflammasome activation in the absence of MLKL. *Nat Commun* **6,** 6282.

246. Dillon CP, Weinlich R, Rodriguez DA, Cripps JG, Quarato G, Gurung P, . . . Green DR. (2014). RIPK1 blocks early postnatal lethality mediated by caspase-8 and RIPK3. *Cell* **157,** 1189-1202.

247. Kaiser WJ, Daley-Bauer LP, Thapa RJ, Mandal P, Berger SB, Huang C, . . . Mocarski ES. (2014). RIP1 suppresses innate immune necrotic as well as apoptotic cell death during mammalian parturition. *Proc Natl Acad Sci U S A* **111,** 7753-7758.

248. Rickard JA, O'Donnell JA, Evans JM, Lalaoui N, Poh AR, Rogers T, . . . Silke J. (2014). RIPK1 regulates RIPK3-MLKL-driven systemic inflammation and emergency hematopoiesis. *Cell* **157,** 1175-1188.

249. Orozco S, Yatim N, Werner MR, Tran H, Gunja SY, Tait SW, . . . Oberst A. (2014). RIPK1 both positively and negatively regulates RIPK3 oligomerization and necroptosis. *Cell Death Differ* **21,** 1511-1521.

250. Chen W, Wu J, Li L, Zhang Z, Ren J, Liang Y, . . . Han J. (2015). Ppm1b negatively regulates necroptosis through dephosphorylating Rip3. *Nat Cell Biol*.

251. Sasaki M, Ohnishi M, Tashiro F, Niwa H, Suzuki A, Miyazaki J, . . . Tamura S. (2007). Disruption of the mouse protein Ser/Thr phosphatase 2Cbeta gene leads to early pre-implantation lethality. *Mech Dev* **124,** 489-499.

252. Sun X, Yin J, Starovasnik MA, Fairbrother WJ and Dixit VM. (2002). Identification of a novel homotypic interaction motif required for the phosphorylation of receptor-interacting protein (RIP) by RIP3. *J Biol Chem* **277,** 9505-9511.

253. Kaiser WJ and Offermann MK. (2005). Apoptosis induced by the toll-like receptor adaptor TRIF is dependent on its receptor interacting protein homotypic interaction motif. *J Immunol* **174,** 4942-4952.

254. Kaiser WJ, Upton JW and Mocarski ES. (2008). Receptor-interacting protein homotypic interaction motif-dependent control of NF-kappa B activation via the DNA-dependent activator of IFN regulatory factors. *J Immunol* **181,** 6427-6434.

255. Rebsamen M, Heinz LX, Meylan E, Michallet MC, Schroder K, Hofmann K, . . . Tschopp J. (2009). DAI/ZBP1 recruits RIP1 and RIP3 through RIP homotypic interaction motifs to activate NF-kappaB. *EMBO Rep* **10,** 916-922.

256. Li J, McQuade T, Siemer AB, Napetschnig J, Moriwaki K, Hsiao YS, . . . Wu H. (2012). The RIP1/RIP3 necrosome forms a functional amyloid signaling complex required for programmed necrosis. *Cell* **150,** 339-350.

257. Wu XN, Yang ZH, Wang XK, Zhang Y, Wan H, Song Y, . . . Han J. (2014). Distinct roles of RIP1-RIP3 hetero- and RIP3-RIP3 homo-interaction in mediating necroptosis. *Cell Death Differ* **21,** 1709-1720.

258. Sun L, Wang H, Wang Z, He S, Chen S, Liao D, . . . Wang X. (2012). Mixed lineage kinase domain-like protein mediates necrosis signaling downstream of RIP3 kinase. *Cell* **148,** 213-227.

259. Xie T, Peng W, Yan C, Wu J, Gong X and Shi Y. (2013). Structural insights into RIP3-mediated necroptotic signaling. *Cell Rep* **5,** 70-78.

260. Chen W, Zhou Z, Li L, Zhong CQ, Zheng X, Wu X, . . . Han J. (2013). Diverse sequence determinants control human and mouse receptor interacting protein 3 (RIP3) and mixed lineage kinase domain-like (MLKL) interaction in necroptotic signaling. *J Biol Chem* **288,** 16247-16261.

261. Murphy JM, Czabotar PE, Hildebrand JM, Lucet IS, Zhang JG, Alvarez-Diaz S, . . . Alexander WS. (2013). The pseudokinase MLKL mediates necroptosis via a molecular switch mechanism. *Immunity* **39,** 443-453.

262. Wu J, Huang Z, Ren J, Zhang Z, He P, Li Y, . . . Han J. (2013). Mlkl knockout mice demonstrate the indispensable role of Mlkl in necroptosis. *Cell Res* **23,** 994-1006.

263. Tait SW, Oberst A, Quarato G, Milasta S, Haller M, Wang R, . . . Green DR. (2013). Widespread mitochondrial depletion via mitophagy does not compromise necroptosis. *Cell Rep* **5,** 878-885.

264. Chen X, Li W, Ren J, Huang D, He WT, Song Y, . . . Han J. (2014). Translocation of mixed lineage kinase domain-like protein to plasma membrane leads to necrotic cell death. *Cell Res* **24,** 105-121.

265. Cai Z, Jitkaew S, Zhao J, Chiang HC, Choksi S, Liu J, . . . Liu ZG. (2014). Plasma membrane translocation of trimerized MLKL protein is required for TNF-induced necroptosis. *Nat Cell Biol* **16,** 55-65.

266. Dondelinger Y, Declercq W, Montessuit S, Roelandt R, Goncalves A, Bruggeman I, . . . Vandenabeele P. (2014). MLKL compromises plasma membrane integrity by binding to phosphatidylinositol phosphates. *Cell Rep* **7,** 971-981.

267. Su L, Quade B, Wang H, Sun L, Wang X and Rizo J. (2014). A plug release mechanism for membrane permeation by MLKL. *Structure* **22,** 1489-1500.

268. Hildebrand JM, Tanzer MC, Lucet IS, Young SN, Spall SK, Sharma P, . . . Silke J. (2014). Activation of the pseudokinase MLKL unleashes the four-helix bundle domain to induce membrane localization and necroptotic cell death. *Proc Natl Acad Sci U S A* **111,** 15072-15077.

269. Ramachandran A, McGill MR, Xie Y, Ni HM, Ding WX and Jaeschke H. (2013). Receptor interacting protein kinase 3 is a critical early mediator of acetaminophen-induced hepatocyte necrosis in mice. *Hepatology* **58,** 2099-2108.

270. Wang H, Sun L, Su L, Rizo J, Liu L, Wang LF, . . . Wang X. (2014). Mixed lineage kinase domain-like protein MLKL causes necrotic membrane disruption upon phosphorylation by RIP3. *Mol Cell* **54,** 133-146.

271. Wang X, Jiang W, Yan Y, Gong T, Han J, Tian Z and Zhou R. (2014). RNA viruses promote activation of the NLRP3 inflammasome through a RIP1-RIP3-DRP1 signaling pathway. *Nat Immunol* **15,** 1126-1133.

272. Upton JW, Kaiser WJ and Mocarski ES. (2008). Cytomegalovirus M45 cell death suppression requires receptor-interacting protein (RIP) homotypic interaction motif (RHIM)-dependent interaction with RIP1. *J Biol Chem* **283,** 16966-16970.

273. Upton JW, Kaiser WJ and Mocarski ES. (2010). Virus inhibition of RIP3-dependent necrosis. *Cell Host Microbe* **7,** 302-313.

274. Omoto S, Guo H, Talekar GR, Roback L, Kaiser WJ and Mocarski E. (2015). Suppression of RIP3-dependent Necroptosis by Human Cytomegalovirus. *J Biol Chem*.

275. Wang X, Li Y, Liu S, Yu X, Li L, Shi C, . . . He S. (2014). Direct activation of RIP3/MLKL-dependent necrosis by herpes simplex virus 1 (HSV-1) protein ICP6 triggers host antiviral defense. *Proc Natl Acad Sci U S A* **111,** 15438-15443.

276. Guo H, Omoto S, Harris PA, Finger JN, Bertin J, Gough PJ, . . . Mocarski ES. (2015). Herpes simplex virus suppresses necroptosis in human cells. *Cell Host Microbe* **17,** 243-251.

277. Huang Z, Wu SQ, Liang Y, Zhou X, Chen W, Li L, . . . Han J. (2015). RIP1/RIP3 Binding to HSV-1 ICP6 Initiates Necroptosis to Restrict Virus Propagation in Mice. *Cell Host Microbe* **17,** 229-242.

278. Rodrigue-Gervais IG, Labbe K, Dagenais M, Dupaul-Chicoine J, Champagne C, Morizot A, . . . Saleh M. (2014). Cellular inhibitor of apoptosis protein cIAP2 protects against pulmonary tissue necrosis during influenza virus infection to promote host survival. *Cell Host Microbe* **15,** 23-35.

279. Dobbelstein M and Shenk T. (1996). Protection against apoptosis by the vaccinia virus SPI-2 (B13R) gene product. *J Virol* **70,** 6479-6485.

280. Robinson N, McComb S, Mulligan R, Dudani R, Krishnan L and Sad S. (2012). Type I interferon induces necroptosis in macrophages during infection with Salmonella enterica serovar Typhimurium. *Nat Immunol* **13,** 954-962.

281. Autheman D, Wyder M, Popoff M, D'Herde K, Christen S and Posthaus H. (2013). Clostridium perfringens beta-toxin induces necrostatin-inhibitable, calpain-dependent necrosis in primary porcine endothelial cells. *PLoS One* **8,** e64644.

282. Murakami Y, Matsumoto H, Roh M, Suzuki J, Hisatomi T, Ikeda Y, . . . Vavvas DG. (2012). Receptor interacting protein kinase mediates necrotic cone but not rod cell death in a mouse model of inherited degeneration. *Proc Natl Acad Sci U S A* **109,** 14598-14603.

283. Hanus J, Zhang H, Wang Z, Liu Q, Zhou Q and Wang S. (2013). Induction of necrotic cell death by oxidative stress in retinal pigment epithelial cells. *Cell Death Dis* **4,** e965.

284. Gunther C, Martini E, Wittkopf N, Amann K, Weigmann B, Neumann H, . . . Becker C. (2011). Caspase-8 regulates TNF-alpha-induced epithelial necroptosis and terminal ileitis. *Nature* **477,** 335-339.

285. Pierdomenico M, Negroni A, Stronati L, Vitali R, Prete E, Bertin J, . . . Cucchiara S. (2014). Necroptosis is active in children with inflammatory bowel disease and contributes to heighten intestinal inflammation. *Am J Gastroenterol* **109,** 279-287.

286. Gautheron J, Vucur M, Reisinger F, Cardenas DV, Roderburg C, Koppe C, . . . Luedde T. (2014). A positive feedback loop between RIP3 and JNK controls non-alcoholic steatohepatitis. *EMBO Mol Med* **6,** 1062-1074.

287. Kyung Kim S, Kim WJ, Yoon JH, Ji JH, Morgan MJ, Cho H, . . . Kim YS. (2015). Upregulated RIP3 Expression Potentiates MLKL Phosphorylation-Mediated Programmed Necrosis in Toxic Epidermal Necrolysis. *J Invest Dermatol*.

288. Saito N, Qiao H, Yanagi T, Shinkuma S, Nishimura K, Suto A, . . . Abe R. (2014). An annexin A1-FPR1 interaction contributes to necroptosis of keratinocytes in severe cutaneous adverse drug reactions. *Sci Transl Med* **6,** 245ra295.

289. Linkermann A, Brasen JH, De Zen F, Weinlich R, Schwendener RA, Green DR, . . . Krautwald S. (2012). Dichotomy between RIP1- and RIP3-mediated necroptosis in tumor necrosis factor-alpha-induced shock. *Mol Med* **18,** 577-586.

290. Duprez L, Takahashi N, Van Hauwermeiren F, Vandendriessche B, Goossens V, Vanden Berghe T, . . . Vandenabeele P. (2011). RIP kinase-dependent necrosis drives lethal systemic inflammatory response syndrome. *Immunity* **35,** 908-918.

291. Ohsumi Y. (2014). Historical landmarks of autophagy research. *Cell Res* **24,** 9-23.

292. Kraft C, Reggiori F and Peter M. (2009). Selective types of autophagy in yeast. *Biochim Biophys Acta* **1793,** 1404-1412.

293. Liu L, Sakakibara K, Chen Q and Okamoto K. (2014). Receptor-mediated mitophagy in yeast and mammalian systems. *Cell Res* **24,** 787-795.

294. Sibirny AA. (2011). Mechanisms of autophagy and pexophagy in yeasts. *Biochemistry (Mosc)* **76,** 1279-1290.

295. Gomes LC and Dikic I. (2014). Autophagy in antimicrobial immunity. *Mol Cell* **54,** 224-233.

296. Devenish RJ and Klionsky DJ. (2012). Autophagy: mechanism and physiological relevance 'brewed' from yeast studies. *Front Biosci (Schol Ed)* **4,** 1354-1363.

297. Komatsu M, Ueno T, Waguri S, Uchiyama Y, Kominami E and Tanaka K. (2007). Constitutive autophagy: vital role in clearance of unfavorable proteins in neurons. *Cell Death Differ* **14,** 887-894.

298. Kim J, Kundu M, Viollet B and Guan KL. (2011). AMPK and mTOR regulate autophagy through direct phosphorylation of Ulk1. *Nat Cell Biol* **13,** 132-141.

299. Meijer AJ, Lorin S, Blommaart EF and Codogno P. (2014). Regulation of autophagy by amino acids and MTOR-dependent signal transduction. *Amino Acids*.

300. Li L, Tan J, Miao Y, Lei P and Zhang Q. (2015). ROS and Autophagy: Interactions and Molecular Regulatory Mechanisms. *Cell Mol Neurobiol*.

301. Ogata M, Hino S, Saito A, Morikawa K, Kondo S, Kanemoto S, . . . Imaizumi K. (2006). Autophagy is activated for cell survival after endoplasmic reticulum stress. *Mol Cell Biol* **26,** 9220-9231.

302. Zhu JH, Horbinski C, Guo F, Watkins S, Uchiyama Y and Chu CT. (2007). Regulation of autophagy by extracellular signal-regulated protein kinases during 1-methyl-4-phenylpyridinium-induced cell death. *Am J Pathol* **170,** 75-86.

303. Feng Y, He D, Yao Z and Klionsky DJ. (2014). The machinery of macroautophagy. *Cell Res* **24,** 24-41.

304. Shibutani ST and Yoshimori T. (2014). A current perspective of autophagosome biogenesis. *Cell Res* **24,** 58-68.

305. Lamb CA, Yoshimori T and Tooze SA. (2013). The autophagosome: origins unknown, biogenesis complex. *Nat Rev Mol Cell Biol* **14,** 759-774.

306. Jahn R and Scheller RH. (2006). SNAREs--engines for membrane fusion. *Nat Rev Mol Cell Biol* **7,** 631-643.

307. Itakura E, Kishi-Itakura C and Mizushima N. (2012). The hairpin-type tail-anchored SNARE syntaxin 17 targets to autophagosomes for fusion with endosomes/lysosomes. *Cell* **151,** 1256-1269.

308. Furuta N, Fujita N, Noda T, Yoshimori T and Amano A. (2010). Combinational soluble N-ethylmaleimide-sensitive factor attachment protein receptor proteins VAMP8 and Vti1b mediate fusion of antimicrobial and canonical autophagosomes with lysosomes. *Mol Biol Cell* **21,** 1001-1010.

309. Pankiv S, Clausen TH, Lamark T, Brech A, Bruun JA, Outzen H, . . . Johansen T. (2007). p62/SQSTM1 binds directly to Atg8/LC3 to facilitate degradation of ubiquitinated protein aggregates by autophagy. *J Biol Chem* **282,** 24131-24145.

310. Lippai M and Low P. (2014). The role of the selective adaptor p62 and ubiquitin-like proteins in autophagy. *Biomed Res Int* **2014,** 832704.

311. Tanida I, Tanida-Miyake E, Komatsu M, Ueno T and Kominami E. (2002). Human Apg3p/Aut1p homologue is an authentic E2 enzyme for multiple substrates, GATE-16, GABARAP, and MAP-LC3, and facilitates the conjugation of hApg12p to hApg5p. *J Biol Chem* **277,** 13739-13744.

312. Klionsky DJ, Abdalla FC, Abeliovich H, Abraham RT, Acevedo-Arozena A, Adeli K, . . . Zuckerbraun B. (2012). Guidelines for the use and interpretation of assays for monitoring autophagy. *Autophagy* **8,** 445-544.

313. Shi J and Luo H. (2012). Interplay between the cellular autophagy machinery and positive-stranded RNA viruses. *Acta Biochim Biophys Sin (Shanghai)* **44,** 375-384.

314. Wong J, Zhang J, Si X, Gao G, Mao I, McManus BM and Luo H. (2008). Autophagosome supports coxsackievirus B3 replication in host cells. *J Virol* **82,** 9143-9153.

315. Alirezaei M, Flynn CT, Wood MR and Whitton JL. (2012). Pancreatic acinar cell-specific autophagy disruption reduces coxsackievirus replication and pathogenesis in vivo. *Cell Host Microbe* **11,** 298-305.

316. Caliguiri LA and Tamm I. (1969). Membranous structures associated with translation and transcription of poliovirus RNA. *Science* **166,** 885-886.

317. Bienz K, Egger D, Troxler M and Pasamontes L. (1990). Structural organization of poliovirus RNA replication is mediated by viral proteins of the P2 genomic region. *J Virol* **64,** 1156-1163.

318. Suhy DA, Giddings TH, Jr. and Kirkegaard K. (2000). Remodeling the endoplasmic reticulum by poliovirus infection and by individual viral proteins: an autophagy-like origin for virus-induced vesicles. *J Virol* **74,** 8953-8965.

319. Jackson WT, Giddings TH, Jr., Taylor MP, Mulinyawe S, Rabinovitch M, Kopito RR and Kirkegaard K. (2005). Subversion of cellular autophagosomal machinery by RNA viruses. *PLoS Biol* **3,** e156.

320. Delorme-Axford E, Morosky S, Bomberger J, Stolz DB, Jackson WT and Coyne CB. (2014). BPIFB3 regulates autophagy and coxsackievirus B replication through a noncanonical pathway independent of the core initiation machinery. *MBio* **5,** e02147.

321. Casrouge A, Zhang SY, Eidenschenk C, Jouanguy E, Puel A, Yang K, . . . Casanova JL. (2006). Herpes simplex virus encephalitis in human UNC-93B deficiency. *Science* **314,** 308-312.

322. Zhang SY, Jouanguy E, Ugolini S, Smahi A, Elain G, Romero P, . . . Casanova JL. (2007). TLR3 deficiency in patients with herpes simplex encephalitis. *Science* **317,** 1522-1527.

323. Nakano S, Morimoto S, Suzuki S, Watanabe T, Amano H and Takasaki Y. (2010). Up-regulation of the endoplasmic reticulum transmembrane protein UNC93B in the B cells of patients with active systemic lupus erythematosus. *Rheumatology (Oxford)* **49,** 876-881.

324. Han KJ, Su X, Xu LG, Bin LH, Zhang J and Shu HB. (2004). Mechanisms of the TRIF-induced interferon-stimulated response element and NF-kappaB activation and apoptosis pathways. *J Biol Chem* **279,** 15652-15661.

325. Colston JT, Chandrasekar B and Freeman GL. (1998). Expression of apoptosis-related proteins in experimental coxsackievirus myocarditis. *Cardiovasc Res* **38,** 158-168.

326. Huang da W, Sherman BT and Lempicki RA. (2009). Bioinformatics enrichment tools: paths toward the comprehensive functional analysis of large gene lists. *Nucleic Acids Res* **37,** 1-13.

327. Huang da W, Sherman BT and Lempicki RA. (2009). Systematic and integrative analysis of large gene lists using DAVID bioinformatics resources. *Nat Protoc* **4,** 44-57.

328. Rintahaka J, Wiik D, Kovanen PE, Alenius H and Matikainen S. (2008). Cytosolic antiviral RNA recognition pathway activates caspases 1 and 3. *J Immunol* **180,** 1749-1757.

329. Kang DC, Gopalkrishnan RV, Lin L, Randolph A, Valerie K, Pestka S and Fisher PB. (2004). Expression analysis and genomic characterization of human melanoma differentiation associated gene-5, mda-5: a novel type I interferon-responsive apoptosis-inducing gene. *Oncogene* **23,** 1789-1800.

330. Kim W, Bennett EJ, Huttlin EL, Guo A, Li J, Possemato A, . . . Gygi SP. (2011). Systematic and quantitative assessment of the ubiquitin-modified proteome. *Mol Cell* **44,** 325-340.

331. Simbulan-Rosenthal CM, Rosenthal DS, Iyer S, Boulares AH and Smulson ME. (1998). Transient poly(ADP-ribosyl)ation of nuclear proteins and role of poly(ADP-ribose) polymerase in the early stages of apoptosis. *J Biol Chem* **273,** 13703-13712.

332. Wee LJ, Tan TW and Ranganathan S. (2006). SVM-based prediction of caspase substrate cleavage sites. *BMC Bioinformatics* **7 Suppl 5,** S14.

333. Estornes Y, Toscano F, Virard F, Jacquemin G, Pierrot A, Vanbervliet B, . . . Lebecque S. (2012). dsRNA induces apoptosis through an atypical death complex associating TLR3 to caspase-8. *Cell Death Differ* **19,** 1482-1494.

334. Blom N, Hansen J, Blaas D and Brunak S. (1996). Cleavage site analysis in picornaviral polyproteins: discovering cellular targets by neural networks. *Protein Sci* **5,** 2203-2216.

335. Presley JF, Cole NB, Schroer TA, Hirschberg K, Zaal KJ and Lippincott-Schwartz J. (1997). ER-to-Golgi transport visualized in living cells. *Nature* **389,** 81-85.

336. Ashida H, Mimuro H, Ogawa M, Kobayashi T, Sanada T, Kim M and Sasakawa C. (2011). Cell death and infection: a double-edged sword for host and pathogen survival. *J Cell Biol* **195,** 931-942.

337. Hornung V, Rothenfusser S, Britsch S, Krug A, Jahrsdorfer B, Giese T, . . . Hartmann G. (2002). Quantitative expression of toll-like receptor 1-10 mRNA in cellular subsets of human peripheral blood mononuclear cells and sensitivity to CpG oligodeoxynucleotides. *J Immunol* **168,** 4531-4537.

338. Rajput A, Kovalenko A, Bogdanov K, Yang SH, Kang TB, Kim JC, . . . Wallach D. (2011). RIG-I RNA helicase activation of IRF3 transcription factor is negatively regulated by caspase-8-mediated cleavage of the RIP1 protein. *Immunity* **34,** 340-351.

339. Golks A, Brenner D, Krammer PH and Lavrik IN. (2006). The c-FLIP-NH2 terminus (p22-FLIP) induces NF-kappaB activation. *J Exp Med* **203,** 1295-1305.

340. Lemmers B, Salmena L, Bidere N, Su H, Matysiak-Zablocki E, Murakami K, . . . Hakem A. (2007). Essential role for caspase-8 in Toll-like receptors and NFkappaB signaling. *J Biol Chem* **282,** 7416-7423.

341. Su H, Bidere N, Zheng L, Cubre A, Sakai K, Dale J, . . . Lenardo M. (2005). Requirement for caspase-8 in NF-kappaB activation by antigen receptor. *Science* **307,** 1465-1468.

342. Berg TO, Fengsrud M, Stromhaug PE, Berg T and Seglen PO. (1998). Isolation and characterization of rat liver amphisomes. Evidence for fusion of autophagosomes with both early and late endosomes. *J Biol Chem* **273,** 21883-21892.

343. Huang J and Brumell JH. (2014). Bacteria-autophagy interplay: a battle for survival. *Nat Rev Microbiol* **12,** 101-114.

344. Jacobs JL, Zhu J, Sarkar SN and Coyne CB. (2014). Regulation of mitochondrial antiviral signaling (MAVS) expression and signaling by the mitochondria-associated endoplasmic reticulum membrane (MAM) protein Gp78. *J Biol Chem* **289,** 1604-1616.

345. Crowther D and Melnick JL. (1961). The incorporation of neutral red and acridine orange into developing poliovirus particles making them photosensitive. *Virology* **14,** 11-21.

346. Kirkin V, Lamark T, Johansen T and Dikic I. (2009). NBR1 cooperates with p62 in selective autophagy of ubiquitinated targets. *Autophagy* **5,** 732-733.

347. Matsuzawa Y, Oshima S, Nibe Y, Kobayashi M, Maeyashiki C, Nemoto Y, . . . Watanabe M. (2015). RIPK3 regulates p62-LC3 complex formation via the caspase-8-dependent cleavage of p62. *Biochem Biophys Res Commun* **456,** 298-304.

348. Harris KG and Coyne CB. (2014). Death waits for no man--does it wait for a virus? How enteroviruses induce and control cell death. *Cytokine Growth Factor Rev* **25,** 587-596.

349. Moriwaki K and Chan FK. (2013). RIP3: a molecular switch for necrosis and inflammation. *Genes Dev* **27,** 1640-1649.

350. Meylan E, Burns K, Hofmann K, Blancheteau V, Martinon F, Kelliher M and Tschopp J. (2004). RIP1 is an essential mediator of Toll-like receptor 3-induced NF-kappa B activation. *Nat Immunol* **5,** 503-507.

351. Sun X, Lee J, Navas T, Baldwin DT, Stewart TA and Dixit VM. (1999). RIP3, a novel apoptosis-inducing kinase. *J Biol Chem* **274,** 16871-16875.

352. Boya P, Gonzalez-Polo RA, Casares N, Perfettini JL, Dessen P, Larochette N, . . . Kroemer G. (2005). Inhibition of macroautophagy triggers apoptosis. *Mol Cell Biol* **25,** 1025-1040.

353. Marino G, Niso-Santano M, Baehrecke EH and Kroemer G. (2014). Self-consumption: the interplay of autophagy and apoptosis. *Nat Rev Mol Cell Biol* **15,** 81-94.

354. Elgendy M, Sheridan C, Brumatti G and Martin SJ. (2011). Oncogenic Ras-induced expression of Noxa and Beclin-1 promotes autophagic cell death and limits clonogenic survival. *Mol Cell* **42,** 23-35.

355. Liu Y, Shoji-Kawata S, Sumpter RM, Jr., Wei Y, Ginet V, Zhang L, . . . Levine B. (2013). Autosis is a Na+,K+-ATPase-regulated form of cell death triggered by autophagy-inducing peptides, starvation, and hypoxia-ischemia. *Proc Natl Acad Sci U S A* **110,** 20364-20371.

356. Yu L, Alva A, Su H, Dutt P, Freundt E, Welsh S, . . . Lenardo MJ. (2004). Regulation of an ATG7-beclin 1 program of autophagic cell death by caspase-8. *Science* **304,** 1500-1502.

357. Kirkegaard K, Taylor MP and Jackson WT. (2004). Cellular autophagy: surrender, avoidance and subversion by microorganisms. *Nat Rev Microbiol* **2,** 301-314.

358. Shelly S, Lukinova N, Bambina S, Berman A and Cherry S. (2009). Autophagy is an essential component of Drosophila immunity against vesicular stomatitis virus. *Immunity* **30,** 588-598.

359. Stolz A, Ernst A and Dikic I. (2014). Cargo recognition and trafficking in selective autophagy. *Nat Cell Biol* **16,** 495-501.

360. Anderson CA, Boucher G, Lees CW, Franke A, D'Amato M, Taylor KD, . . . Rioux JD. (2011). Meta-analysis identifies 29 additional ulcerative colitis risk loci, increasing the number of confirmed associations to 47. *Nat Genet* **43,** 246-252.

361. Benjamin JL, Sumpter R, Jr., Levine B and Hooper LV. (2013). Intestinal epithelial autophagy is essential for host defense against invasive bacteria. *Cell Host Microbe* **13,** 723-734.

362. Mizushima N and Levine B. (2010). Autophagy in mammalian development and differentiation. *Nat Cell Biol* **12,** 823-830.

363. Newton K, Sun X and Dixit VM. (2004). Kinase RIP3 is dispensable for normal NF-kappa Bs, signaling by the B-cell and T-cell receptors, tumor necrosis factor receptor 1, and Toll-like receptors 2 and 4. *Mol Cell Biol* **24,** 1464-1469.

364. Yu PW, Huang BC, Shen M, Quast J, Chan E, Xu X, . . . Luo Y. (1999). Identification of RIP3, a RIP-like kinase that activates apoptosis and NFkappaB. *Curr Biol* **9,** 539-542.

365. Longdon B, Brockhurst MA, Russell CA, Welch JJ and Jiggins FM. (2014). The evolution and genetics of virus host shifts. *PLoS Pathog* **10,** e1004395.

366. Zaharia M, Bolosky WJ, Curtis K, Fox A, Patterson D, Shenker S, . . . Sittler T. (2011). Faster and More Accurate Sequence Alignment with SNAP (eprint arXiv:1111.5572).

367. Warrens AN, Jones MD and Lechler RI. (1997). Splicing by overlap extension by PCR using asymmetric amplification: an improved technique for the generation of hybrid proteins of immunological interest. *Gene* **186,** 29-35.

368. Kimura S, Noda T and Yoshimori T. (2007). Dissection of the autophagosome maturation process by a novel reporter protein, tandem fluorescent-tagged LC3. *Autophagy* **3,** 452-460.

369. Delorme-Axford E, Donker RB, Mouillet JF, Chu T, Bayer A, Ouyang Y, . . . Coyne CB. (2013). Human placental trophoblasts confer viral resistance to recipient cells. *Proc Natl Acad Sci U S A* **110,** 12048-12053.

Parts of the introduction were reprinted, with permission from Elsevier, from the following publications:

- Cytokine & Growth Factor Reviews, Volume 25, Katharine G Harris and Carolyn B Coyne, Death waits for no man – Does it wait for a virus? How enteroviruses induce and control cell death, Pages 587-596, ©2014

- Cytokine, Volume 63, Katharine G Harris and Carolyn B Coyne, Enter at your own risk: How enteroviruses navigate the dangerous world of pattern recognition receptor signaling, Pages 230-236, ©2013